Lecture 2

The Microscopic Picture of Magnetic Materials

- **We will now revisit the experimentally observed magnetic behaviours and try to understand them from a microscopic point of view**

Lecture 2

The Microscopic Picture of Magnetic Materials

- **We will now revisit the experimentally observed magnetic behaviours and try to understand them from a microscopic point of view**

Paramagnetic gas

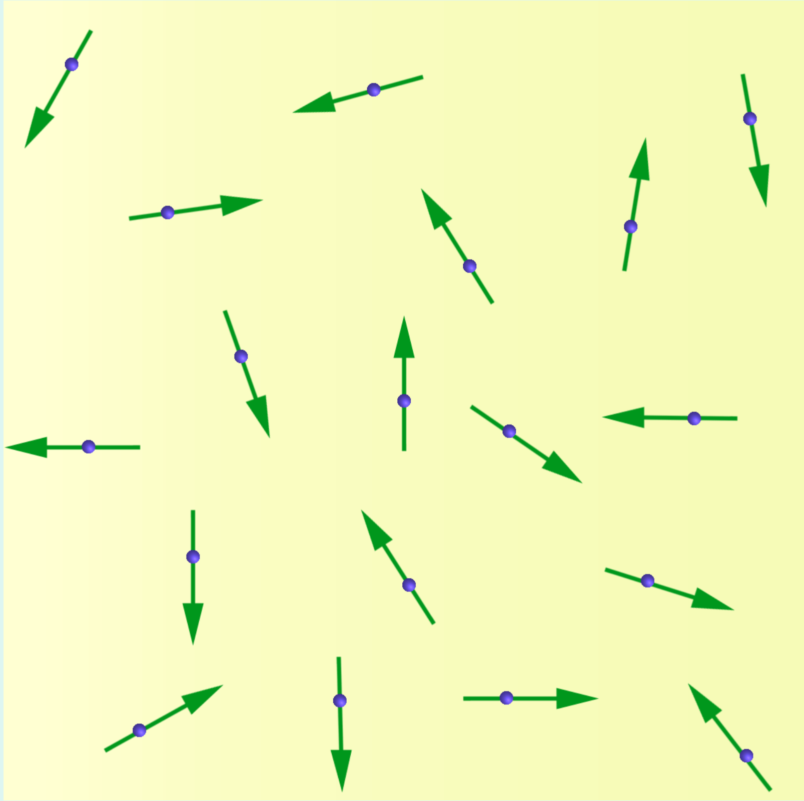

- **Imagine a classical gas of molecules each with a magnetic dipole moment**
- **In zero field the gas would have zero magnetization**

Paramagnetic gas

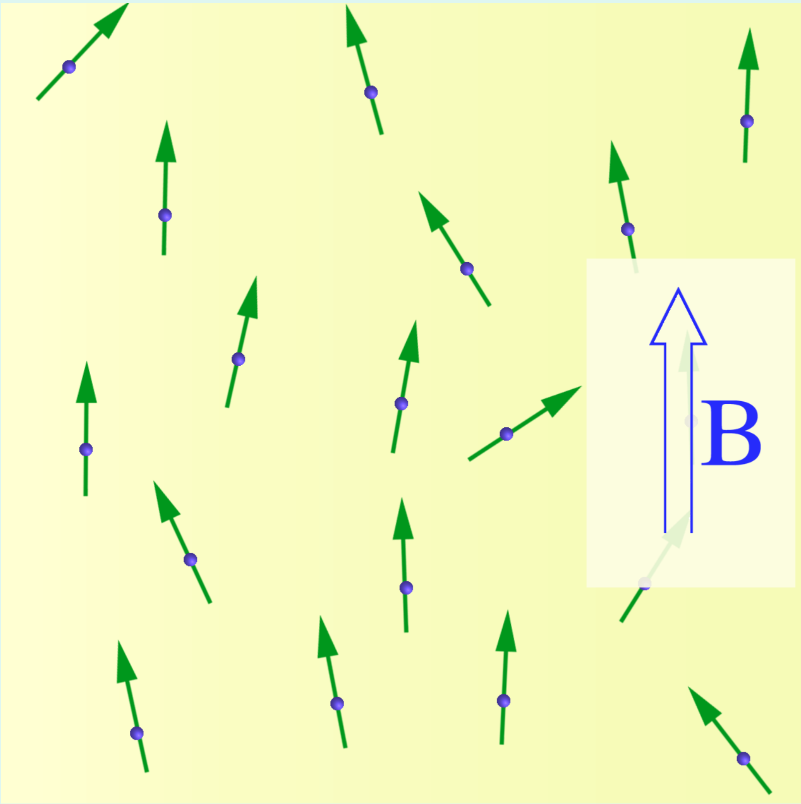

- Applying a magnetic field would tend to orient the dipole moments
- Gas attains a magnetization

Paramagnetic gas

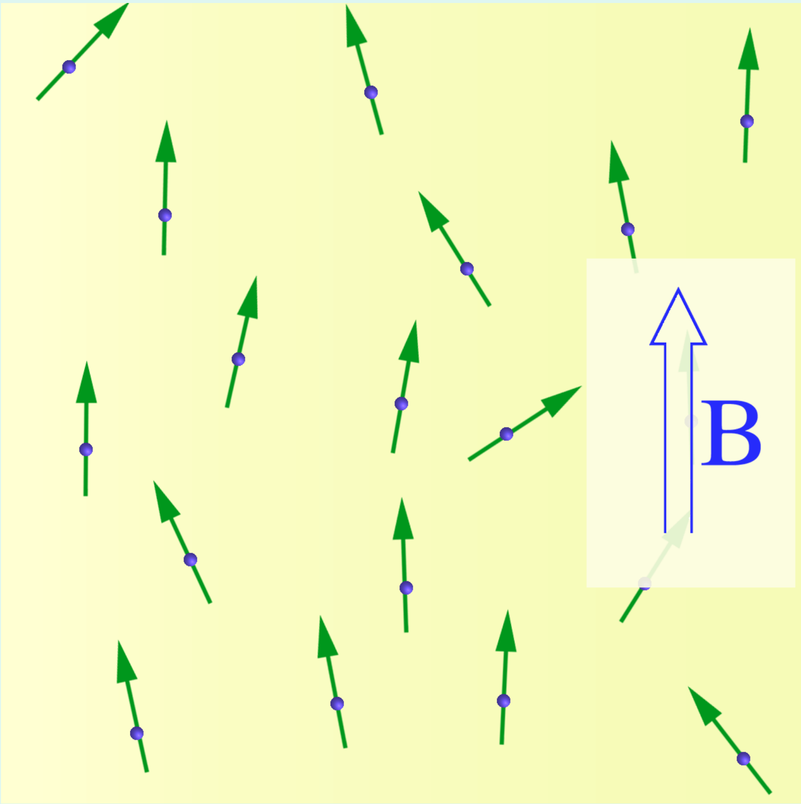

- Very high fields would saturate magnetization
- Heating the gas would tend to disorder the moments and hence decrease magnetization

Paramagnetic gas

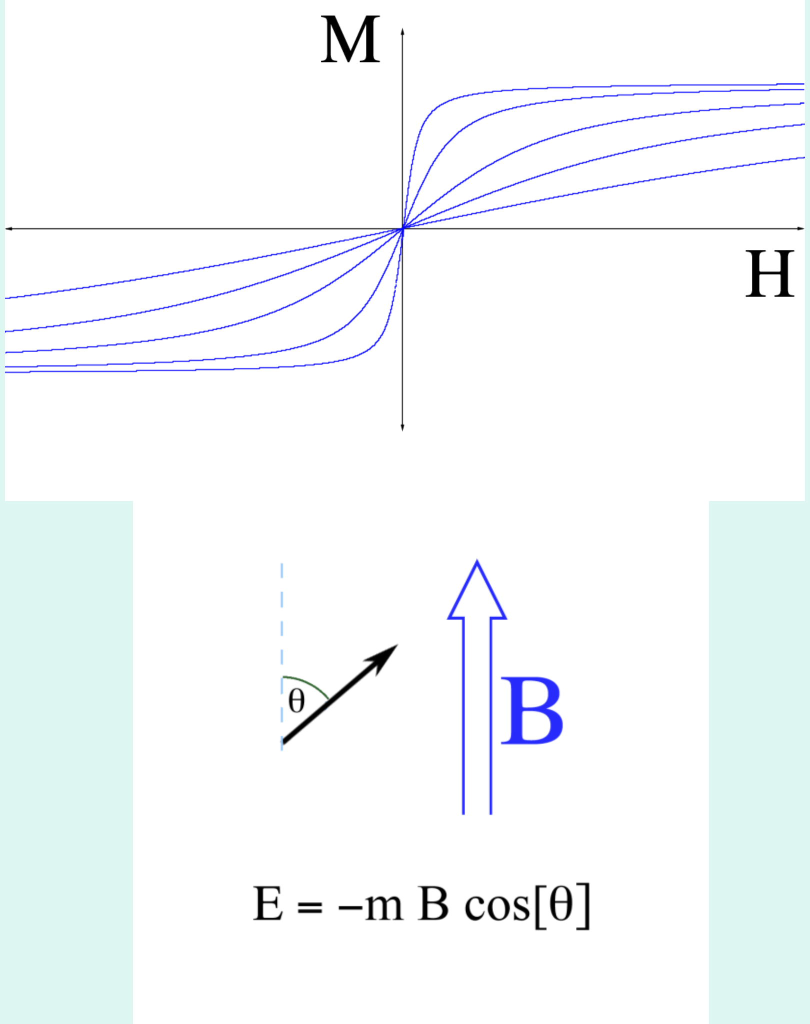

- **Theoretical model**
- **Non-interacting moments**
- **Boltzmann statistics**
- **Dipole interaction with *B***
- **Yields good model for many materials**
- **Examples: ferrous sulfate crystals, ionic solutions of magnetic atoms**

Paramagnetic gas

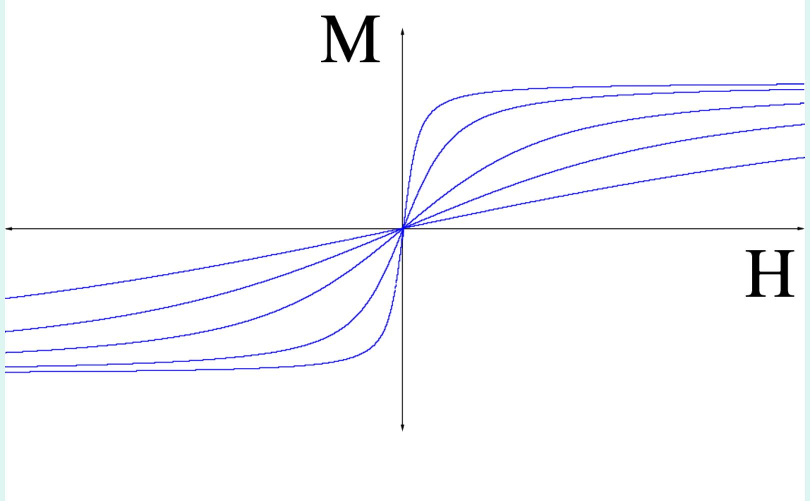

- **Classical model yields Langevin function**
- **Quantum model yields Brillouin function**

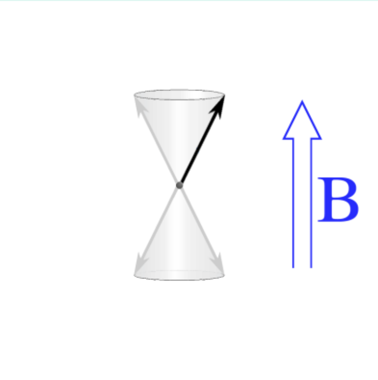

Exchange Interaction

- **Direct exchange**

Direct exchange operates between moments, which are close enough to have sufficient overlap of their wavefunctions. It gives a strong but short-range coupling which decreases rapidly as the ions are separated. An initial simple way of understanding direct exchange is to look at two atoms with one electron each. When the atoms are very close together the Coulomb interaction is minimal when the electrons spend most of their time in between the nuclei. Since the electrons are then required to be at the same place in space at the same time, Pauli's exclusion principle requires that they possess opposite spins. According to Bethe and Slater the electrons spend most of their time in between neighboring atoms when the interatomic distance is small. This gives rise to antiparallel alignment and therefore negative exchange. (antiferromagnetic).

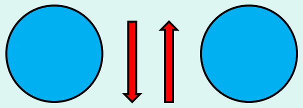

If the atoms are far apart the electrons spend their time away from each other in order to minimize the electron-electron repulsion. This gives rise to parallel alignment or positive exchange (ferromagnetism)

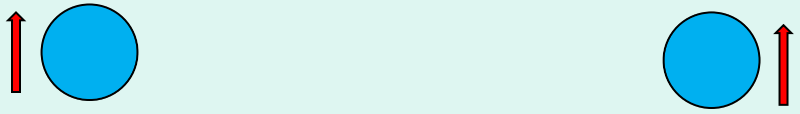

Bethe-Slater curve

- **The exchange Heisenberg energy, suitably scaled, replaces the Weiss molecular field constant in the mean field theory of ferromagnetism to explain the temperature dependence of the magnetization**

$$E_p = -J_{ex} S_i \times S_{i+1}$$

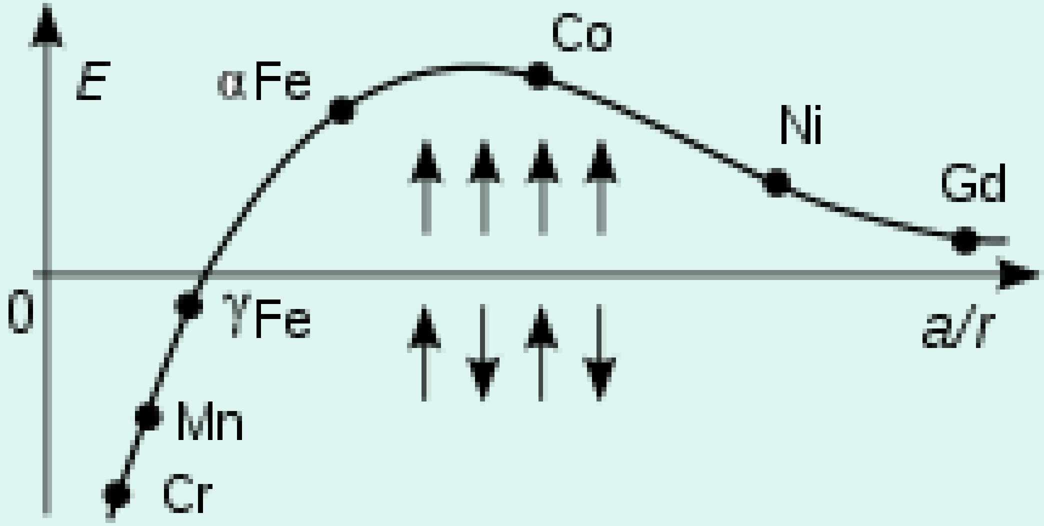

Differences in exchange energy of transition metals as due to the ratio of the interatomic distance a to the radius r of the 3d electron shell

Ferromagnetism

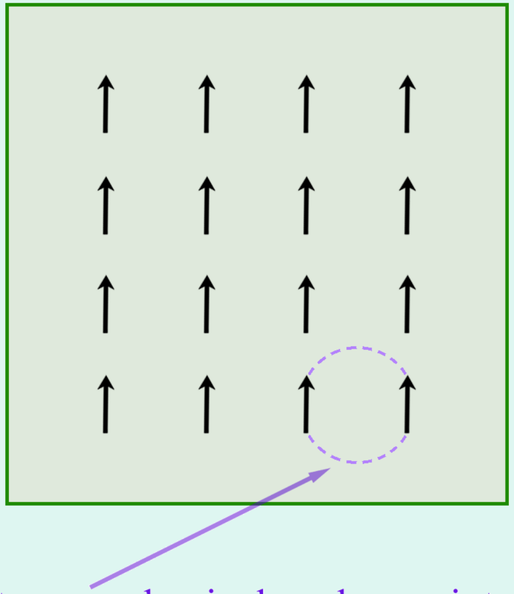

- **Materials that retain a magnetization in zero field**
- **Quantum mechanical exchange interactions favour parallel alignment of moments**
- **Examples: iron, cobalt**

Ferromagnetism

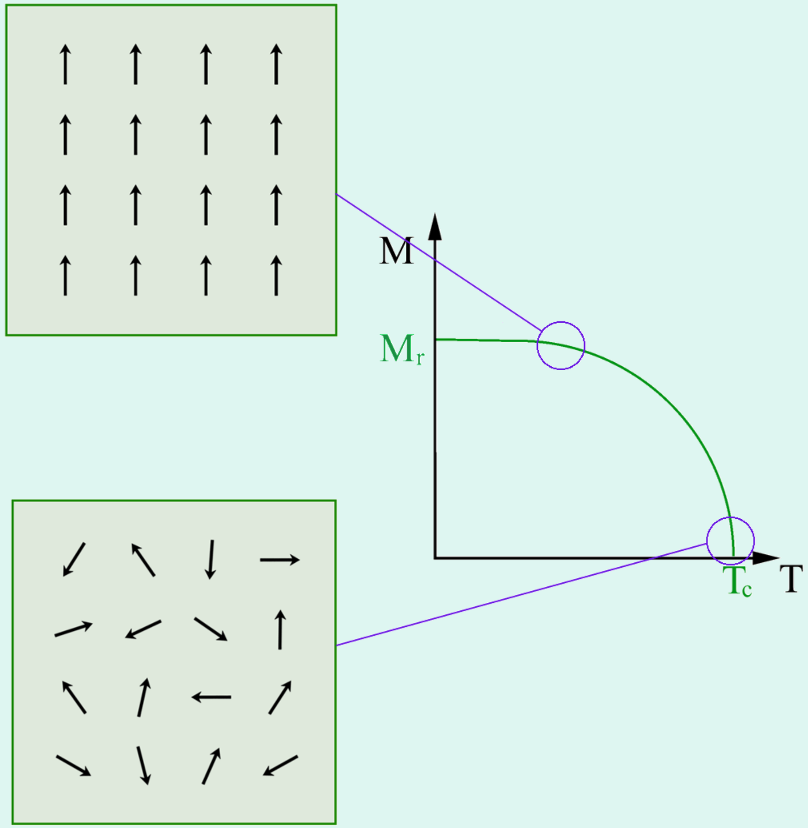

- **Thermal energy can be used to overcome exchange interactions**
- **Curie temp is a measure of exchange interaction strength**
- **Note: exchange interactions much stronger than dipole-dipole interactions**

Magnetic domains

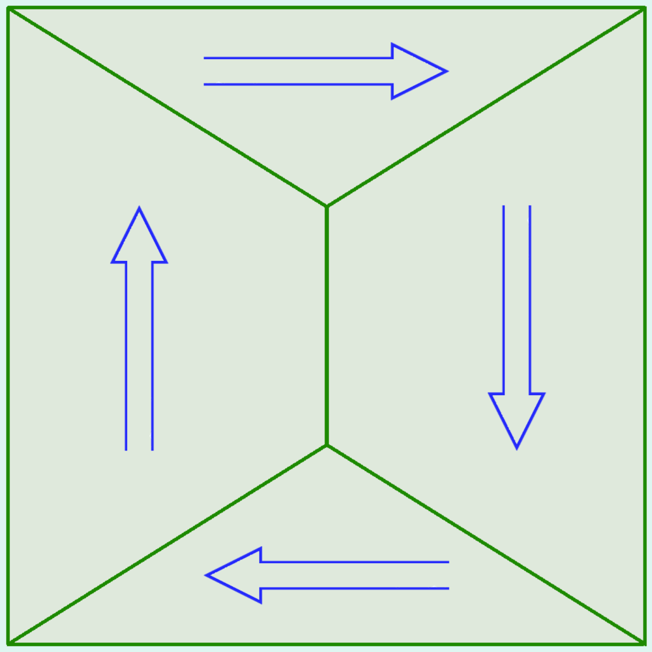

- Ferromagnetic materials tend to form magnetic domains
- Each domain is magnetized in a different direction
- Domain structure minimizes energy due to stray fields

Magnetic domains

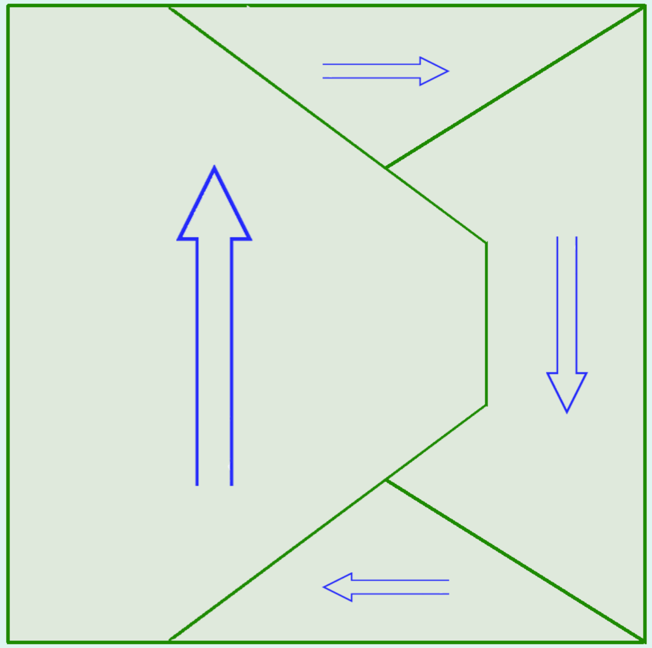

- **Applying a field changes domain structure**
- **Domains with magnetization in direction of field grow**
- **Other domains shrink**

Magnetic domains

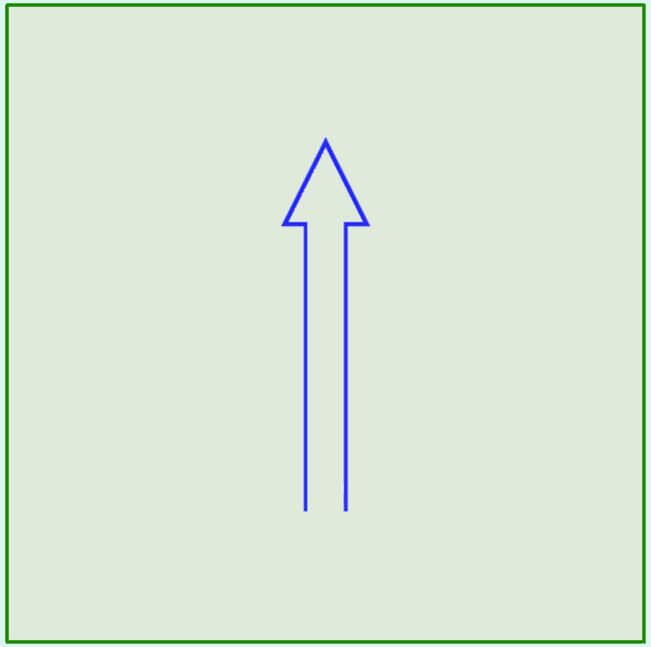

- **Applying very strong fields can saturate magnetization by creating single domain**

Magnetic domains

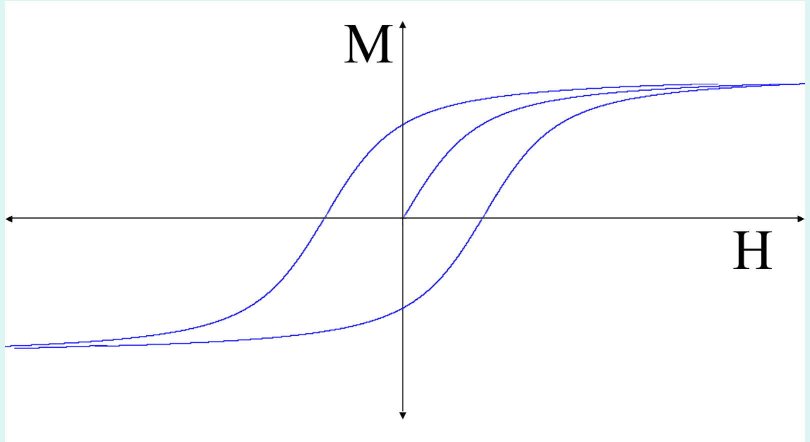

- Removing the field does not necessarily return domain structure to original state

- Hence results in magnetic hysteresis

Magnetic domain walls

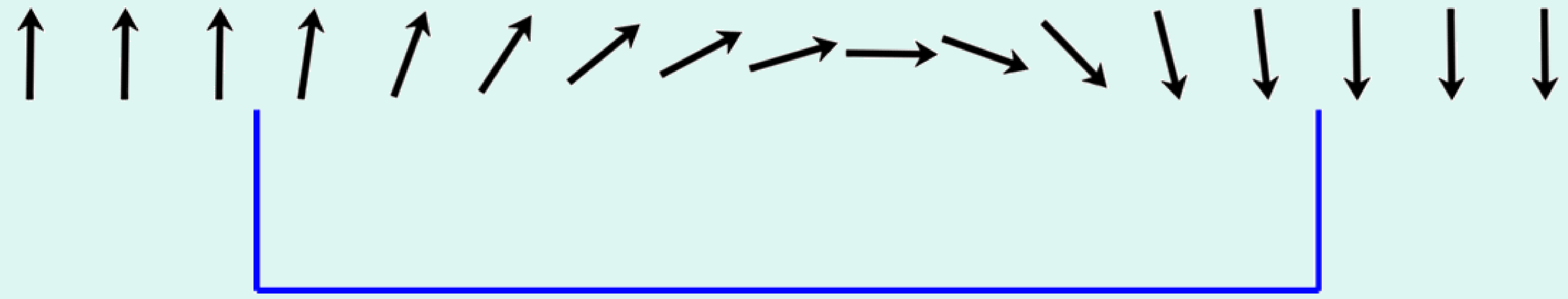

Wall Thickness "t"

Wall thickness, t, is typically about 100 nm

Single domain particles

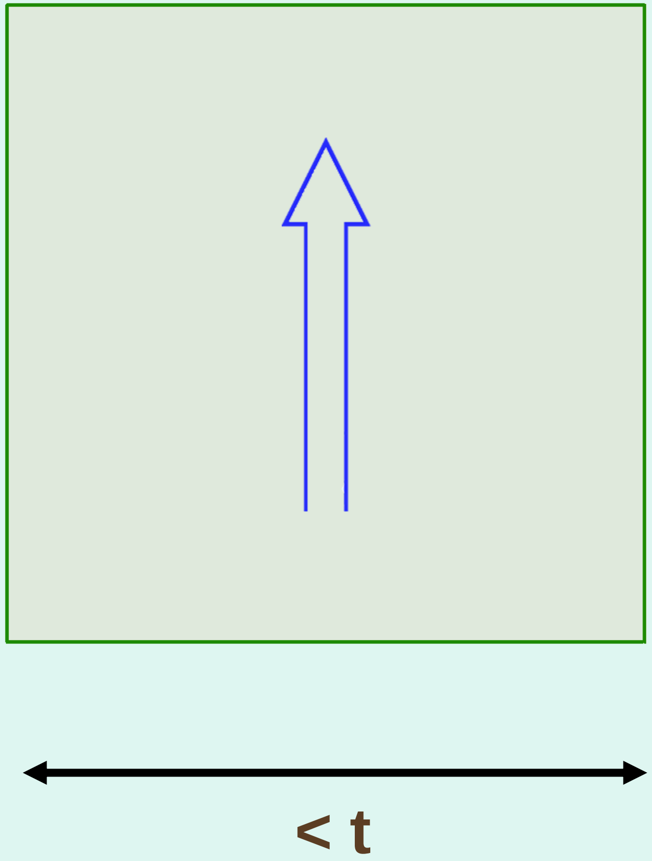

- **Particles smaller than “t” have no domains**

Antiferromagnetism

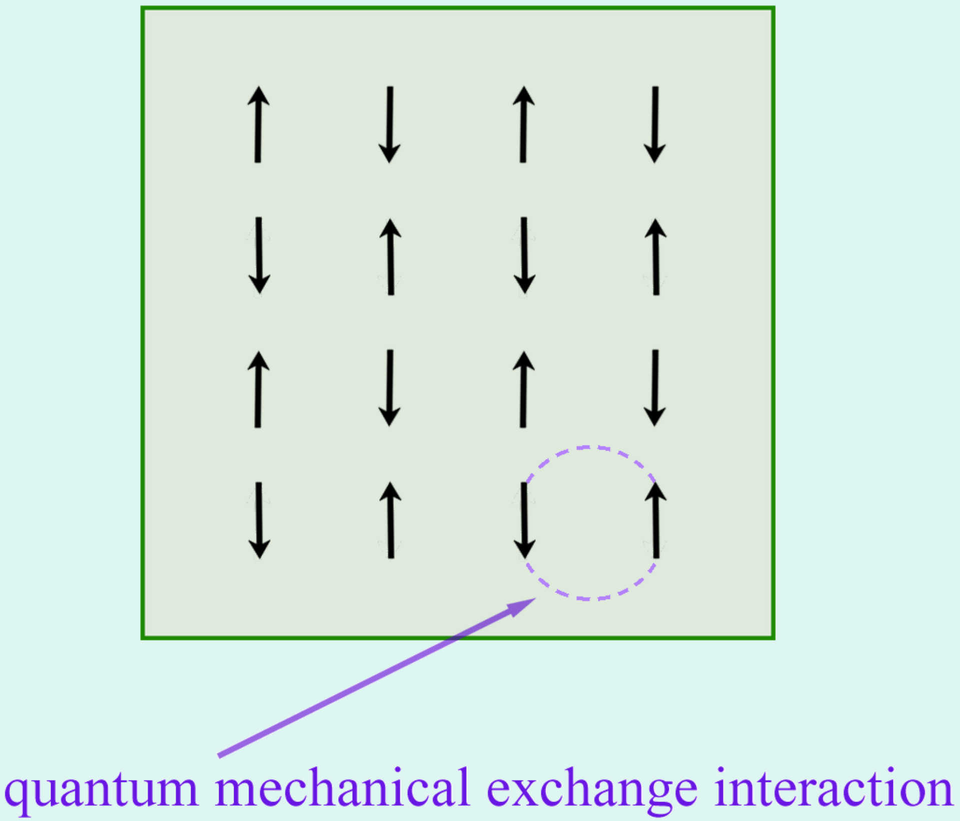

- **In some materials, exchange interactions favour antiparallel alignment of atomic magnetic moments**
- **Materials are magnetically ordered but have zero remnant magnetization and very low χ**
- **Many metal oxides are antiferromagnetic**

Antiferromagnetism

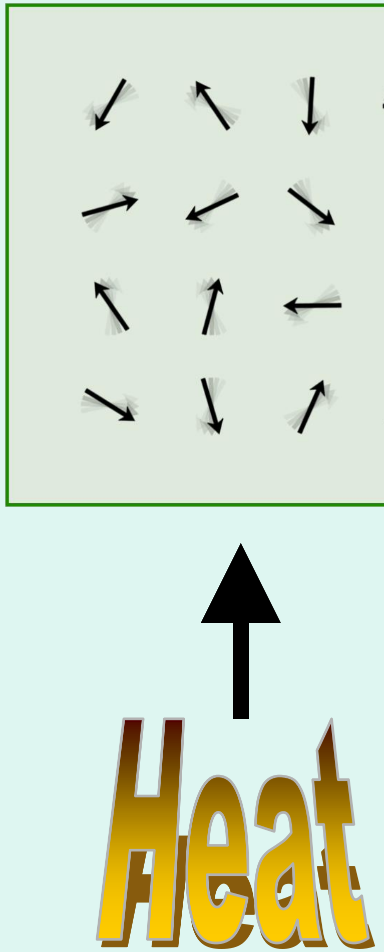

- **Thermal energy can be used to overcome exchange interactions**

- **Magnetic order is broken down at the Néel temperature (c.f. Curie temp)**

Ferrimagnetism

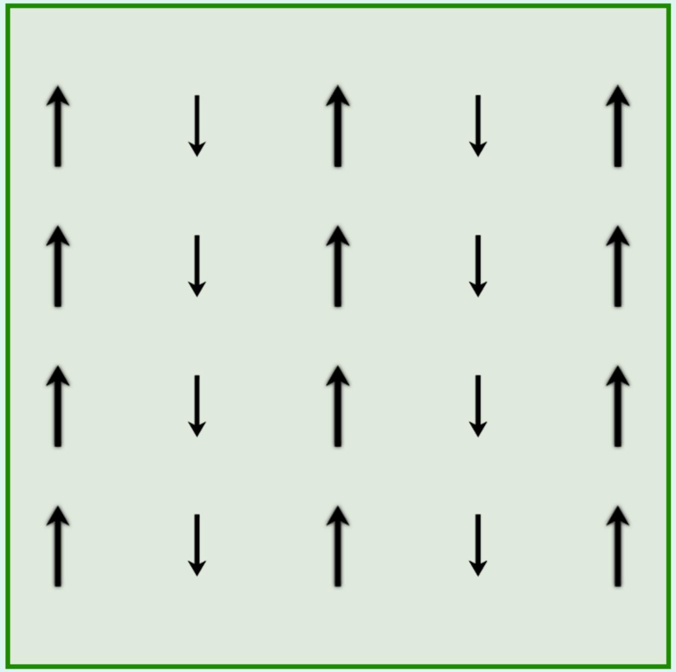

- **Antiferromagnetic exchange interactions**
- **Different sized moments on each sublattice**
- **Results in net magnetization**
- **Example: magnetite, maghemite**

Small Particle Magnetism

Stoner-Wohlfarth Particle

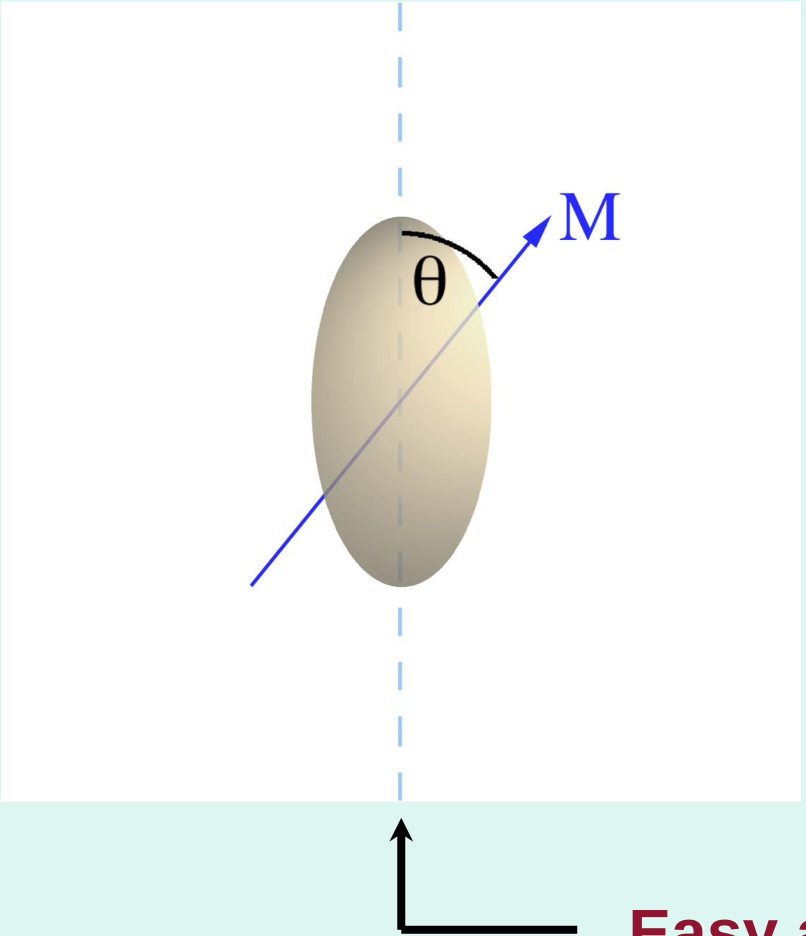

- **Magnetic anisotropy energy favours magnetization along certain axes relative to the crystal lattice**

Easy axis of magnetization

Stoner-Wohlfarth Particle

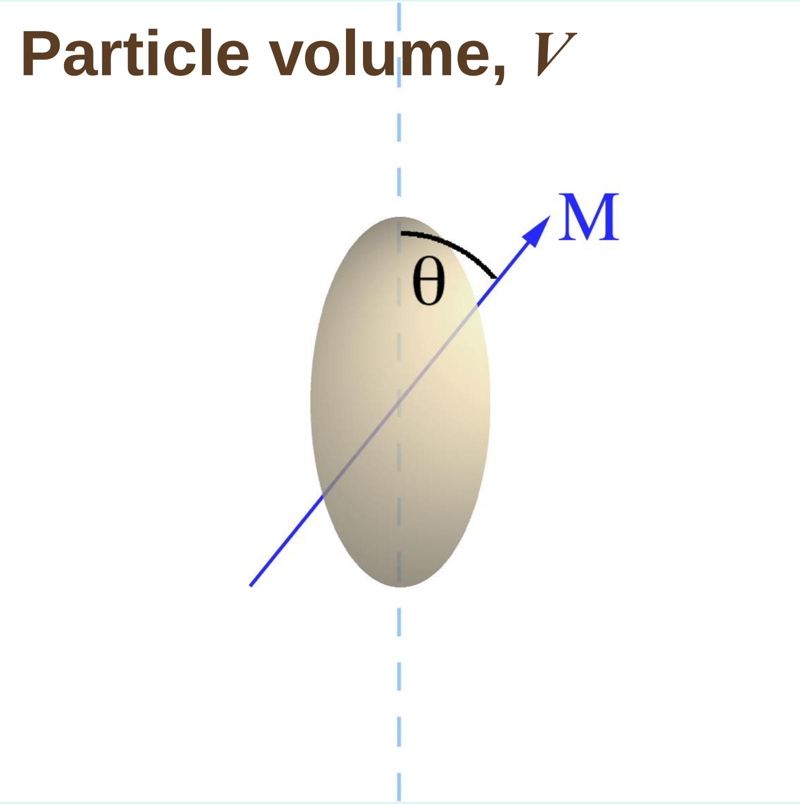

- **Uniaxial single domain particle**
- **Magnetocrystalline magnetic anisotropy energy given by**

$$E_a = KV \sin^2(\theta)$$

- ***K* is a constant for the material**

Stoner-Wohlfarth Particle

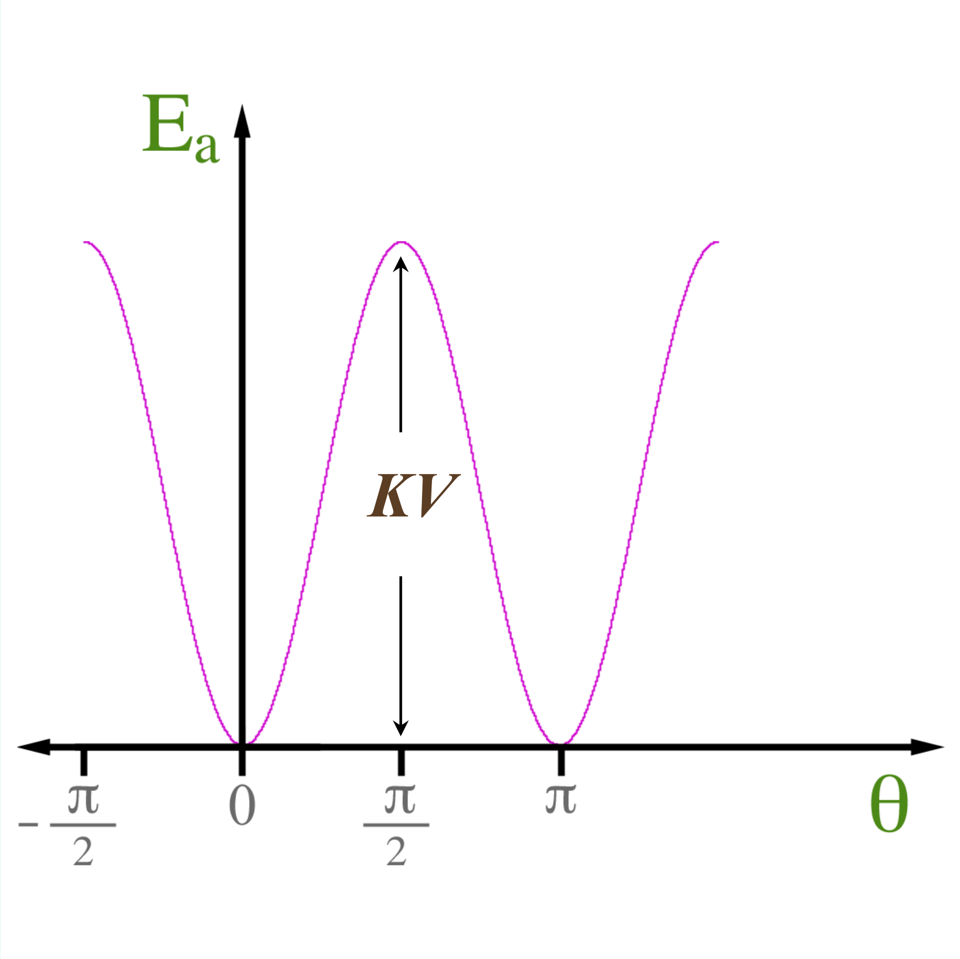

$$E_a = KV\sin^2(\theta)$$

Thermal activation

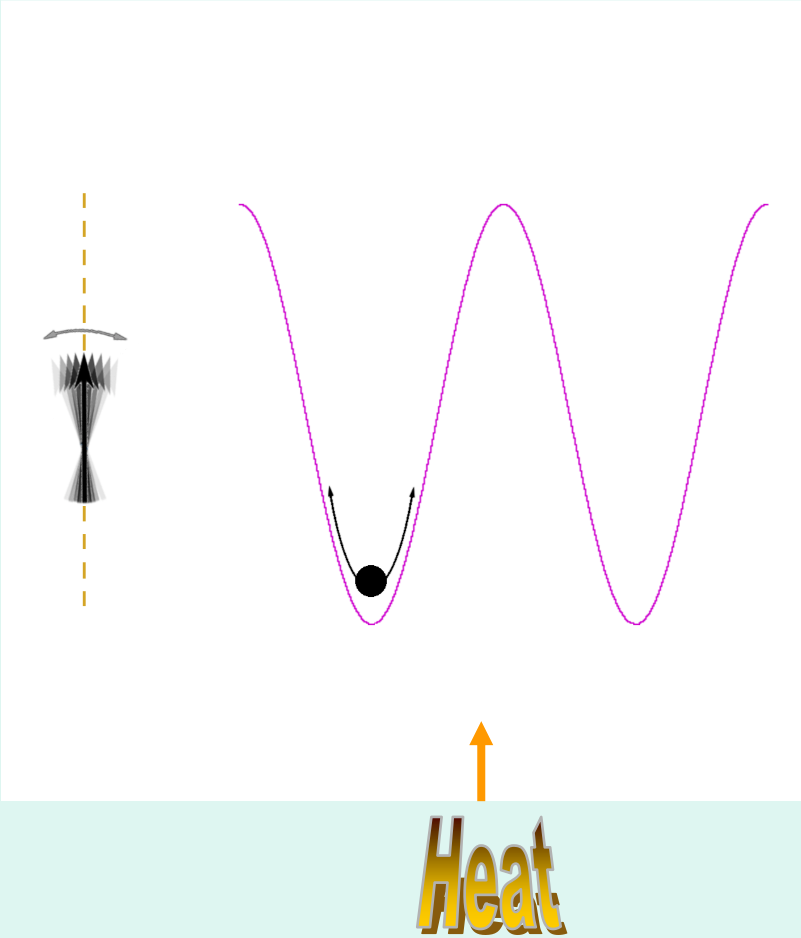

- **At low temperature magnetic moment of particle trapped in one of the wells**
- **Particle magnetic moment is "blocked"**

Thermal activation

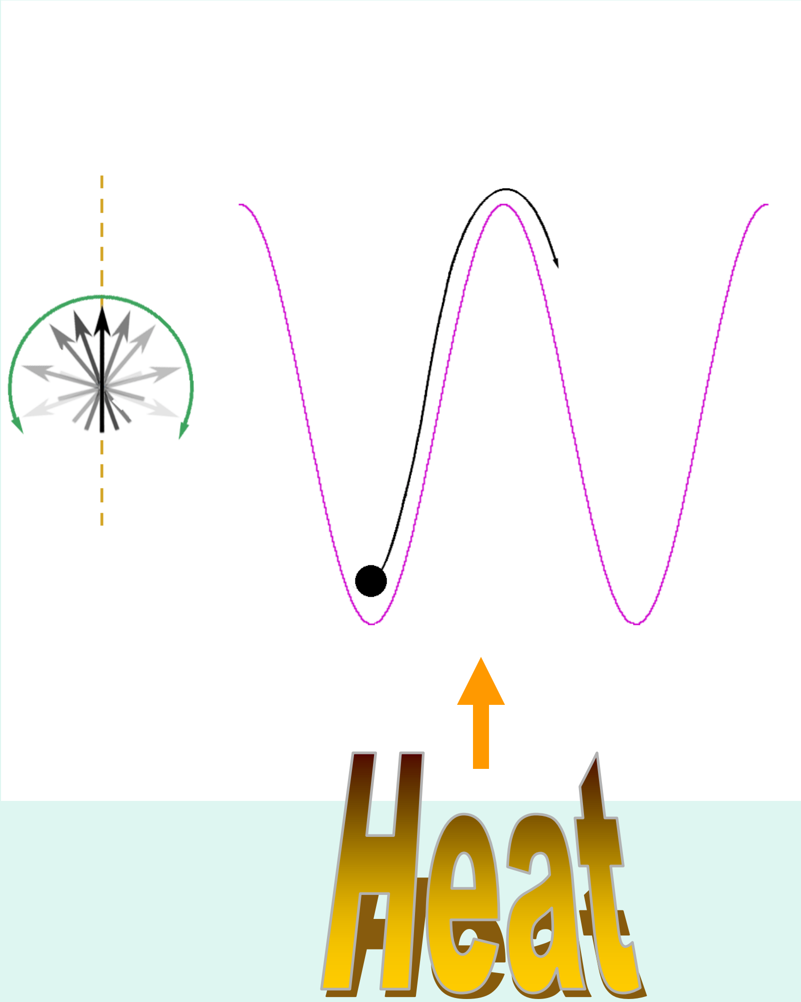

- At higher temps, thermal energy can buffet magnetic moment between the wells
- Results in rapid fluctuation of moment
- Particle moment becomes “unblocked”

Thermally Activated Jump

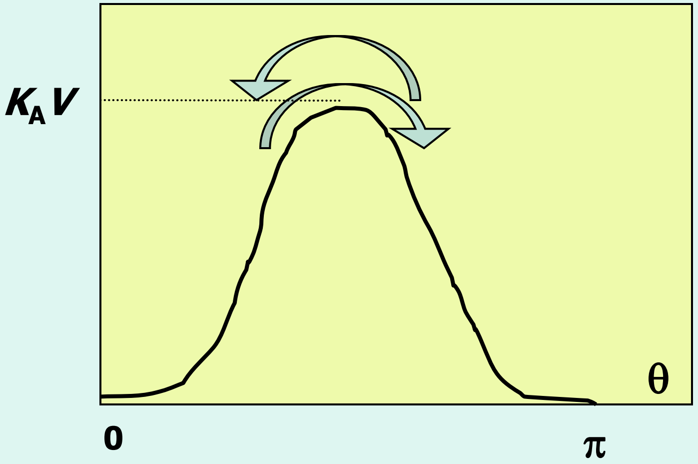

Thermally Activated Jump (Classical Behaviour!!)

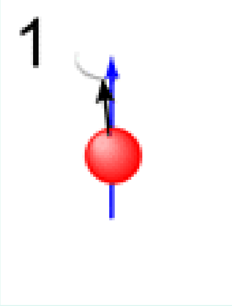

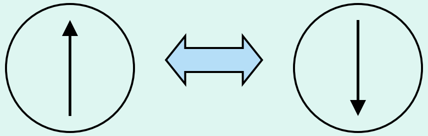

- **Jump frequency**: $$\upsilon = \tau_0^{-1} \exp\left(-\frac{K_a V}{k_B T}\right)$$
- **Relaxation time:** $$\tau = \tau_0 \exp\left(\frac{K_a V}{k_B T}\right)$$
- **theoretical predictions:** τ_0**=10^{-9} ÷ 10^{-10} (see later)**

Demagnetization rate of an assembly of uniaxial particles

$$-\frac{dM}{dt} = f_0 M e^{-KV/kT} = \frac{M}{\tau}$$

f_0 : frequency factor ($\approx 10^9$ sec^{-1})
τ : relaxation time

Turn-off external field at $t = 0$ with M_i

$$M_r = M_i e^{-t/\tau}$$

$\longrightarrow$ τ : time for M_r to decrease to 1/e of its initial value

$$\frac{1}{\tau} = f_0 e^{-KV/kT}$$

For Co ($K = 4.5 \times 10^6$ ergs/cm^3) at room temp. ($T = 300\ K$)

D = 68 Å (V = 1.6 × 10^{-19} cm^3)

$$\frac{1}{\tau} = 10^9 \cdot e^{-(4.5\times10^6 \times 1.6\times10^{-19}/(1.38\times10^{-16}\times300))} \approx 279.9\ \frac{1}{\text{sec}}$$

$$\tau \approx 3\times10^{-2}\ \text{sec}$$

An assembly of such particles would reach thermal equilibrium state ($M_r = 0$) almost instantaneously.
No hysteresis

Magnetization Relaxation

- **Two Regimes:**

$\tau < t_m$ $\qquad t_m \qquad$ $\tau > t_m$ **time**

Superparamagnetic | *Measuring time (time needed to do a measurement)* | **Blocked**

- **Standard Magnetic Measurements: $t_m \approx 100$ s**
- **Mössbauer: $t_m \approx 10^{-8}$ s**

- **Define a critical volume at constant T (e.g., RT≡T_0) by requiring $\tau = t_m$:**

$$\ln\tau = \ln\tau_0 + \frac{K_a V_{crit}}{k_B T_0} = \begin{cases} \ln 10^2 \\ \cdots \\ \ln 10^{-8} \end{cases}$$

$\approx 10^{-10}$

For $t_m \approx 100$ s:

$$V_{crit} \approx \frac{25 k_B T}{K_a}$$

$$D_{crit} = \left[\frac{6}{\pi} V_{crit}\right]^{1/3}$$

Magnetic blocking temperature

- **The magnetic blocking temp, T_b, is the temp below which moment is blocked**
- **Blocking temperature depends on particle size and timescale of observation**
- **Larger particles have higher blocking temperatures**
- **The longer the observation time, the more likely it is that the moment will be observed to flip**

Fluctuation timescales, τ

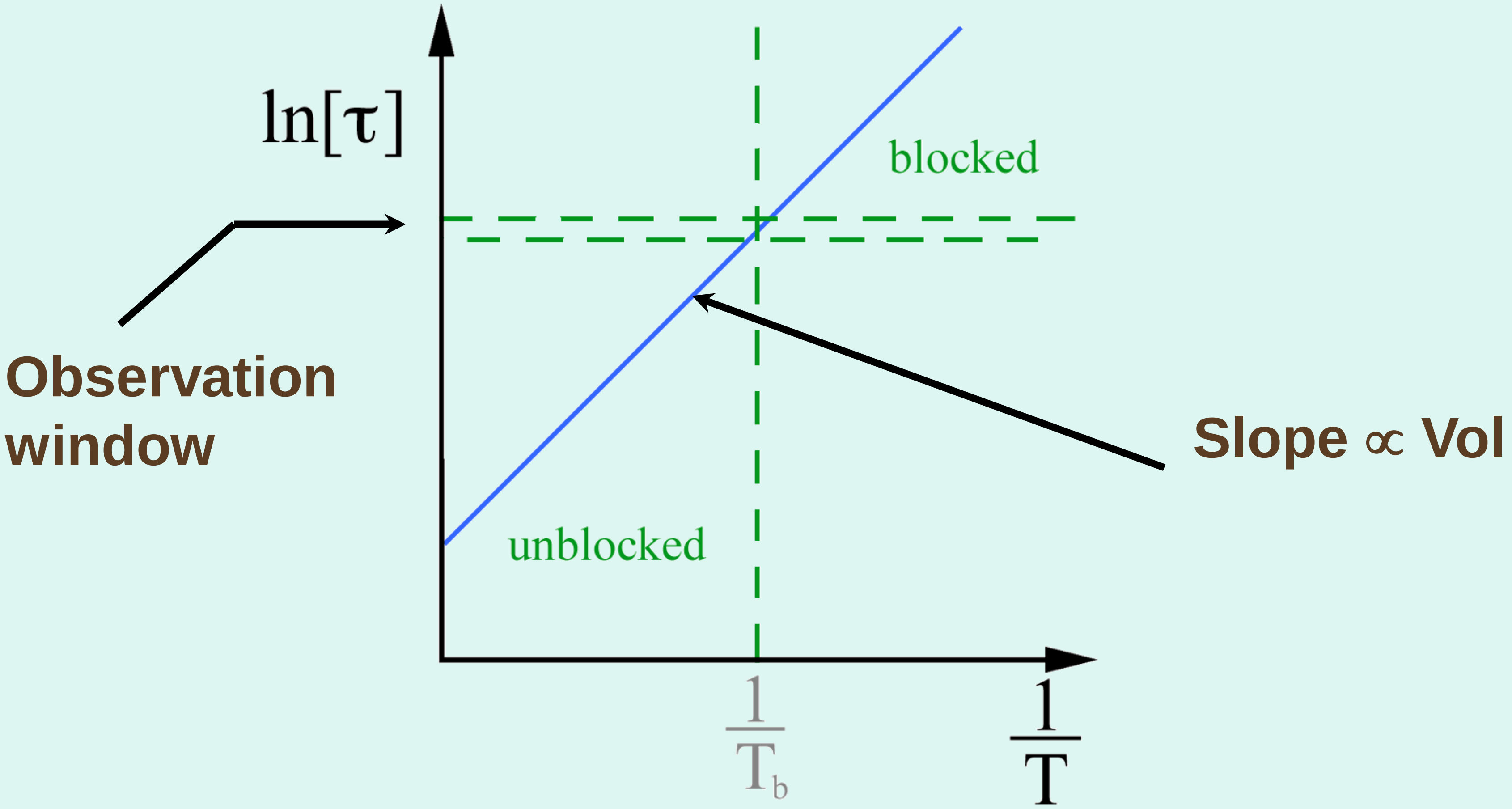

Effect of applied field on single domain particles

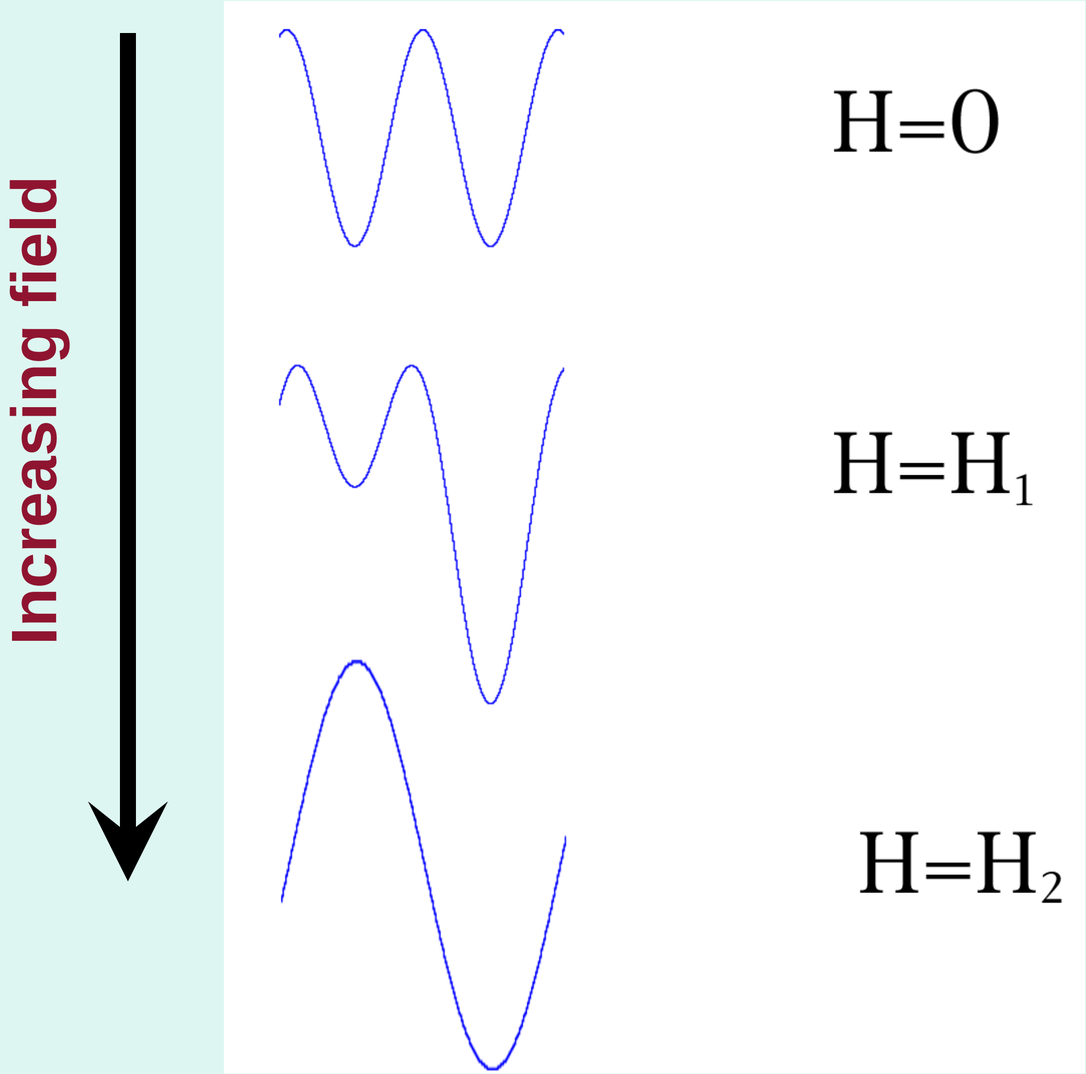

- Applying field along easy axis favours moment aligned with field
- Above T_b this results in moment spending more time in lower well
- Particle exhibits time averaged magnetization in direction of field

Superparamagnetism

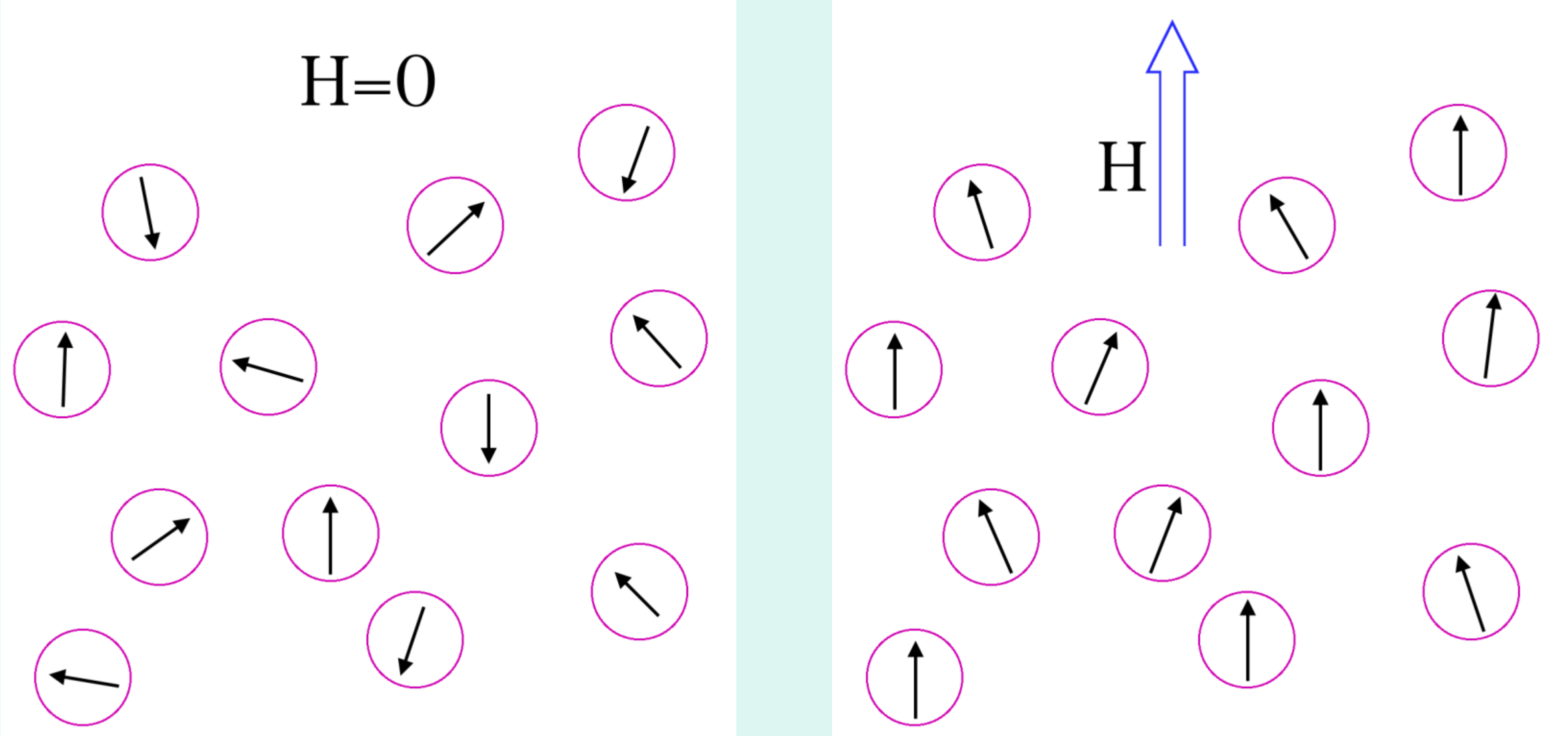

- **Unblocked particles that respond to a field are known as superparamagnetic**

Superparamagnetism

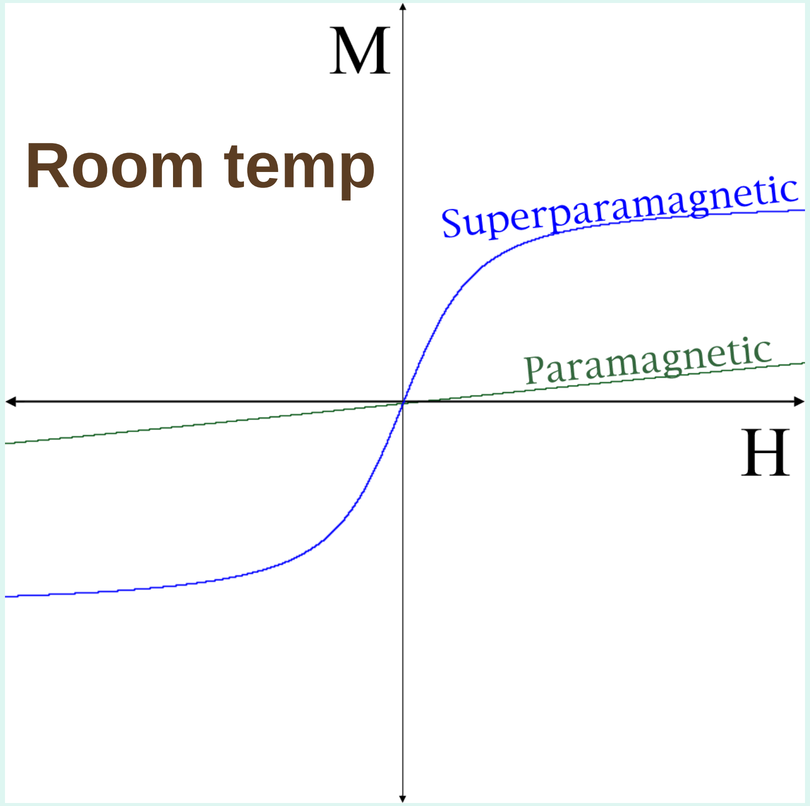

- **Response of superparamagnets to applied field described by Langevin model**
- **Qualitatively similar to paramagnets**
- **At room temperature superparamagnetic materials have a much greater magnetic susceptibility per atom than paramagnetic materials**

Superparamagnetism

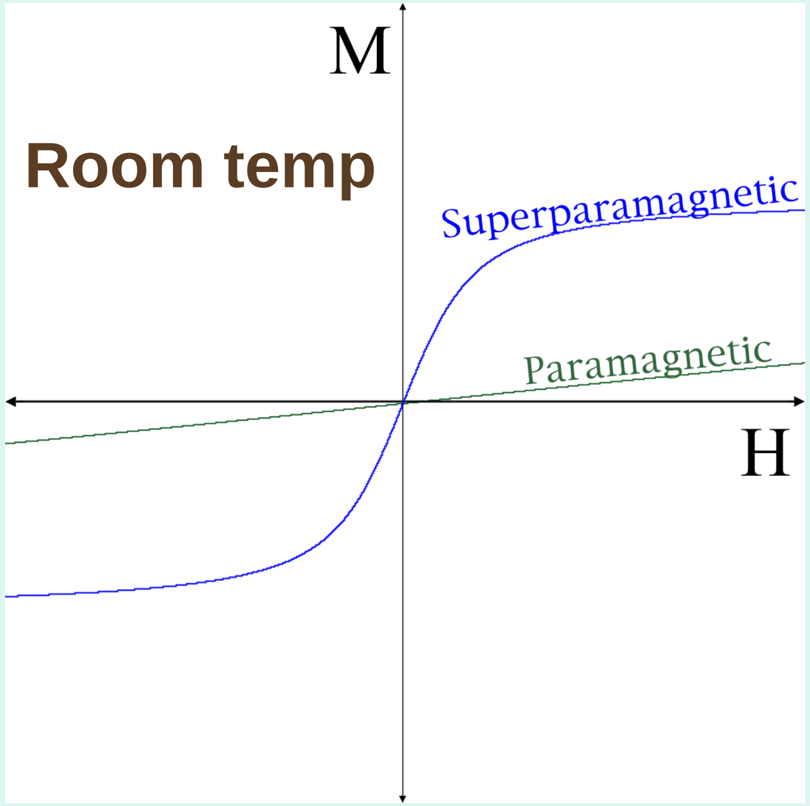

Superparamagnets are often ideal for applications where…

- a high magnetic susceptibility is required
- zero magnetic remanence is required

Ferromagnetic Resonance

FMR is a spectroscopic technique to probe the magnetization of ferromagnetic materials.

Landau-Lifshitz-Gilbert equation:

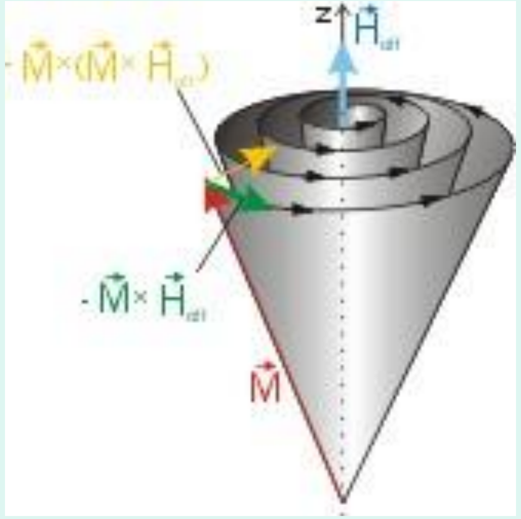

$$\frac{\partial \vec{M}}{\partial t} = -\gamma(\vec{M} \times \vec{H}_{eff}) + \frac{G}{\gamma M_S^2}\left[\vec{M} \times \frac{\partial \vec{M}}{\partial t}\right]$$

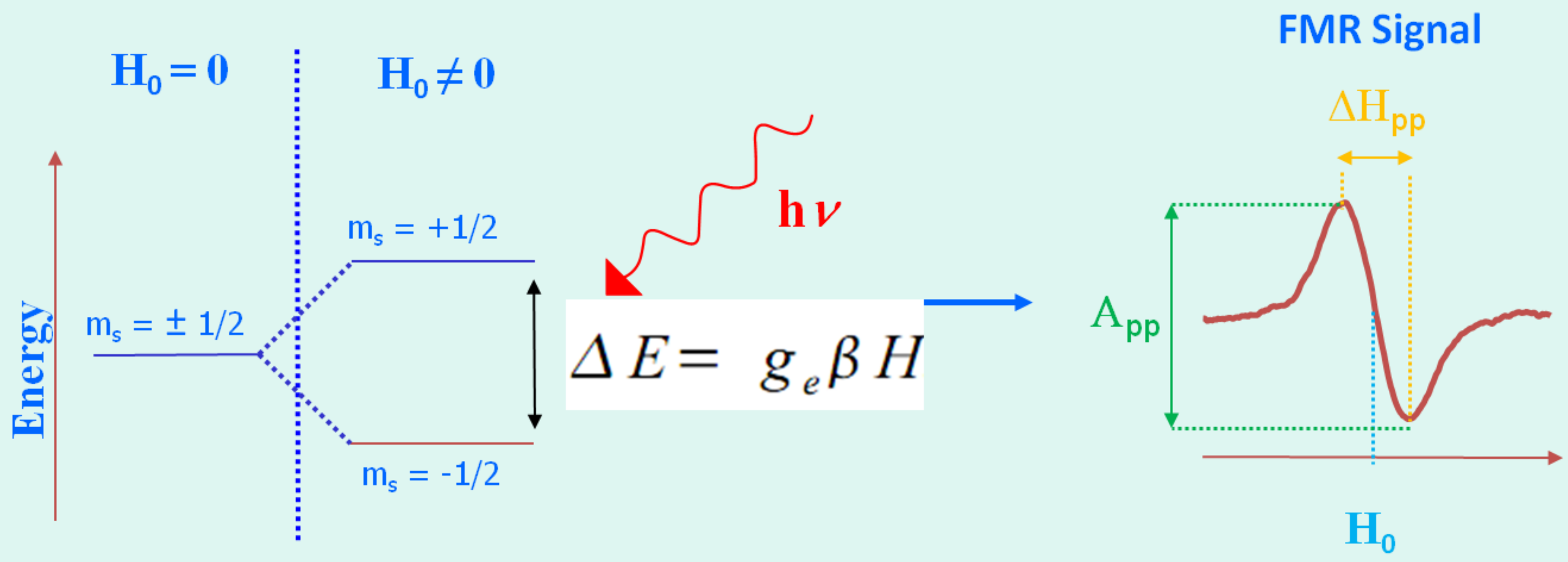

$H_0 = 0$
$H_0 \neq 0$
Energy
$m_s = \pm 1/2$
$m_s = +1/2$
$m_s = -1/2$
$h\nu$
$\Delta E = g_e \beta H$
FMR Signal
ΔH_{pp}
A_{pp}
H_0

FMR: what we calculate?

The following parameters are directly determined from the FMR spectrum:	What are their physical meaning?
• amplitude of the first derivative absorption line A	No immediate meaning (indirectly number of spins)
• resonance field (apparent or true) B_r	Internal magnetic field
• peak-to-peak linewidth (apparent or true) ΔB_{pp}	Dynamics of the spin system
• integrated intensity $I_{int}=A\cdot(\Delta B_{pp})^2$	Magnetic susceptibility at microwave frequency and/or number of spins

Source: Janusz Typek, Institute of Physics, West Pomeranian University of Technology, Szczecin, Poland

JOURNAL OF MAGNETIC RESONANCE, Series A **122,** 100–103 (1996) ARTICLE NO. 0184

Investigation of the Magnetic Anisotropy in Manganese Ferrite Nanoparticles Using Magnetic Resonance

A. F. BAKUZIS,* P. C. MORAIS,* AND F. A. TOURINHO†

The dynamics of the magnetic moment of the particle is described by the Landau–Lifschitz equation, and for uniaxial particles the resonance condition is given by (*16*)

$$\omega_r = \gamma[H_r + 2(K/I_s)(L_2/L_1)P_2(\cos\theta)], \qquad [2]$$

where K is the effective anisotropy, $L_2 = 1 - 3(L_1/\xi)$, and $L_1 = \coth\xi - 1/\xi$ ($\xi = \mu H_r/kT$). The magnetic moment per particle (μ) is related to the saturation magnetization (I_s) by $\mu = I_s V$, where V is the particle volume. It must be pointed out that Eq. [2] is valid over a wide temperature range, including high temperatures, where the fluctuation field is typically of the order of the anisotropy field.

FMR resonance field

$$H_r = (\omega_r/\gamma) - (K/I_s)(3\cos^2\theta - 1).$$

Experimental Results

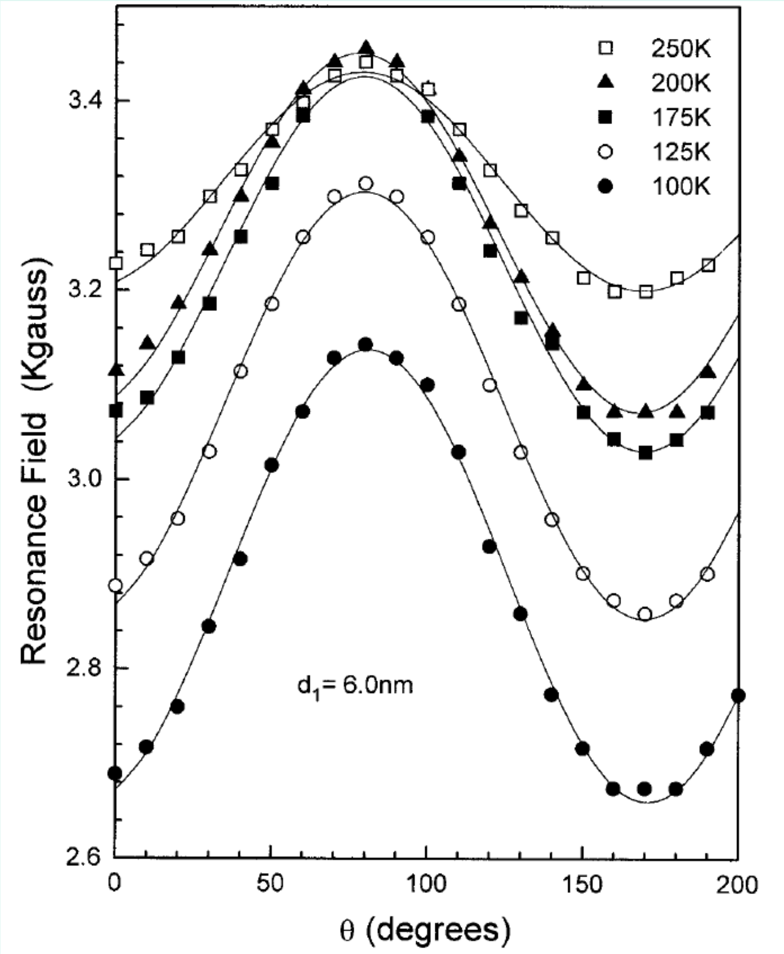

Angular dependence of the resonance field for a magnetic fluid sample of MnFe2O4 with particles having an average diameter of 6.0 nm. The solid lines represent the best fit of the experimental data according to Eq. [4].

Magnetization Curve

ifmpan.poznan.pl/~urbaniak/Wyklady2014/urbaniakUAM2014L2_magnetic%20measurements.pdf

M. Urbaniak Magnetic materials in nanoelectronics... IFM PAN Poznań 2014

Introduction

Measurement of magnetic field strength

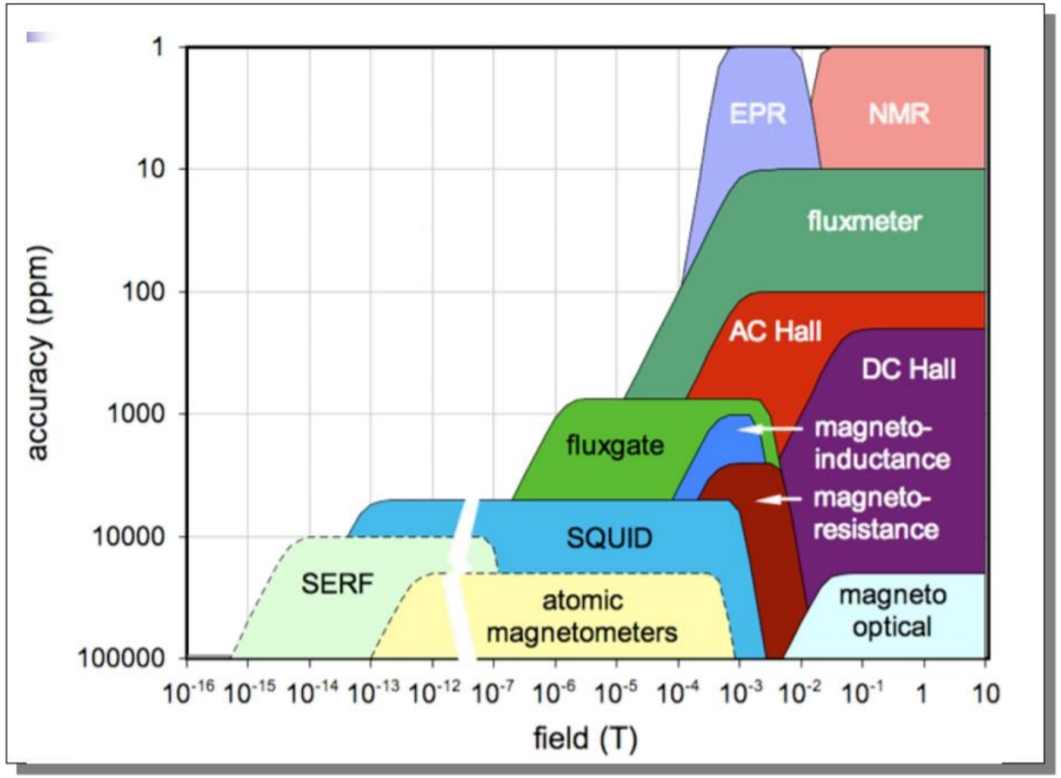

methods most relevant in spintronic measurements:
AC and DC Hall probes

The sensitivity range of the probe should cover whole range of fields in which magnetic configuration significantly changes

graphics from *Field Measurement Methods* lecture delivered during The Cern Accelerator School; Novotel Brugge Centrum, Bruges, Belgium, 16 - 25 June, 2009; author: Luca Bottura

Introduction

- Magnetic sensor can be divided according to different criteria:

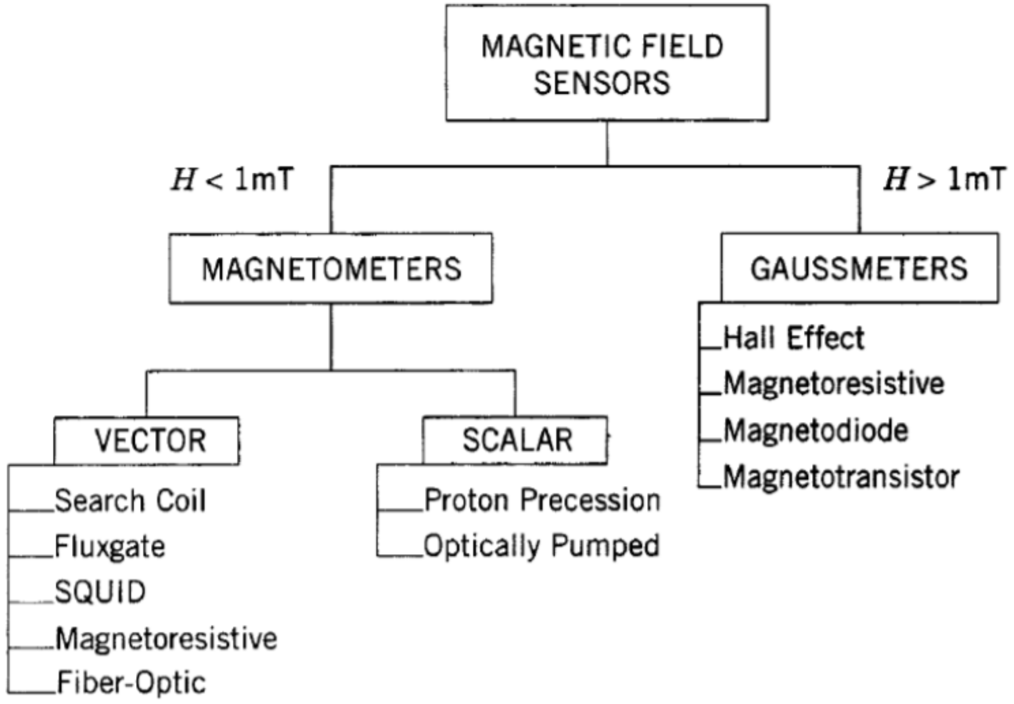

FIGURE 48.1 Magnetic field sensors are divided into two categories based on their field strengths and measurement range: magnetometers measure low fields and gaussmeters measure high fields.

- Distinction magnetometer-gaussmeter is rather arbitrary and not commonly used.

graphics from [7]: S.A. Macintyre, Magnetic Field Measurement

Introduction – Hall magnetometer

- Lorentz force acting on electrons in a circuit deflects them perpendicularly to drift direction:

$$\vec{F}_{Lorentz} = q\vec{E} + q\vec{v}\times\vec{B}$$

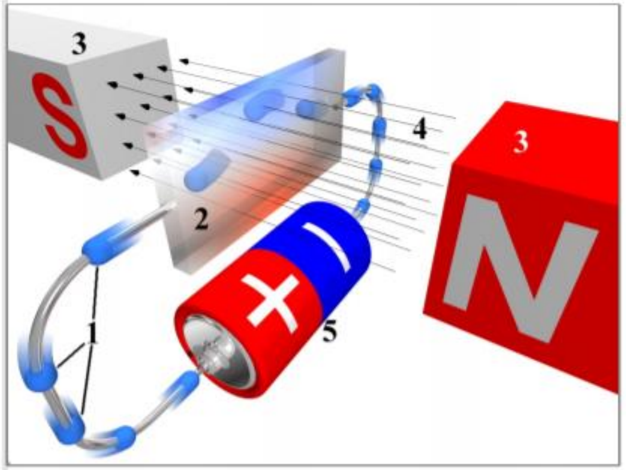

image from Wikimedia Commons; authors: Peo (modification by Church of emacs)

The new HFC probe is able to measure intense fields in tiny gaps.

image from http://metrolab.com/

Hall sensors are relatively easy to miniaturize

- The build-up of charges on outer limits of the circuit induces Hall voltage which depends on the field strength and is used to sense it.
- The Hall voltage is given by (t-film thickness, R_H- Hall coefficient*):

$$U_y = R_H \frac{I}{t} B_z$$

- The main figure of interest is field sensitivity of the sensor** (for a given driving current I_c):

$$\boxed{\gamma_b = \frac{U_y}{B_z} = \frac{R_H I_c}{t}}$$

- Semiconductors are used to obtain high sensitivity combined with temperature stability (InAs)
- The Hall sensors have a limited use at high fields and low temperatures (conductivity quantization)

*for InAs R_H is about 0.0001 m^3/As

**some tenths of mV per kA/m for I_c of several mA (www.lakeshore.com/products/Hall-Magnetic-Sensors/pages/Specifications.aspx)

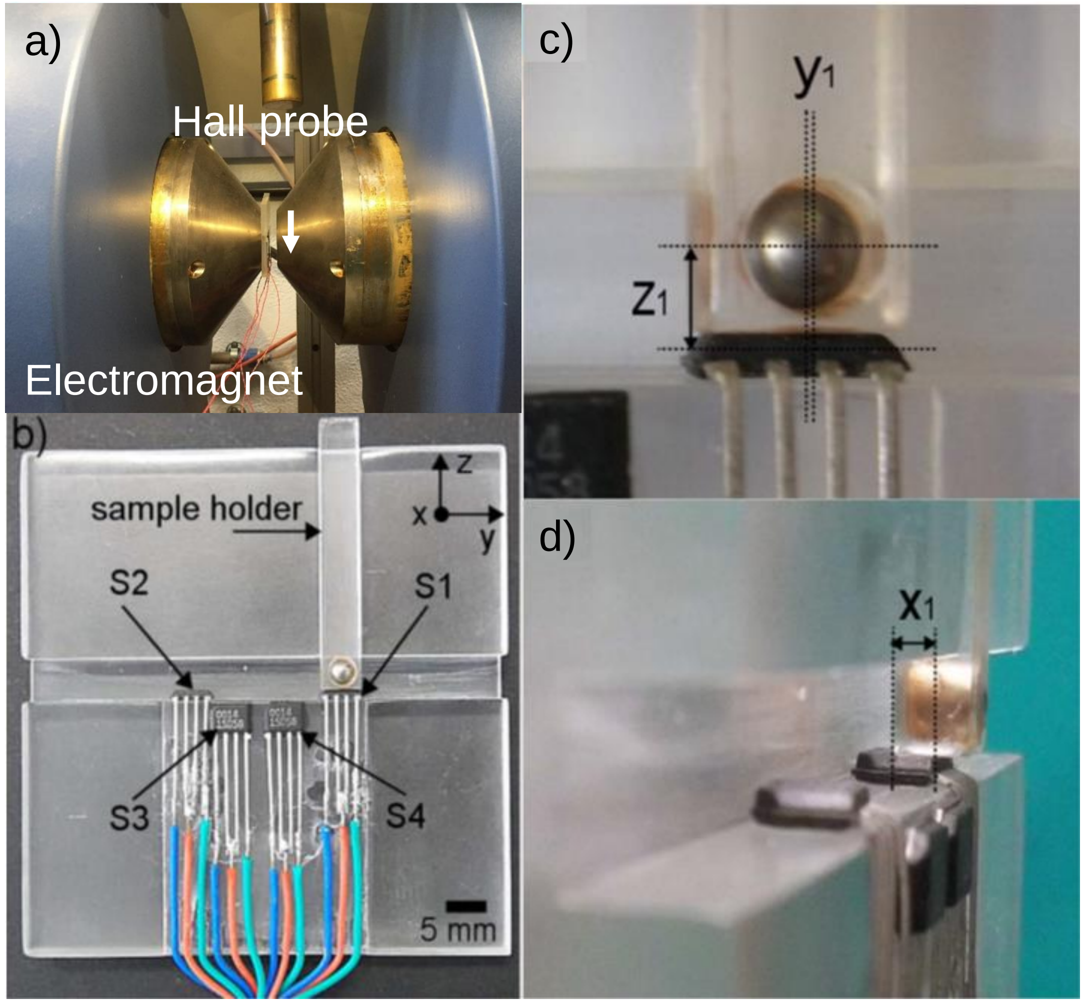

Jefferson F. D. F. Araujo, et al. ***J. Magn. Magn. Mater***. 426, 159-162 **(2017)**.

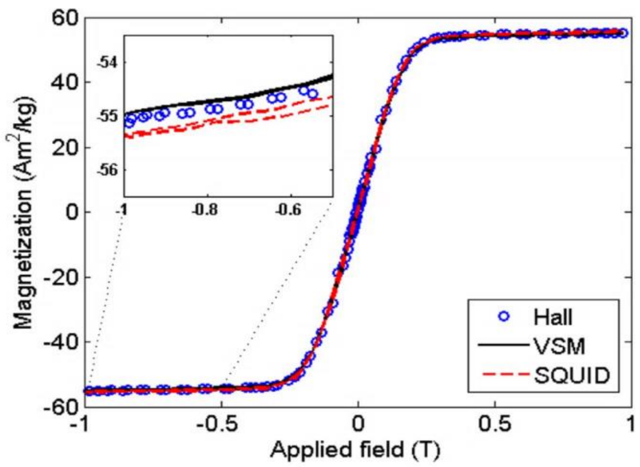

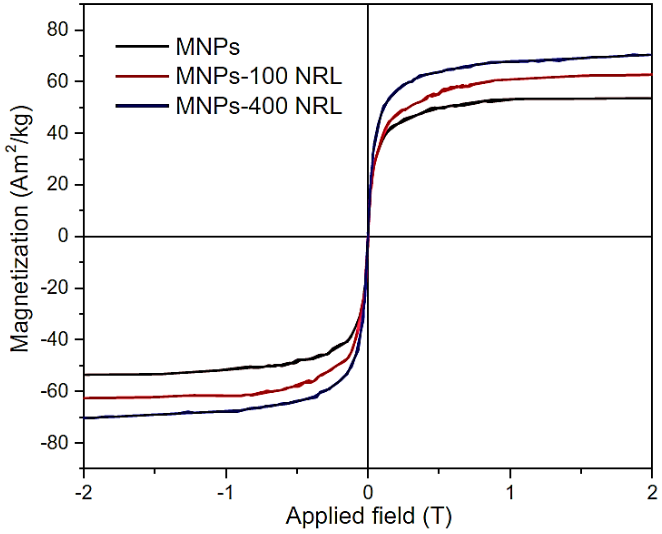

Soudabeh Arsalani, et al. ***J. Magn. Magn. Mater***. 475, 458-464 **(2019)**.

- Sensibilidade **3.5×10^{-7} Am^2**
- Massa da Amostra **15 mg**
- $B_{máx}$ **3.0 T**

- Modelo Teórico

$$B_z(x,y,z) = \frac{\mu_0 I}{4\pi}\int_0^{2\pi}\frac{xasen\varphi}{r'^3}d\varphi$$

$$B_z(x,y,z) = \frac{\mu_0 m}{4\pi}[\int_{-L/2}^{L/2}\int_0^{2\pi}\frac{xasen\varphi}{r'^3}d\varphi dx]/\pi a^2$$

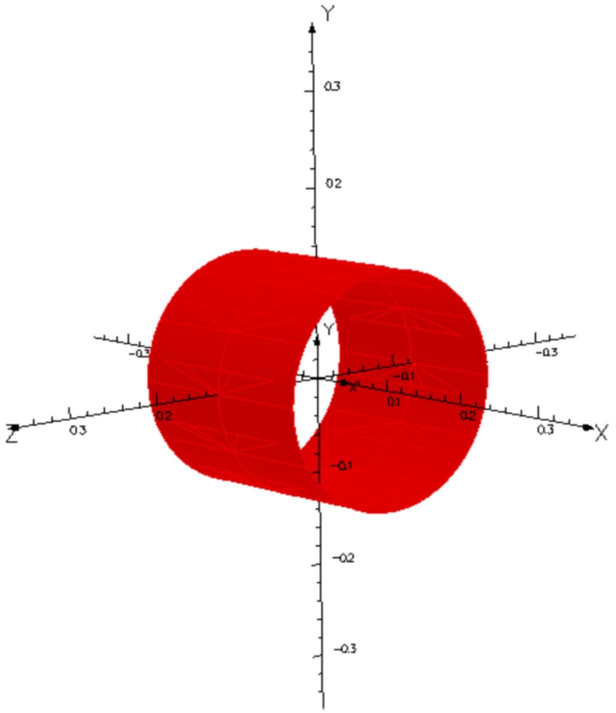

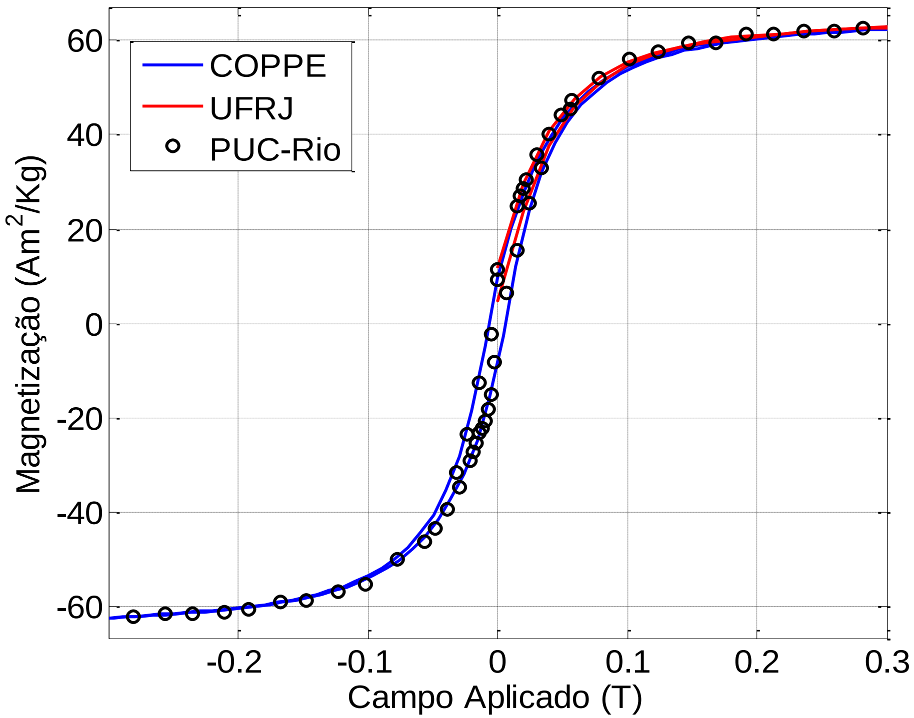

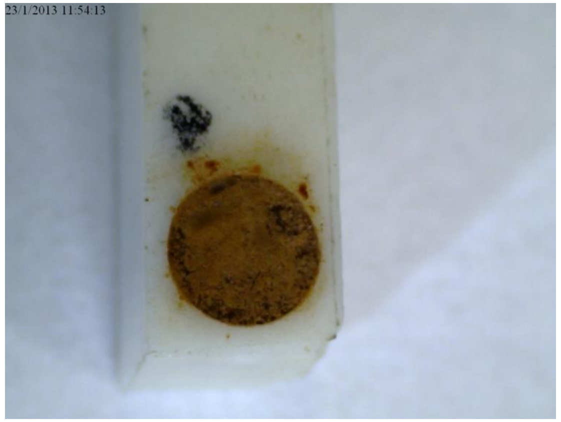

Jefferson F. D. F. Araujo, et al. ***J. Magn. Magn. Mater***. 426, 159-162 **(2017)**.

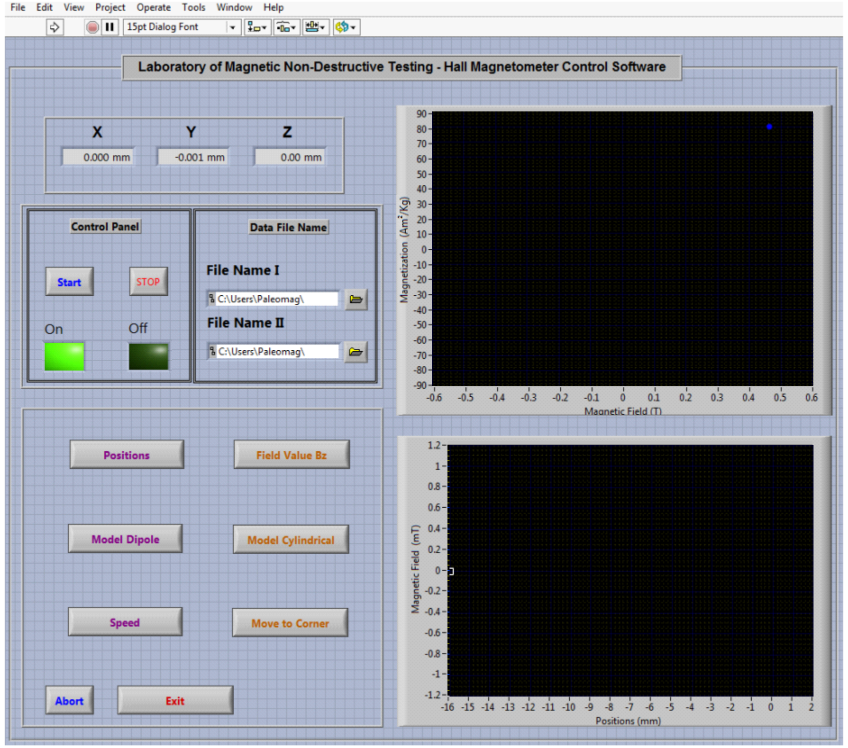
File Edit View Project Operate Tools Window Help
15pt Dialog Font
Laboratory of Magnetic Non-Destructive Testing - Hall Magnetometer Control Software
X
Y
Z
0.000 mm
-0.001 mm
0.00 mm
Control Panel
Start
STOP
On
Off
Data File Name
File Name I
C:\Users\Paleomag\
File Name II
C:\Users\Paleomag\
Positions
Field Value Bz
Model Dipole
Model Cylindrical
Speed
Move to Corner
Abort
Exit
Magnetization (Am²/Kg)
Magnetic Field (T)
Magnetic Field (mT)
Positions (mm)

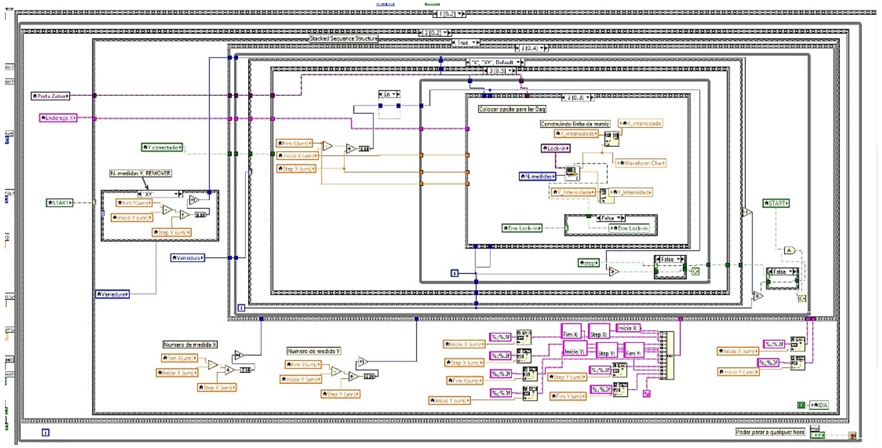

❖ Magnetômetro Baixa Temperatura

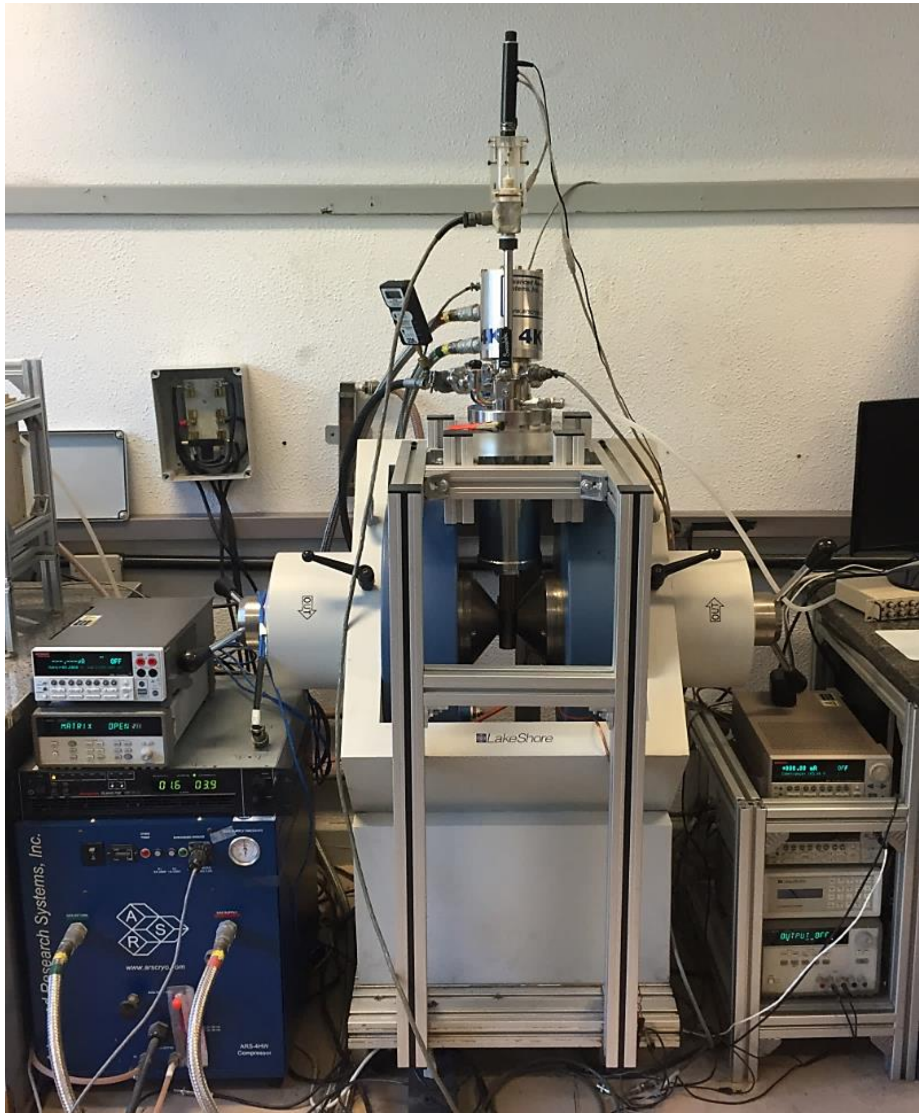

Jefferson F. D. F. Araujo, A. C. Bruno, and S. R. W. Louro, ***Review of Scientific Instruments*** 86, 105103 **(2015)**.

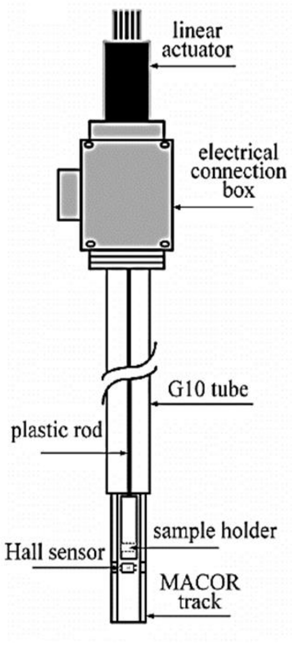

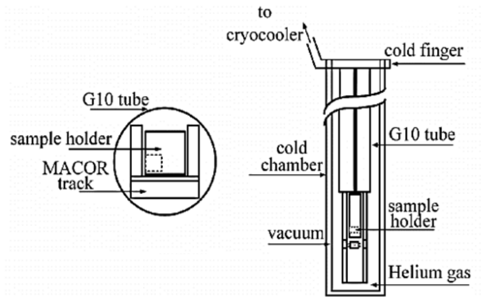

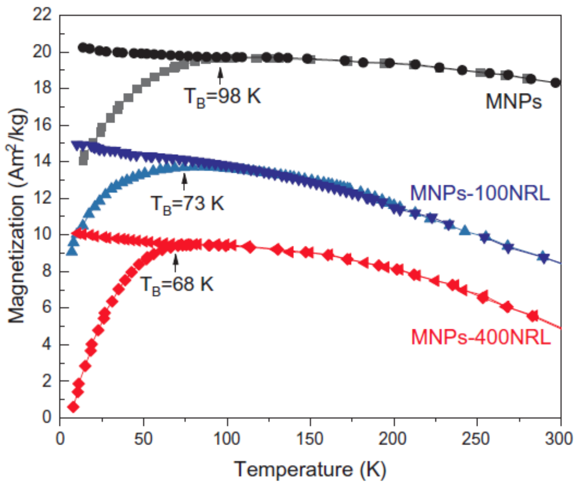

Soudabeh Arsalani, et al. ***J. Magn. Magn. Mater***. 475, 458-464 **(2019)**.

- Sensibilidade: **$8.5\mathrm{x}10^{-8}$ Am²**
- Massa da Amostra: **15 mg**
- $B_{máx}$: **1.0 T**
- T_{mim}: **6.0 K**

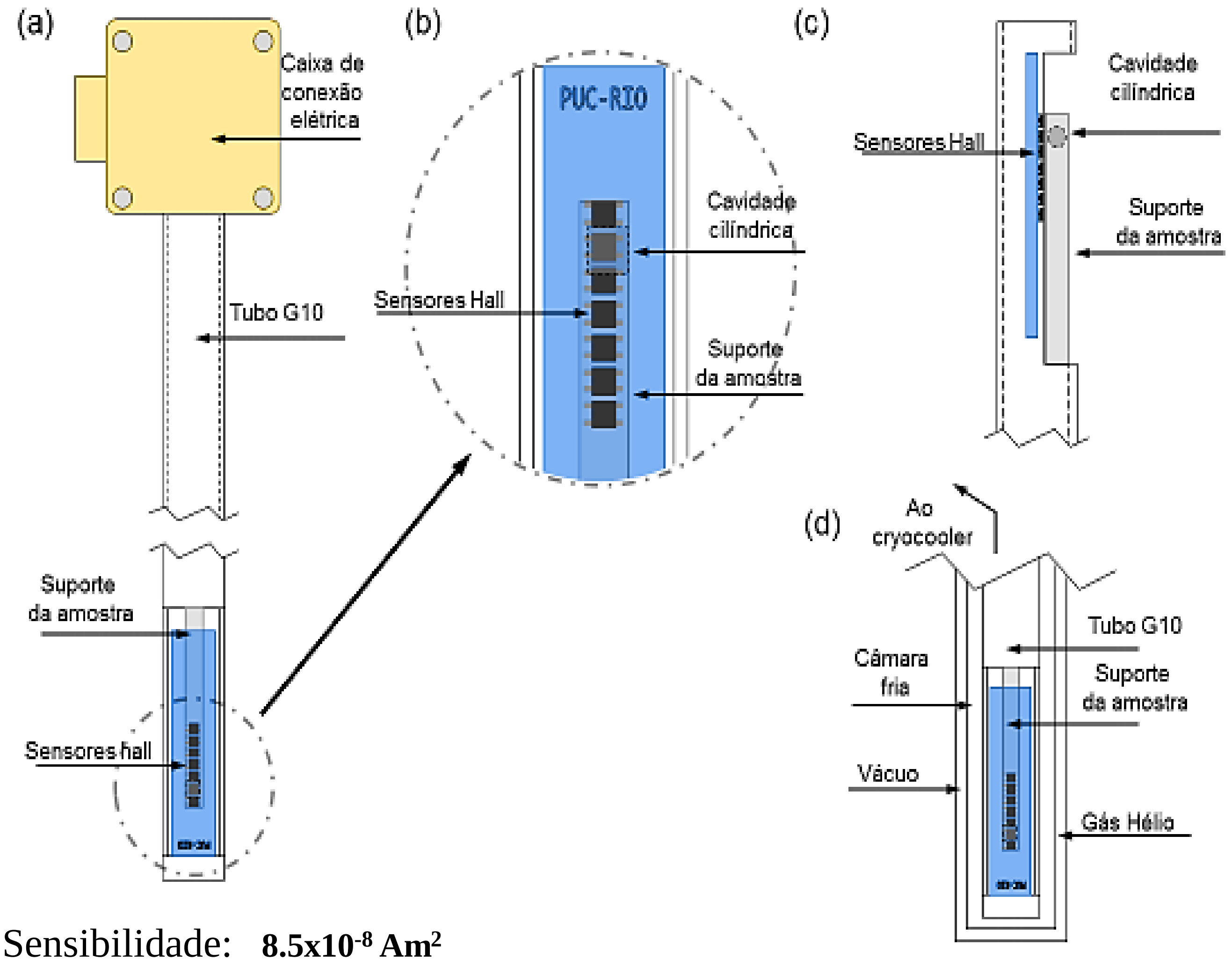

- Sensibilidade: **8.5x10^{-8} Am^{2}**
- Massa da Amostra: **10 - 200 mg**

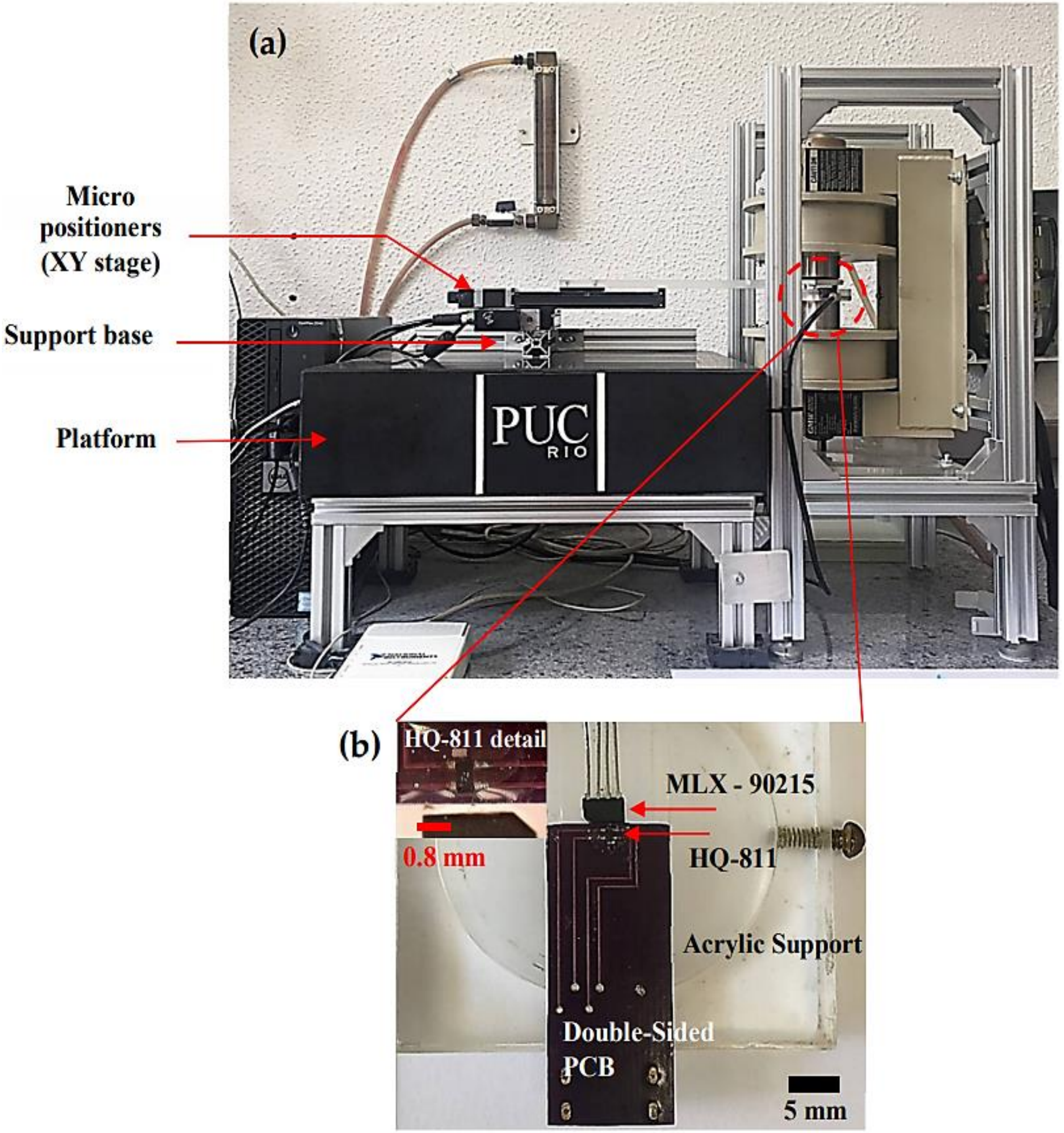

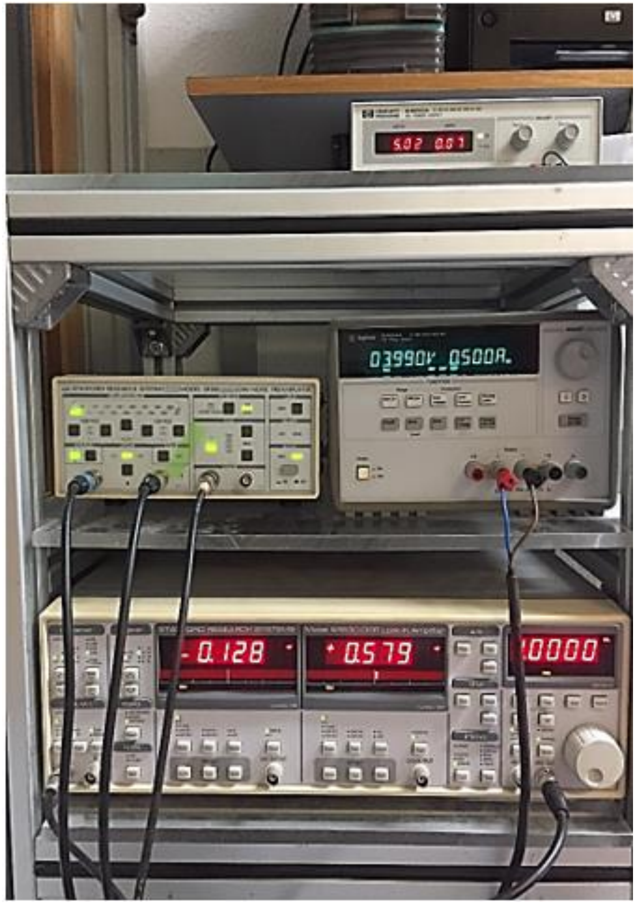

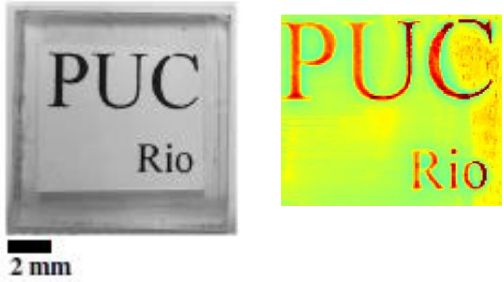

Desenvolvido de forma pioneira

Jefferson F. D. F. Araujo, et al. ***J. Magn. Magn. Mater***. 499, 166300-9 **(2020)**.

Gan.: 2 mV/mT @ 3 mA

BW: 100 kHz

Ruído: 300 nT/√Hz

Sens.: 2,5 x 10^{-11} Am^2

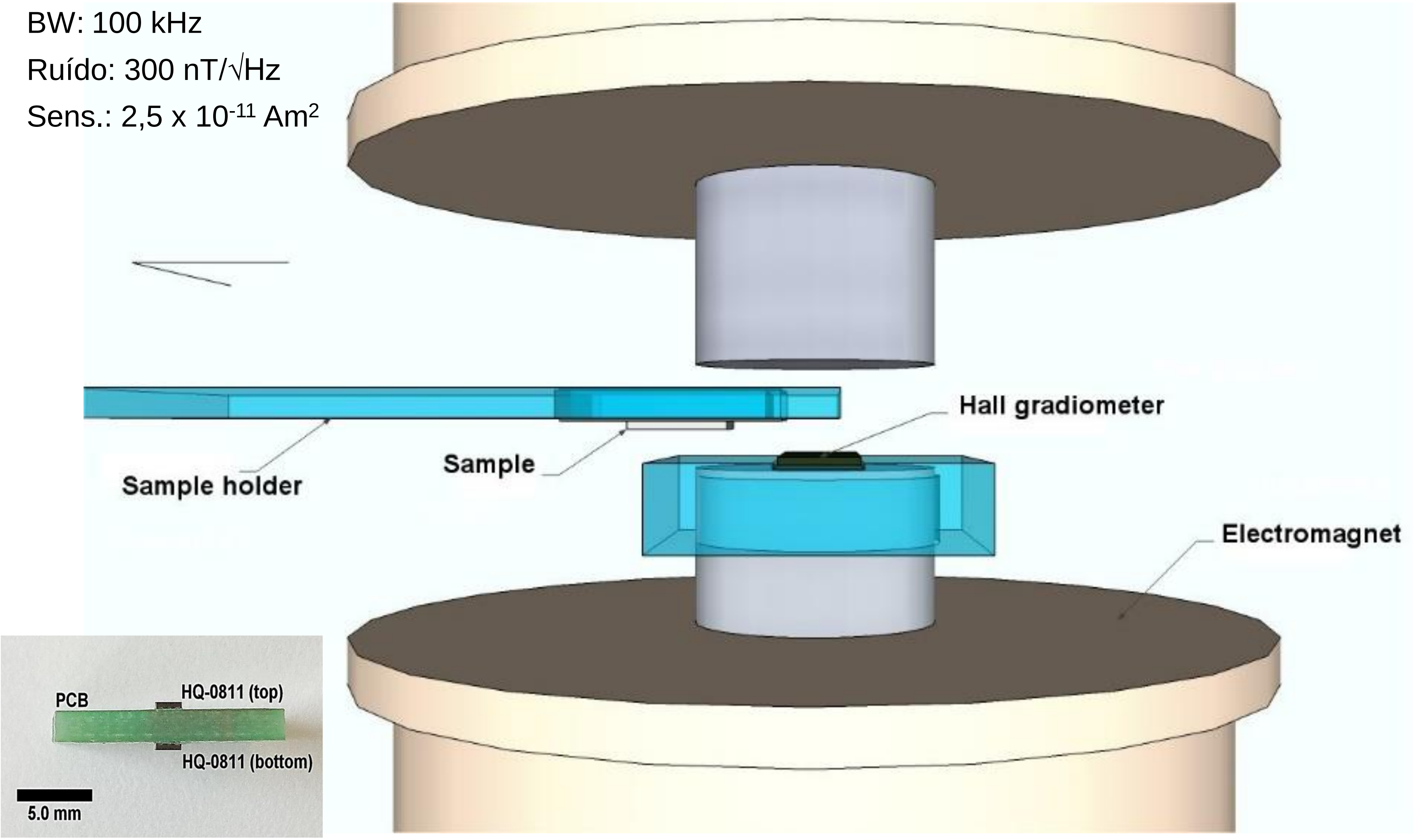

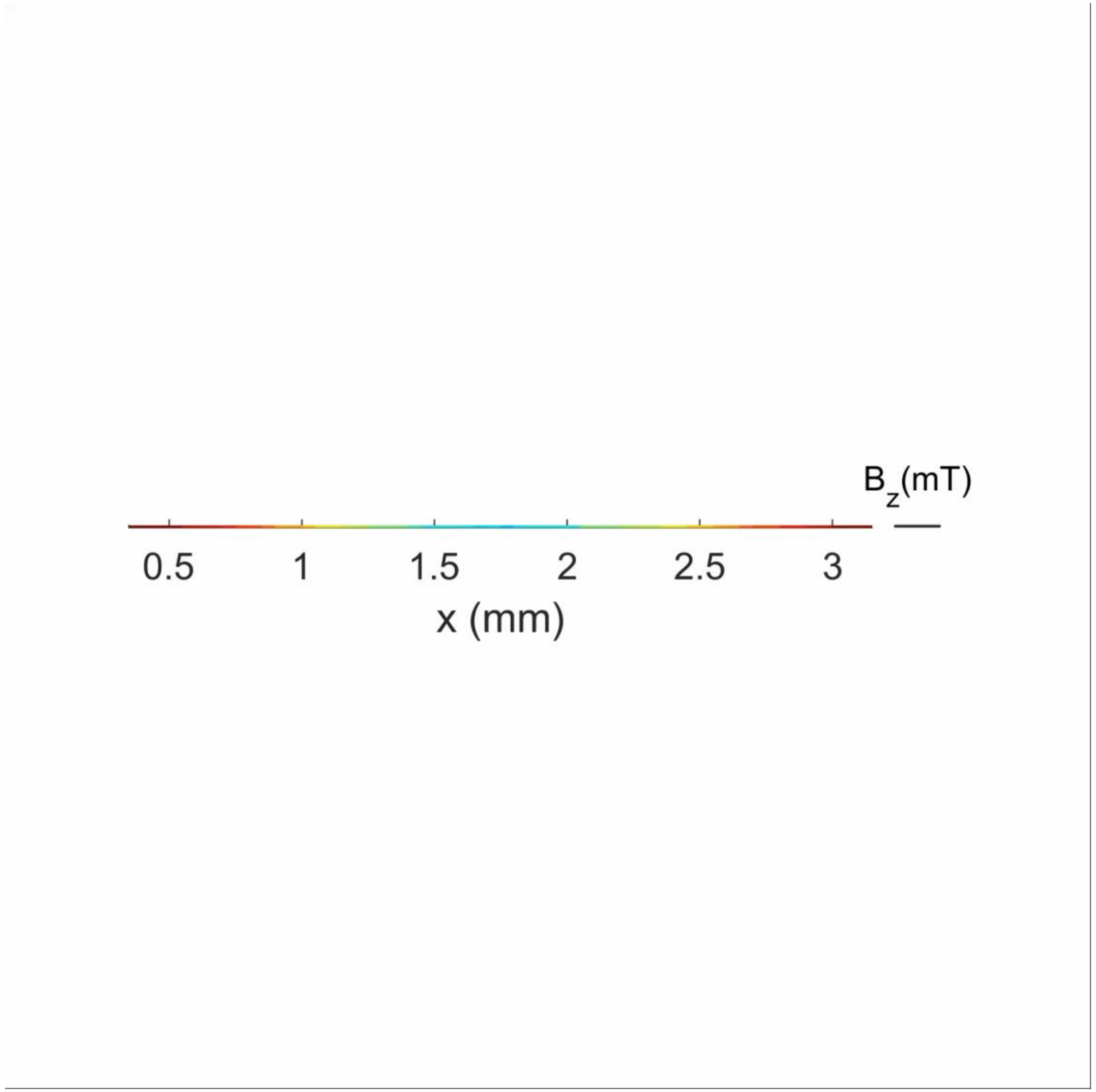

B_z(mT)
0.5
1
1.5
2
2.5
3
x (mm)

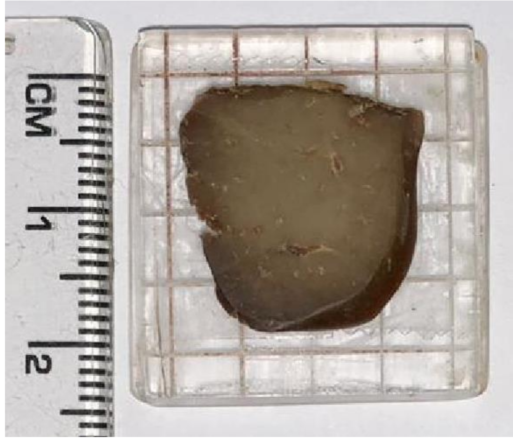

Colaboração: USP - UNESP
Prof. Oswaldo Baffa
Prof. José Ricardo de Arruda

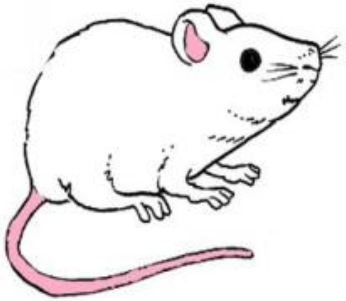

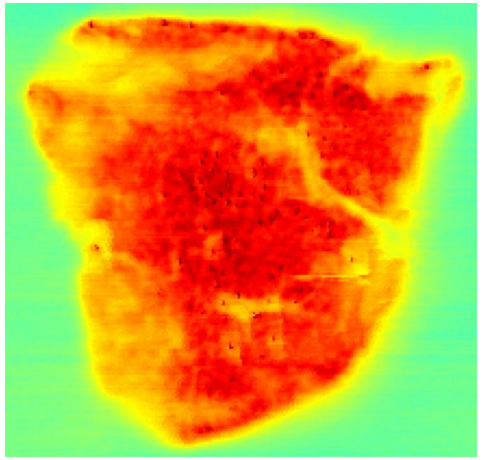

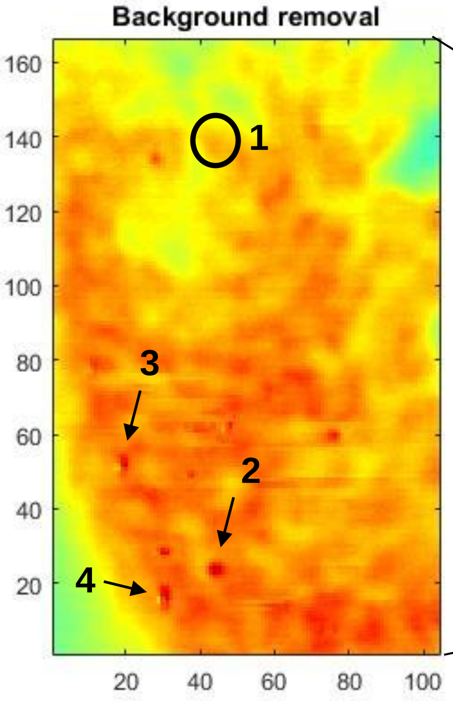

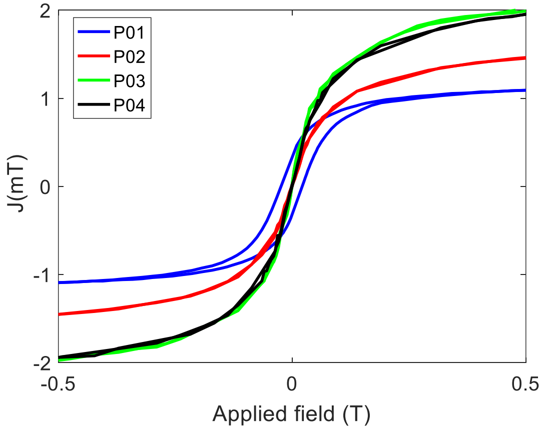

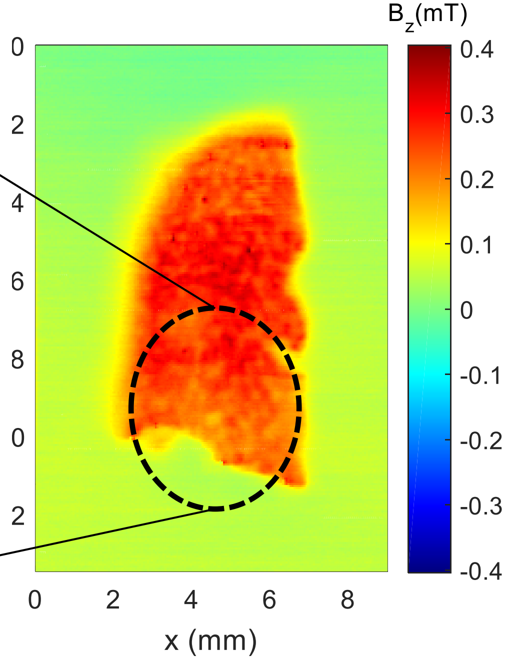

Magnetic Separation

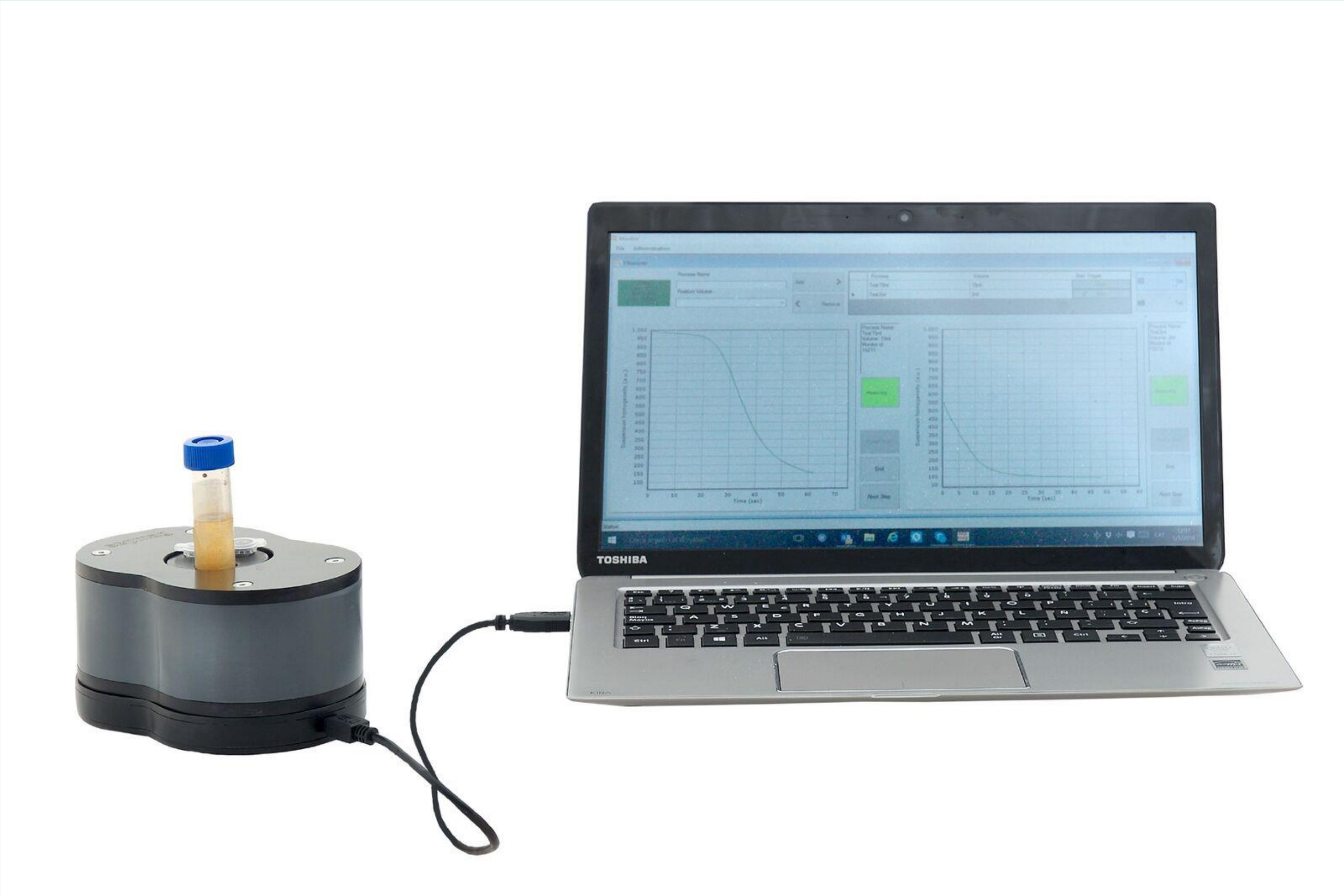

Magnetic separation setup (magnetophoresis device)

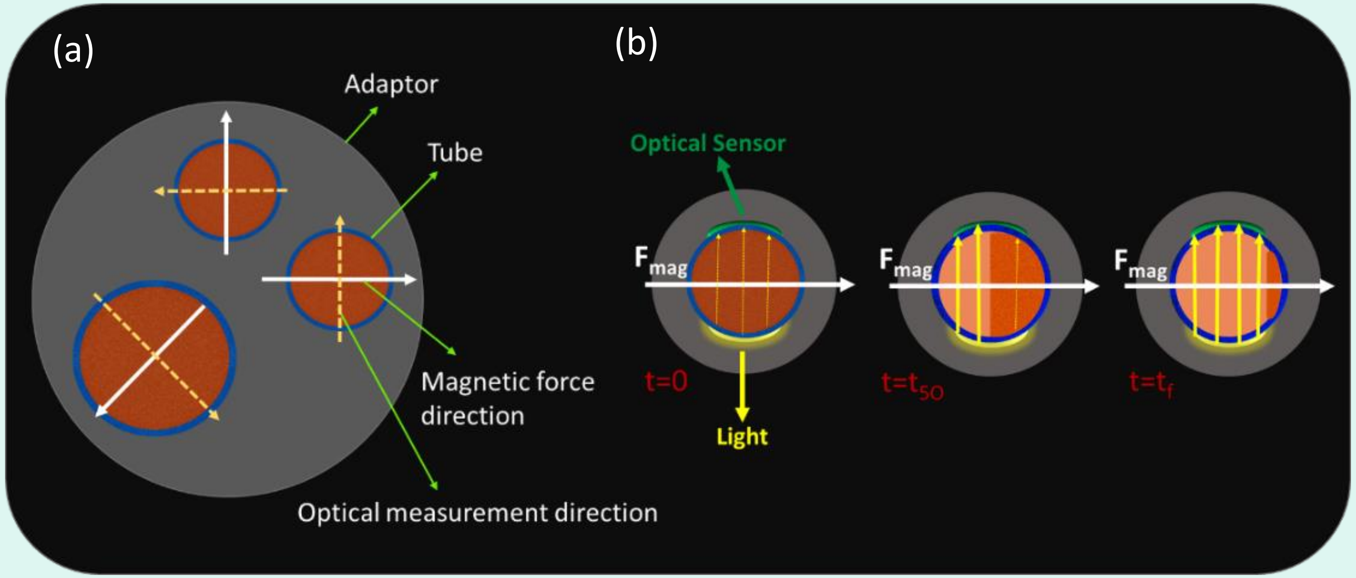

F_d= $6\pi r\eta v$

F_m=m$\mu_0 \frac{\partial H}{\partial r}$

Schematic setup of magnetophoresis device (top view) contains three cylindrical cavities, two of them for 2 mL volume tubes and one for 15 mL tube. (b) The MS process for one tube is illustrated.

Magnetophoresis curve and DLS

Characteristics of the EM10 sample before MS and during 3 h of MS by DLS.

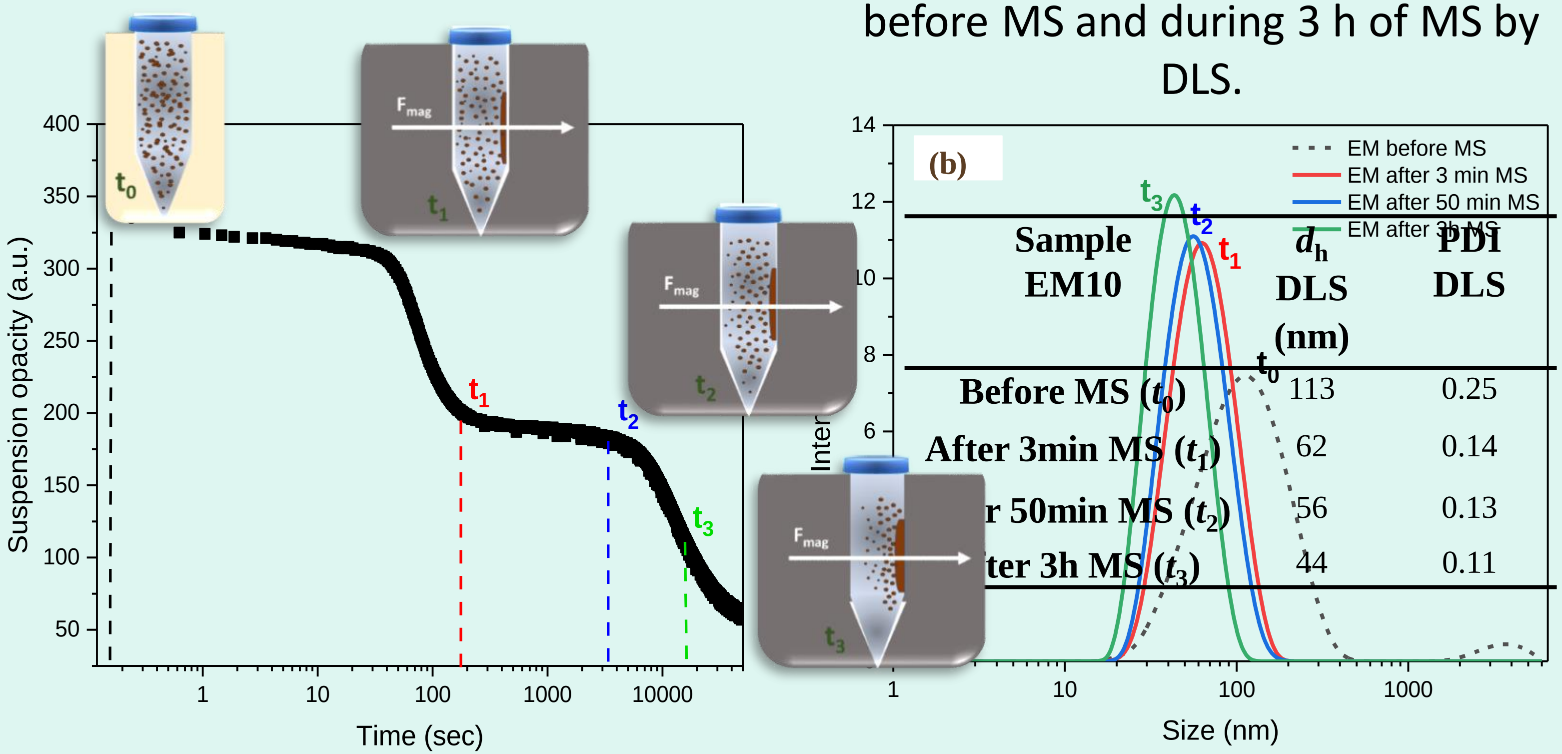

Sample EM10	d_h DLS (nm)	PDI DLS
Before MS (t_0)	113	0.25
After 3min MS (t_1)	62	0.14
r 50min MS (t_2)	56	0.13
ter 3h MS (t_3)	44	0.11

(a) The magnetophoresis curve of EM10 over a 14 h time period, and (b) DLS of EM10 sample at t_0 before separation, t_1 after 3 min, t_2 after 50 min, and t_3 after 3h of inserting sample in separation system.

Magnetic Particle Spectrometer

Single driving field-based MPS

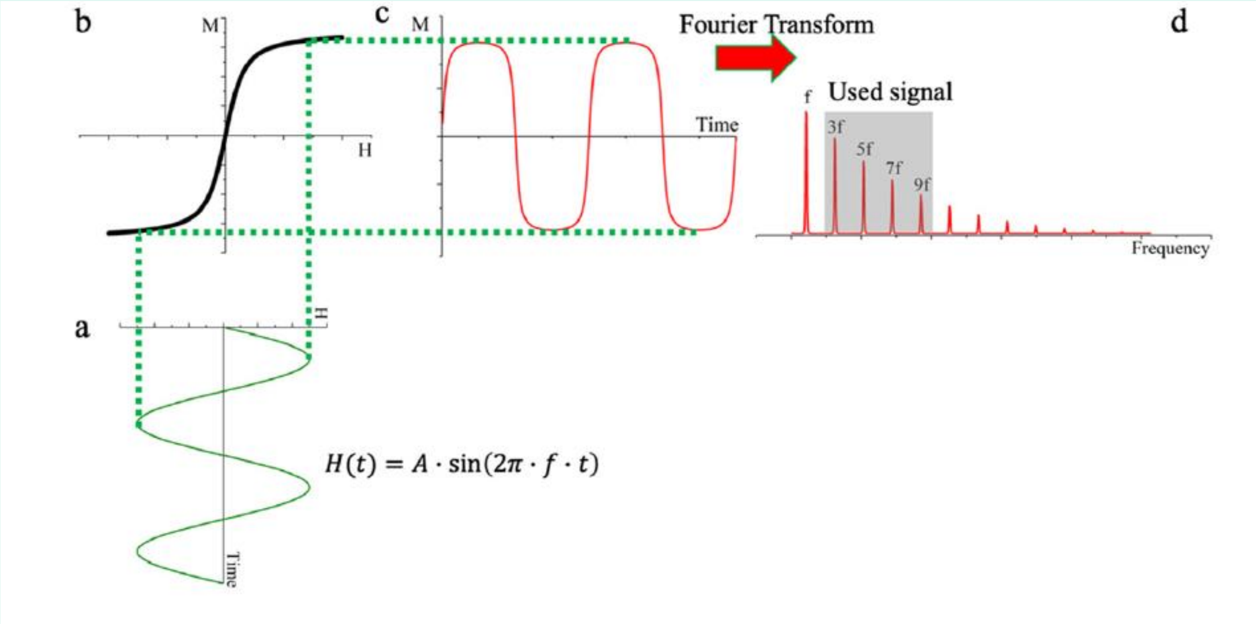

(a) Time varying sinusoidal magnetic field; (b) MH response curve of SPIONs; (c) time domain magnetization response of SPIONs; (d) power spectrum of collected signal contains higher harmonic components 3*f* (third harmonic), 5*f* (fifth harmonic), etc

Picture from: J. Phys. D: Appl. Phys. 52 (2019) 173001 (17pp)

Magnetization Coil Electrical and Geometrical Specifications

R_1= 35 mm

R_2= 41.5 mm

R_3= 52 mm

l=160mm

N= 1.360 turns

L=20.6 mH

R=8.7Ω

C= 12.3nF

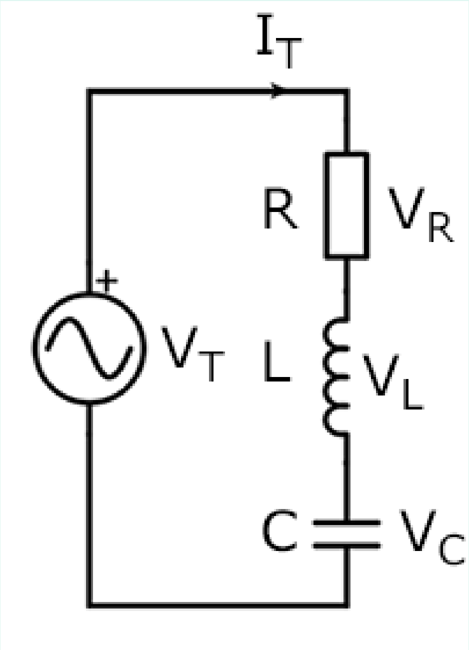

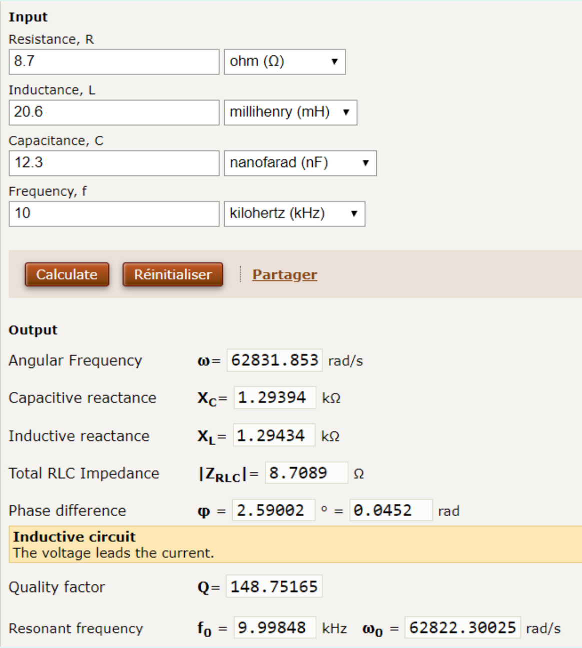

https://www.translatorscafe.com/unit-converter/fr/calculator/series-rlc-impedance/

Magnetic Characteristics

$$\oint_C \mathbf{B} \cdot d\mathbf{l} = \mu_0 I$$

$$\mu_0 = 4\pi \times 10^{-7} \frac{\mathrm{N}}{\mathrm{A}^2}$$

N= 1360 turns

L= 160 mm

B= 10.7 mT/A

Experimental Checks

Search coil positioned at the center of the magnetization coil

N= 10 turns

R= 5 mm

$V_{mag\text{-}coil}$ = 74Vpp

$V_{search\text{-}coil}$ = 81 mVpp

B_{exp}= 0.60 mT/A

Excitation, detection & monitoring coils

Detection coils, 1st order gradiometer

Monitoring coil (center)

Excitation coil- solenoid with two layers of winding.

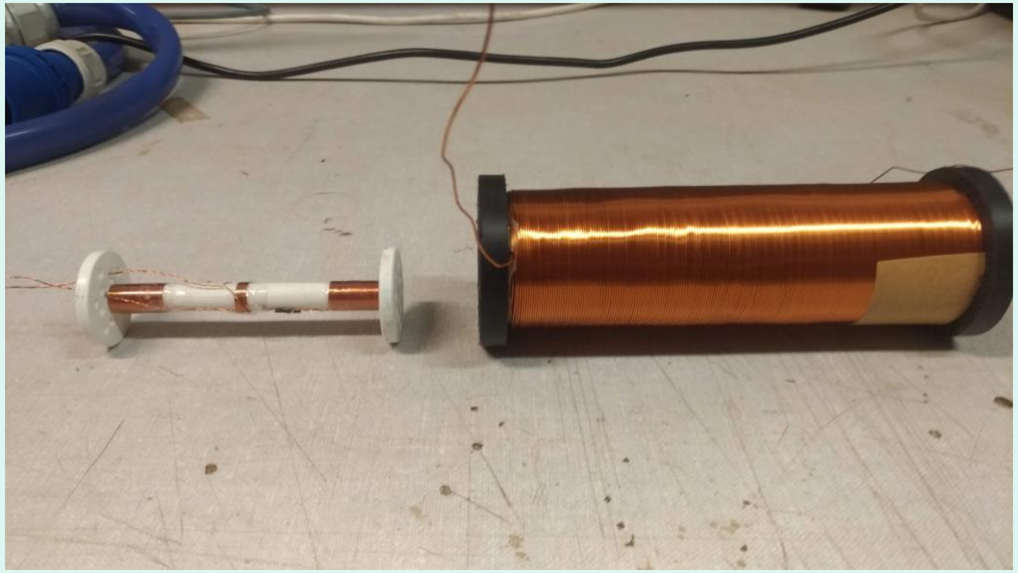

Resonance of Driving Coil

- **The RLC circuit is usually driven at the resonance frequency to optimize power transfer from the power amplifier**

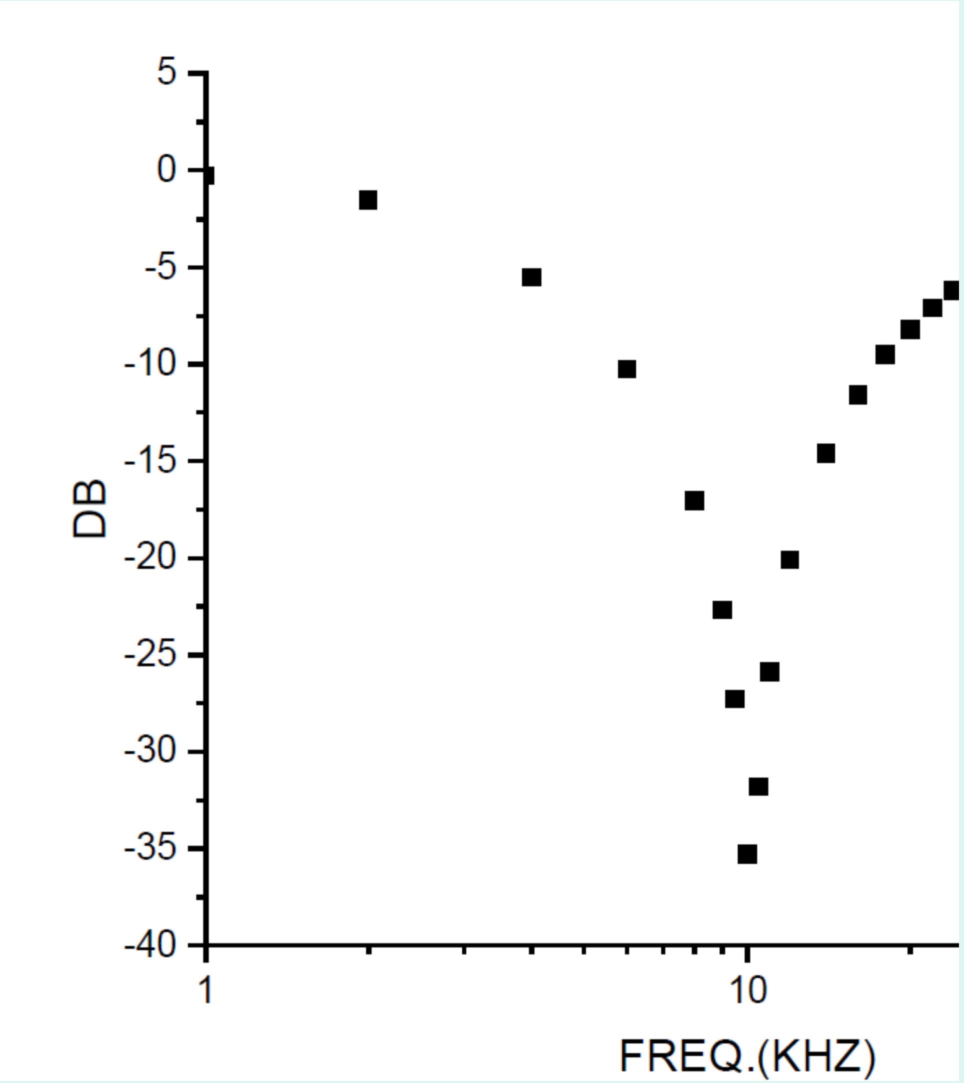

Power Amplifier

A power amplifier with low level of distortion must be employed in the excitation circuit.

Dual driving field-based MPS

(e) dual sinusoidal magnetic fields; (f) MH response curve of SPIONs; (g) time domain magnetization response of SPIONs; (h) power spectrum of collected signal contains higher harmonic components *fH* ± 2*fL* (third harmonics), *fH* ± 4*fL* (fifth harmonics).

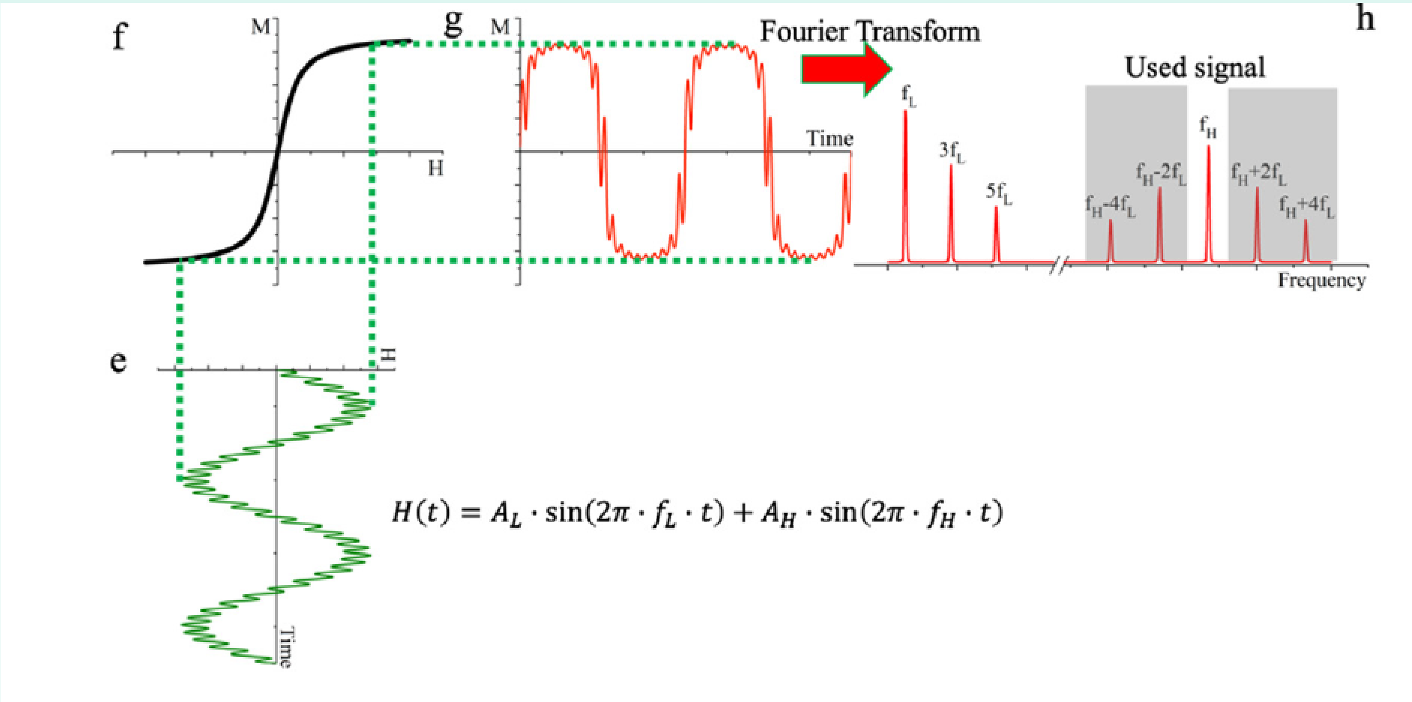

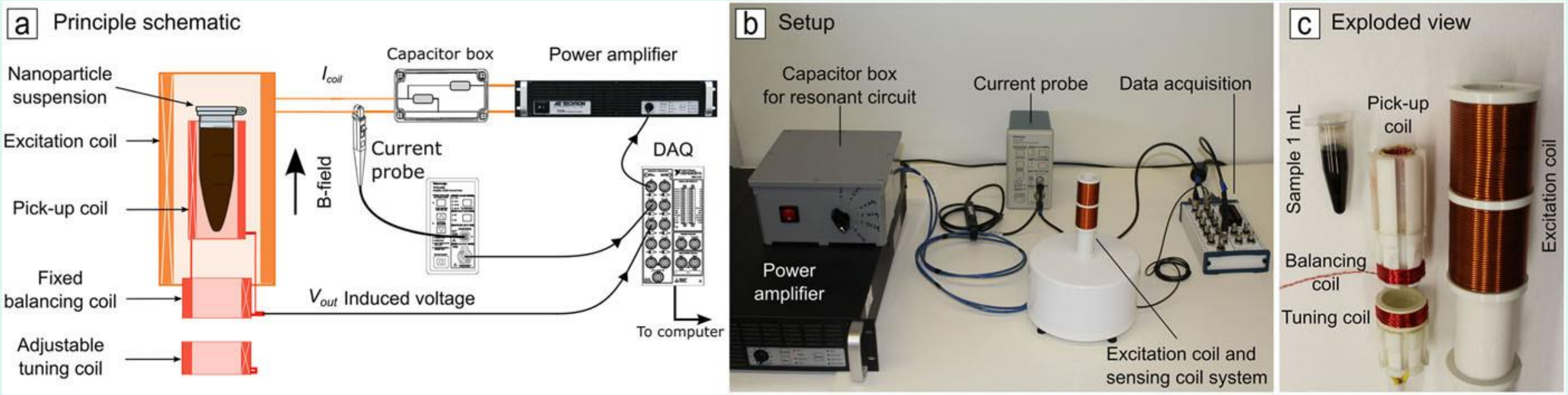

FIG. 1. The nanoparticle suspension is driven by a time-varying magnetic field provided by the excitation field. The sample magnetization change induces a voltage in a pick-up coil system which is recorded by a DAQ.

Published in: Nicolas Garraud; Rohan Dhavalikar; Lorena Maldonado-Camargo; David P. Arnold; Carlos Rinaldi; *AIP Advances* 7, 056730 (2017) DOI: 10.1063/1.4978003

Paramagnetic gas

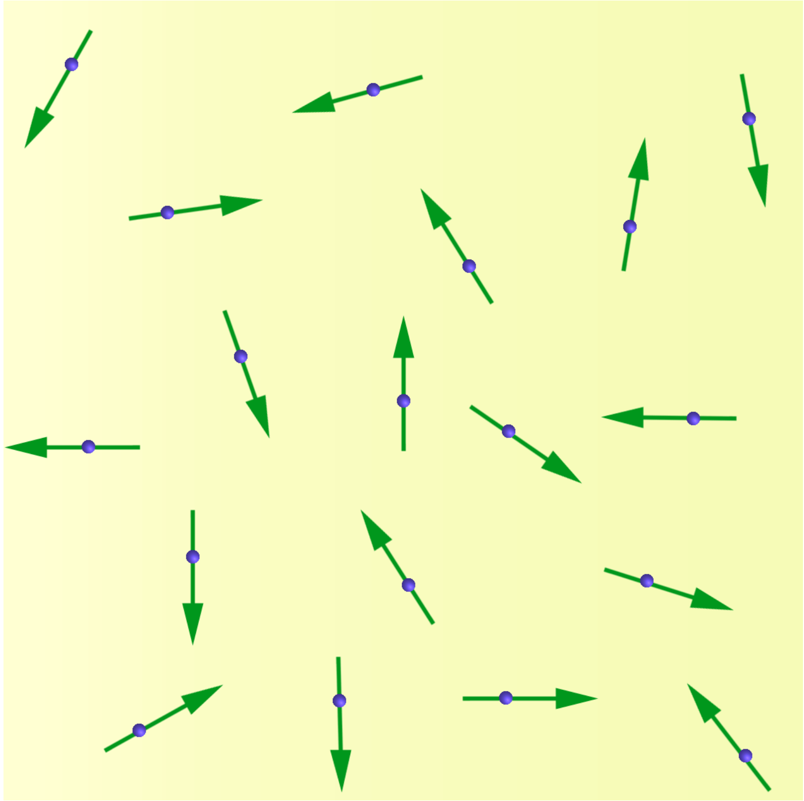

- Imagine a classical gas of molecules each with a magnetic dipole moment
- In zero field the gas would have zero magnetization

Paramagnetic gas

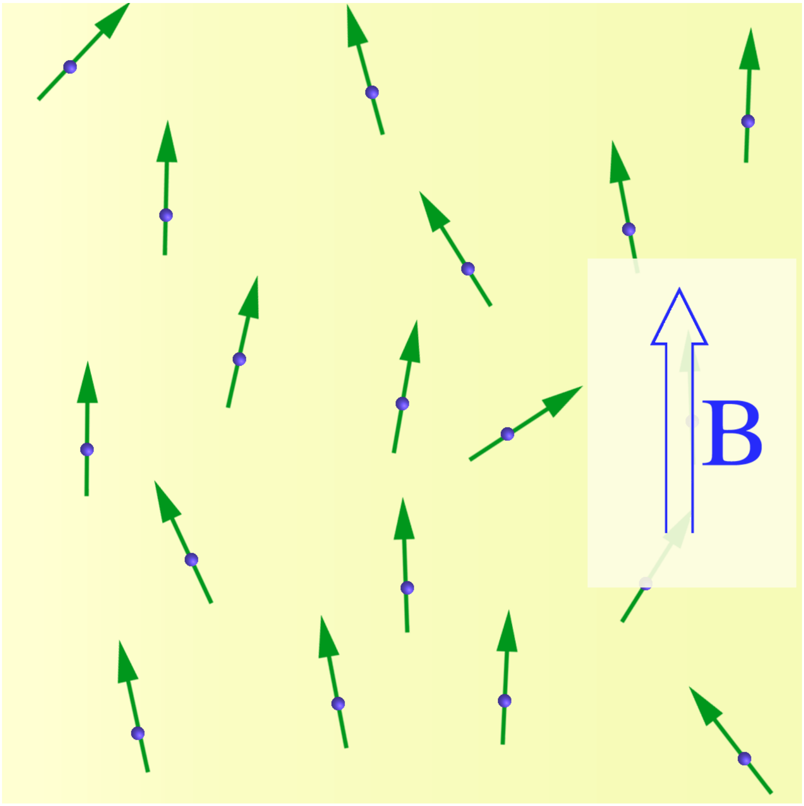

- Applying a magnetic field would tend to orient the dipole moments
- Gas attains a magnetization

Paramagnetic gas

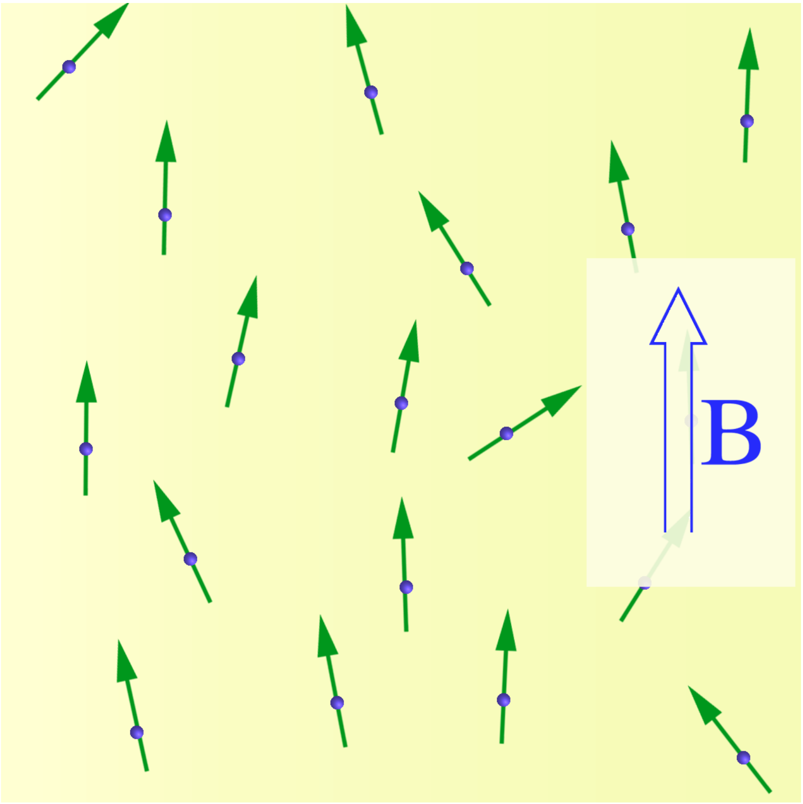

- **Very high fields would saturate magnetization**
- **Heating the gas would tend to disorder the moments and hence decrease magnetization**

Paramagnetic gas

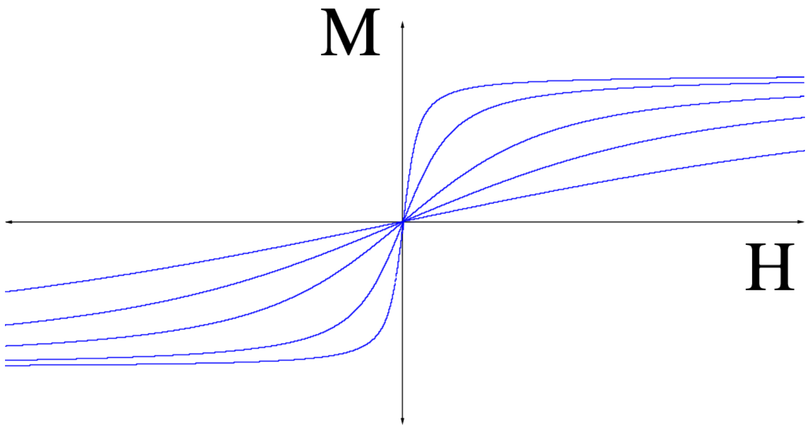

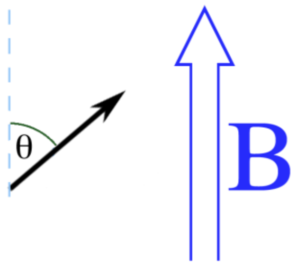

$E = -m\,B\cos[\theta]$

- Theoretical model
- Non-interacting moments
- Boltzmann statistics
- Dipole interaction with B
- Yields good model for many materials
- Examples: ferrous sulfate crystals, ionic solutions of magnetic atoms

Paramagnetic gas

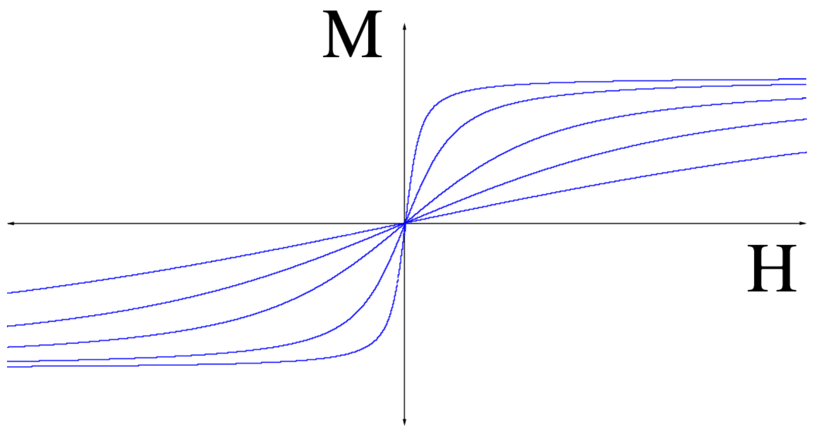

- **Classical model yields Langevin function**

- **Quantum model yields Brillouin function**

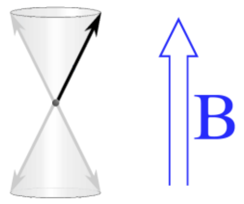

Exchange Interaction

- Direct exchange

Direct exchange operates between moments, which are close enough to have sufficient overlap of their wavefunctions. It gives a strong but short-range coupling which decreases rapidly as the ions are separated. An initial simple way of understanding direct exchange is to look at two atoms with one electron each. When the atoms are very close together the Coulomb interaction is minimal when the electrons spend most of their time in between the nuclei. Since the electrons are then required to be at the same place in space at the same time, Pauli's exclusion principle requires that they possess opposite spins. According to Bethe and Slater the electrons spend most of their time in between neighboring atoms when the interatomic distance is small. This gives rise to antiparallel alignment and therefore negative exchange. (antiferromagnetic).

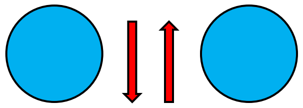

If the atoms are far apart the electrons spend their time away from each other in order to minimize the electron-electron repulsion. This gives rise to parallel alignment or positive exchange (ferromagnetism)

Bethe-Slater curve

- The exchange Heisenberg energy, suitably scaled, replaces the Weiss molecular field constant in the mean field theory of ferromagnetism to explain the temperature dependence of the magnetization

$$E_p = -J_{ex} S_i \times S_{i+1}$$

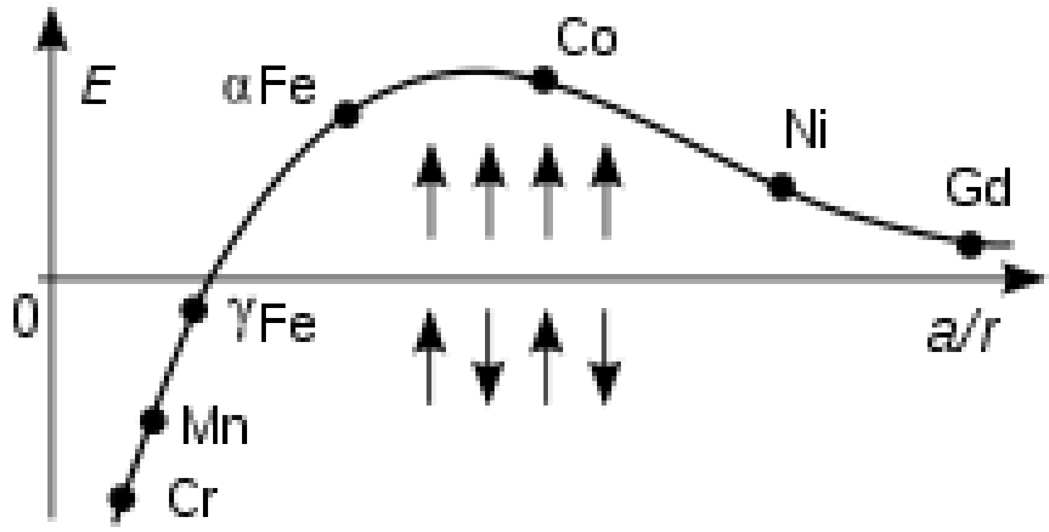

Differences in exchange energy of transition metals as due to the ratio of the interatomic distance a to the radius r of the 3d electron shell

Ferromagnetism

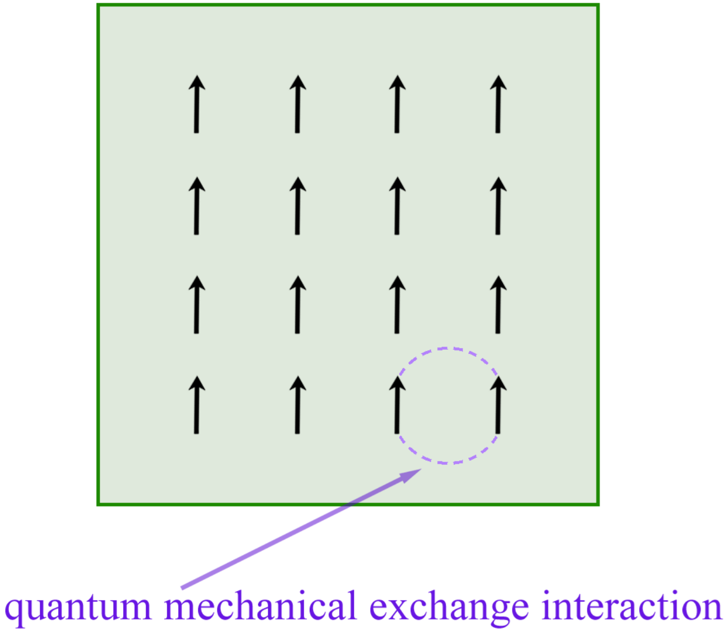

- Materials that retain a magnetization in zero field
- Quantum mechanical exchange interactions favour parallel alignment of moments
- Examples: iron, cobalt

Ferromagnetism

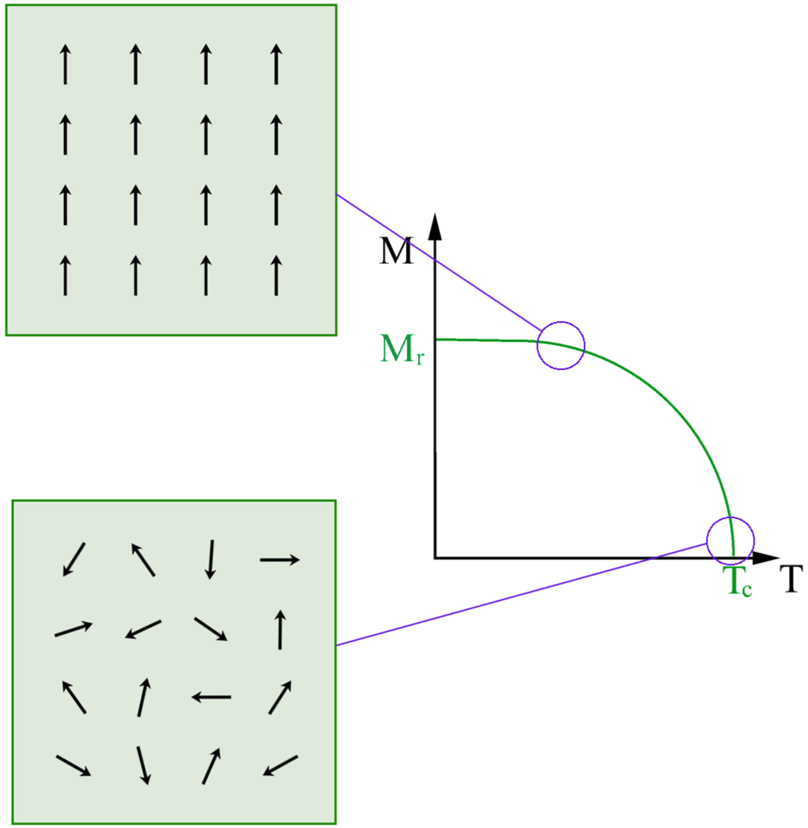

- Thermal energy can be used to overcome exchange interactions
- Curie temp is a measure of exchange interaction strength
- Note: exchange interactions much stronger than dipole-dipole interactions

Magnetic domains

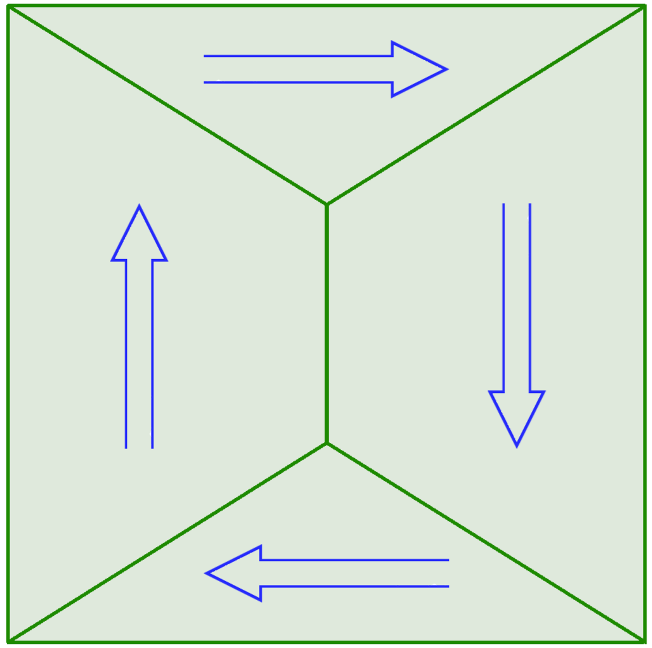

- Ferromagnetic materials tend to form magnetic domains
- Each domain is magnetized in a different direction
- Domain structure minimizes energy due to stray fields

Magnetic domains

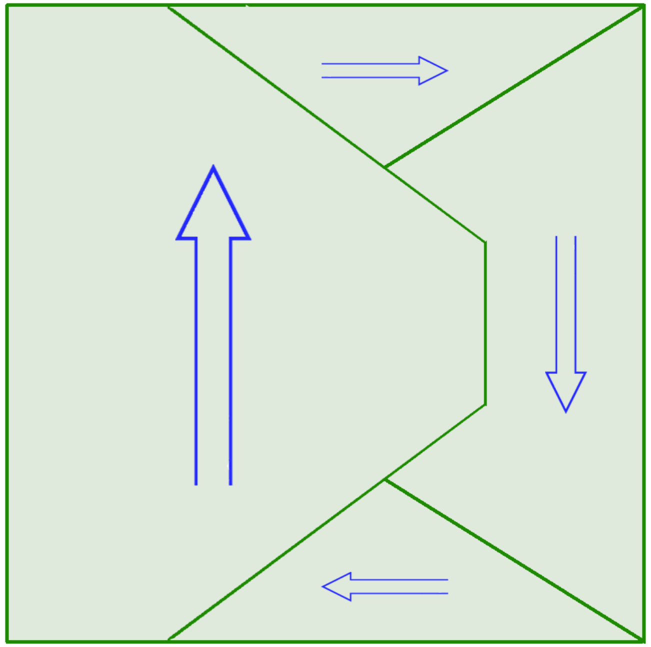

- Applying a field changes domain structure
- Domains with magnetization in direction of field grow
- Other domains shrink

Magnetic domains

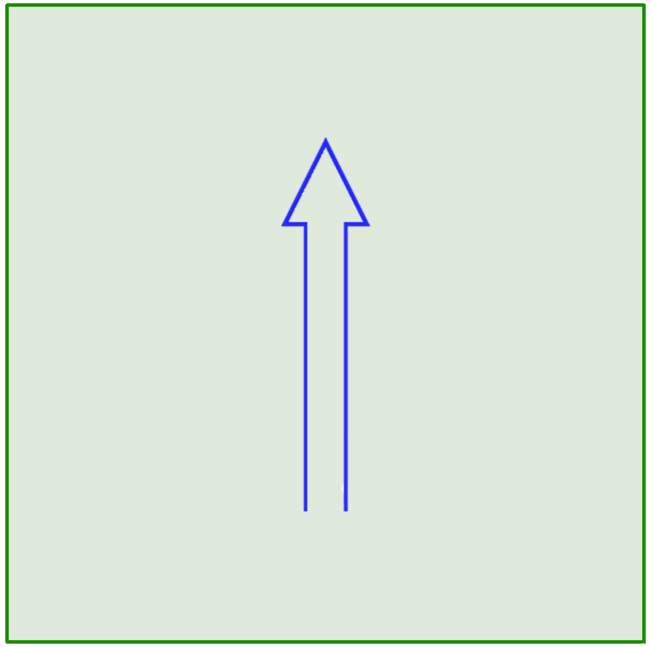

- Applying very strong fields can saturate magnetization by creating single domain

Magnetic domains

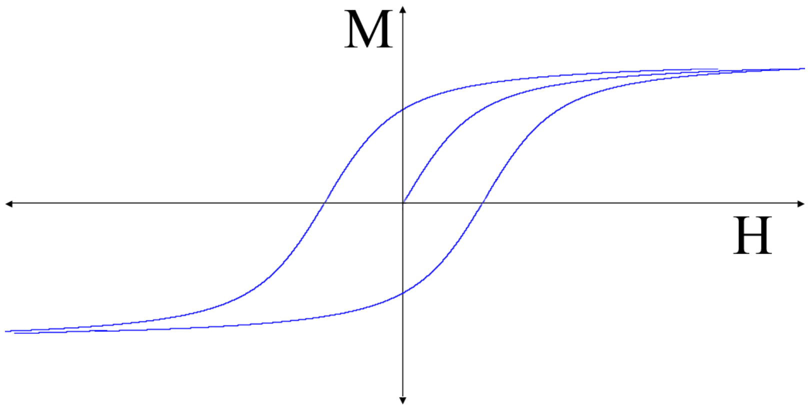

- Removing the field does not necessarily return domain structure to original state

- Hence results in magnetic hysteresis

Magnetic domain walls

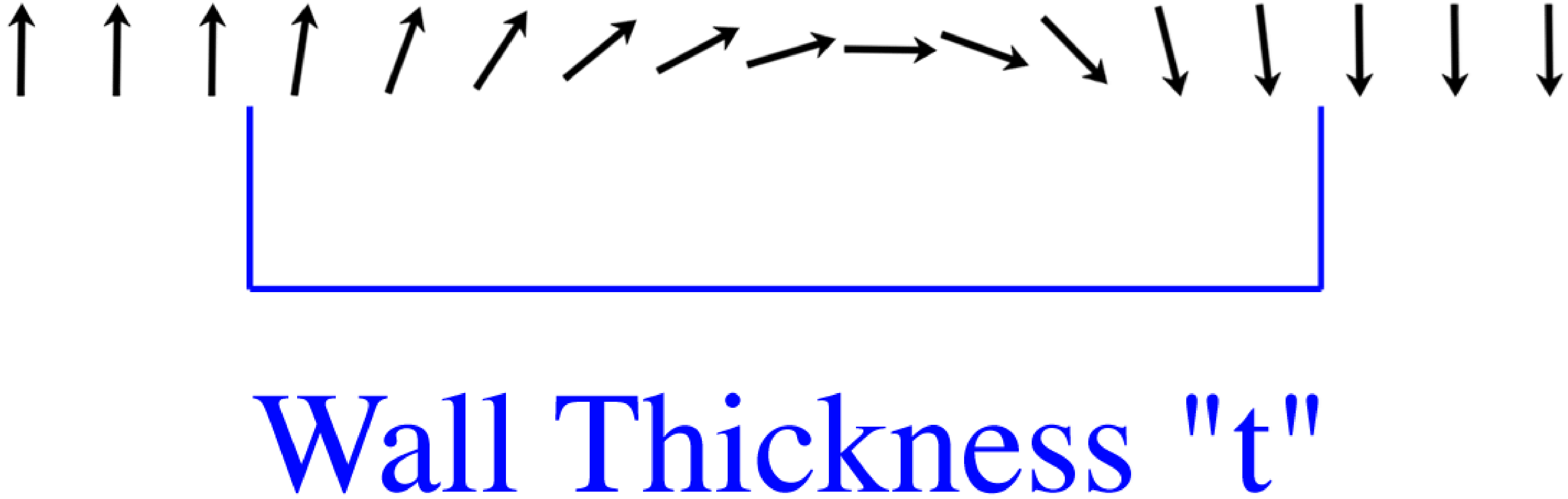

Wall thickness, t, is typically about 100 nm

Single domain particles

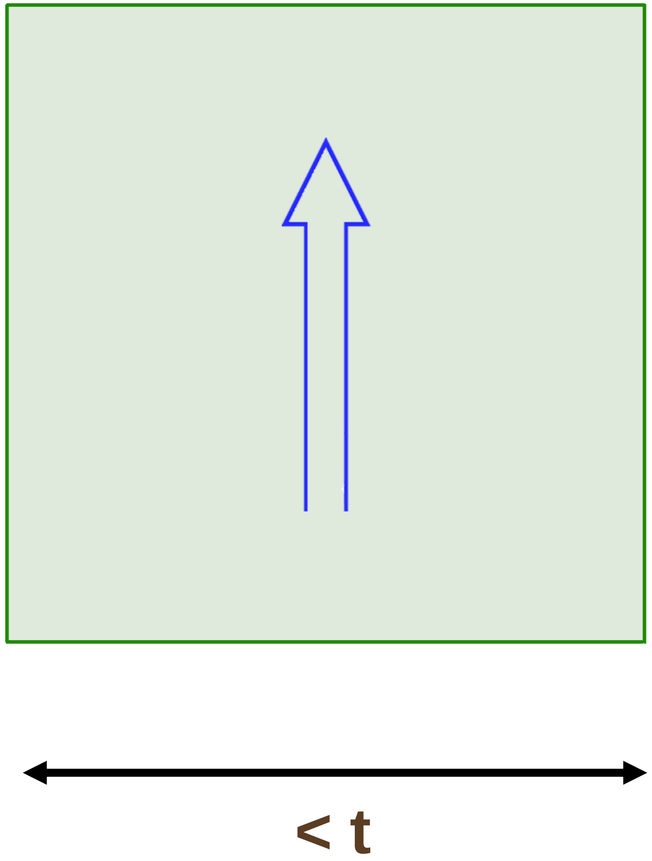

- Particles smaller than "t" have no domains

Antiferromagnetism

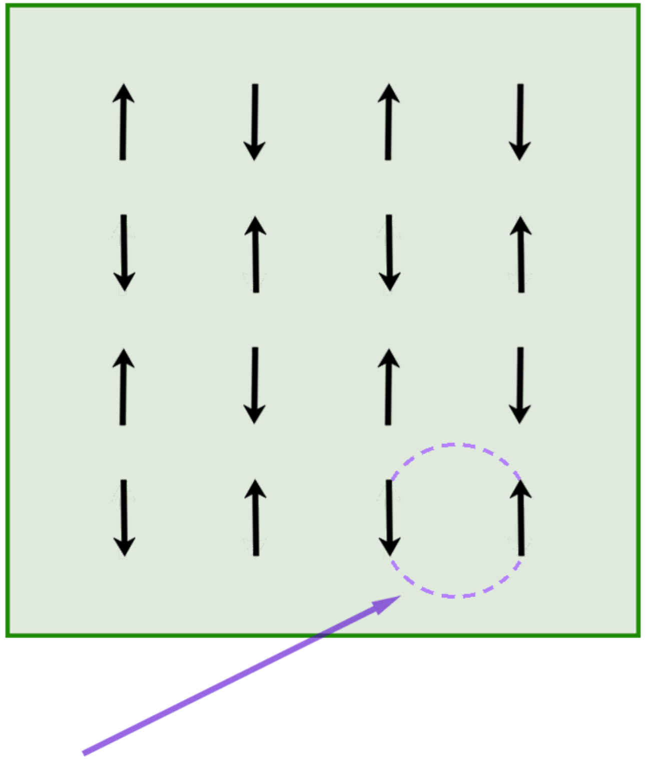

quantum mechanical exchange interaction

- In some materials, exchange interactions favour antiparallel alignment of atomic magnetic moments
- Materials are magnetically ordered but have zero remnant magnetization and very low χ
- Many metal oxides are antiferromagnetic

Antiferromagnetism

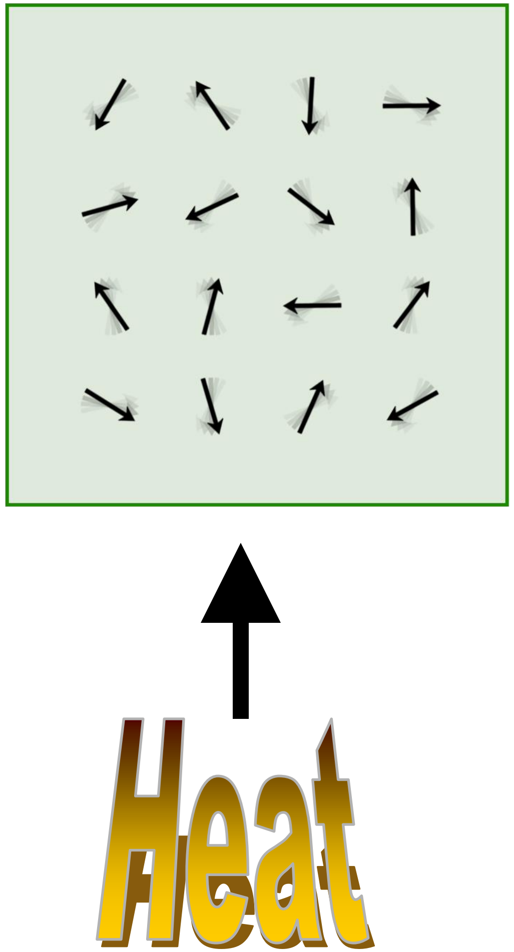

- Thermal energy can be used to overcome exchange interactions

- Magnetic order is broken down at the Néel temperature (c.f. Curie temp)

Ferrimagnetism

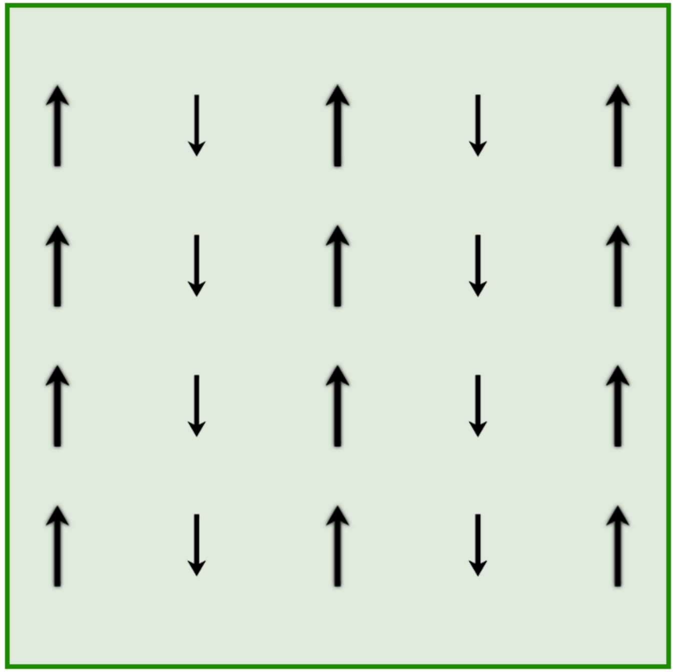

- Antiferromagnetic exchange interactions
- Different sized moments on each sublattice
- Results in net magnetization
- Example: magnetite, maghemite

Small Particle Magnetism

Stoner-Wohlfarth Particle

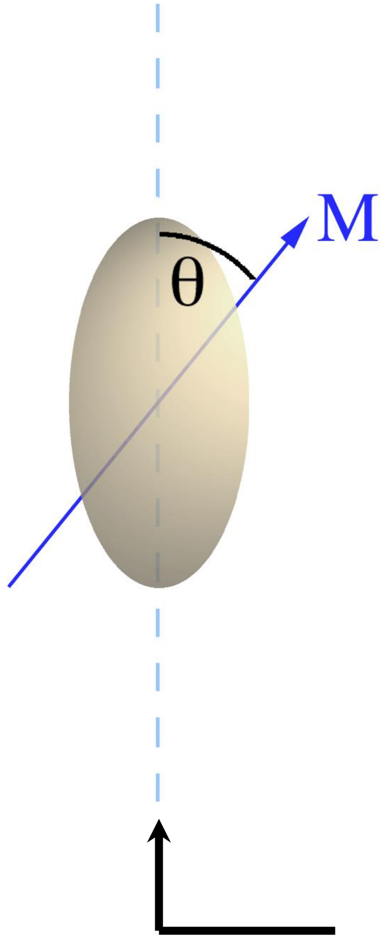

- Magnetic anisotropy energy favours magnetization along certain axes relative to the crystal lattice

Easy axis of magnetization

Stoner-Wohlfarth Particle

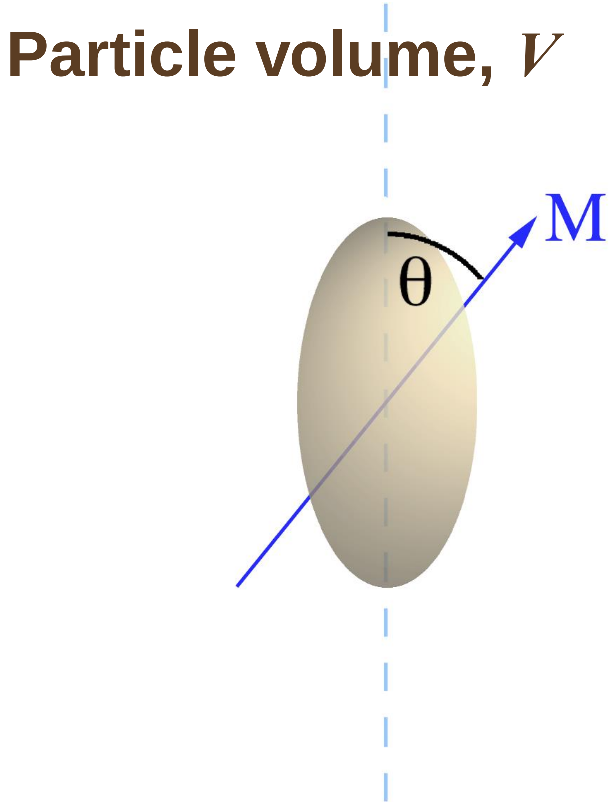

- **Uniaxial single domain particle**
- **Magnetocrystalline magnetic anisotropy energy given by**

$$E_a = KV\sin^2(\theta)$$

- ***K* is a constant for the material**

Stoner-Wohlfarth Particle

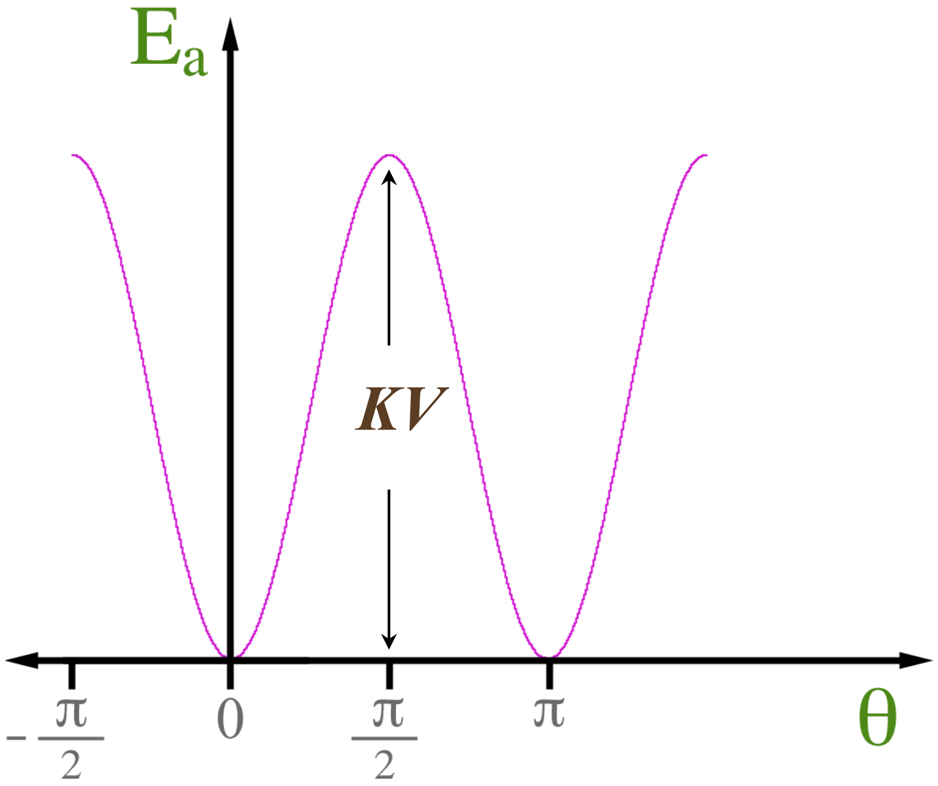

$$E_a = KV\sin^2(\theta)$$

Thermal activation

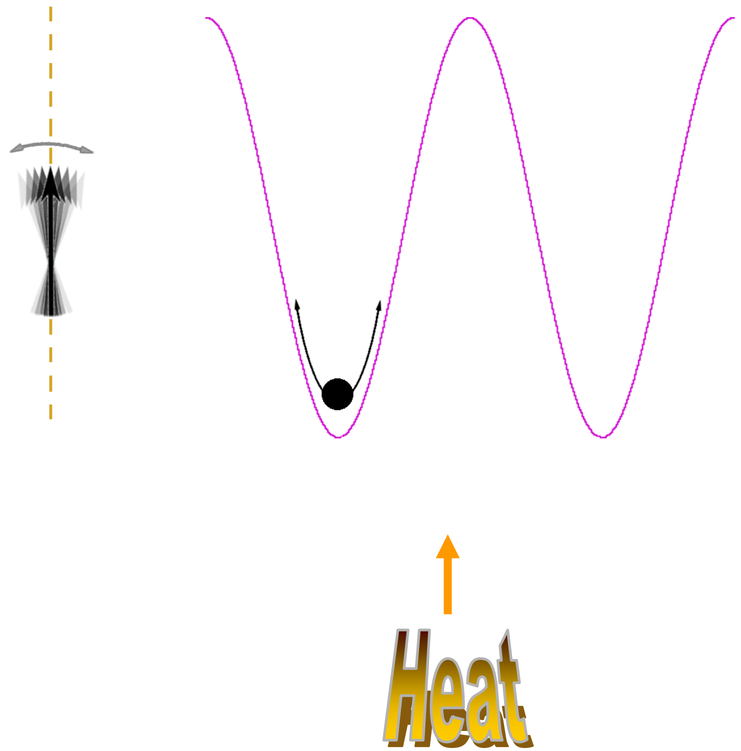

- At low temperature magnetic moment of particle trapped in one of the wells

- Particle magnetic moment is “blocked”

Thermal activation

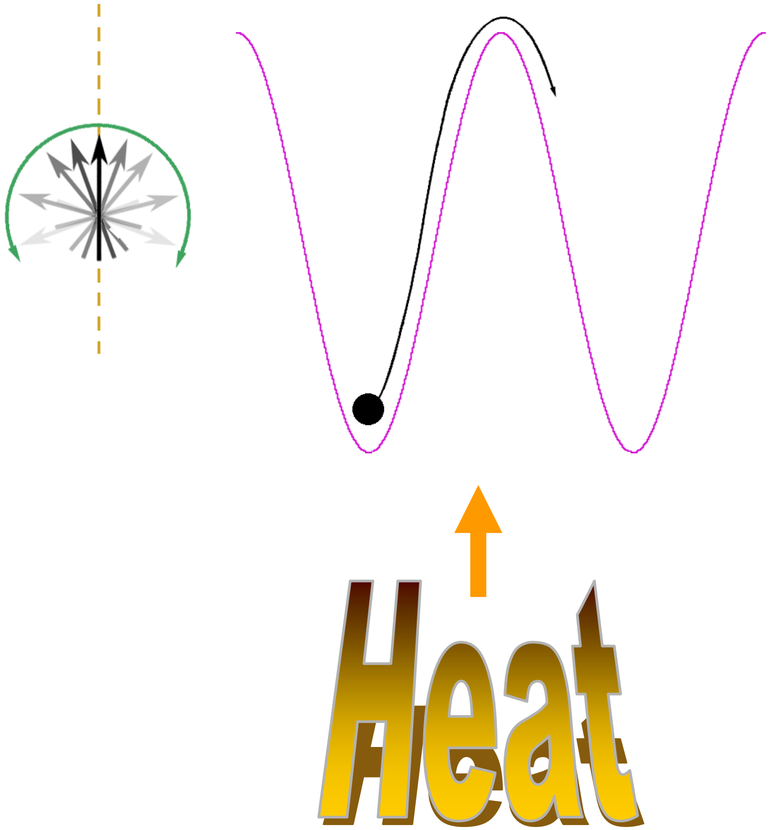

- At higher temps, thermal energy can buffet magnetic moment between the wells
- Results in rapid fluctuation of moment
- Particle moment becomes "unblocked"

Thermally Activated Jump

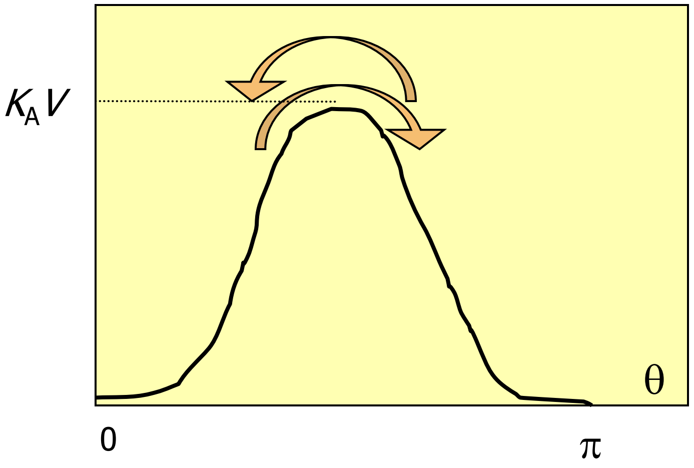

Thermally Activated Jump (Classical Behaviour!!)

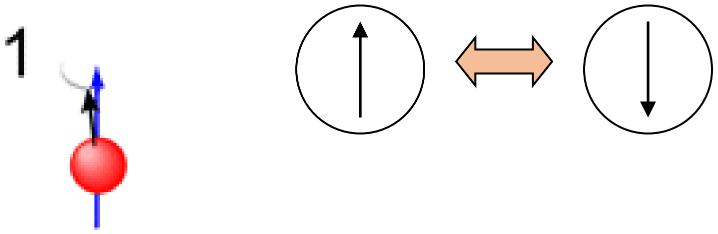

- Jump frequency: $$\upsilon = \tau_0^{-1} \exp\left(-\frac{K_a V}{k_B T} \right)$$
- Relaxation time: $$\tau = \tau_0 \exp\left(\frac{K_a V}{k_B T} \right)$$
- theoretical predictions: $\tau_0 = 10^{-9} \div 10^{-10}$ (see later)

Demagnetization rate of an assembly of uniaxial particles

$$-\frac{dM}{dt} = f_0 M e^{-KV/kT} = \frac{M}{\tau}$$

f_0 : frequency factor ($\approx 10^9$ sec^{-1})
τ : relaxation time

Turn-off external field at t = 0 with M_i

$$M_r = M_i e^{-t/\tau}$$

$\longrightarrow$ τ : time for M_r to decrease to 1/e of its initial value

$$\frac{1}{\tau} = f_0 e^{-KV/kT}$$

For Co (K = 4.5×10^6 ergs/cm^3) at room temp. (T = 300 K)

D = 68 Å (V = 1.6 × 10^{-19} cm^3)

$$\frac{1}{\tau} = 10^9 \cdot e^{-(4.5\times10^6 \times 1.6\times10^{-19}/(1.38\times10^{-16}\times300))} \approx 279.9\ \frac{1}{\text{sec}}$$

$$\tau \approx 3\times10^{-2}\ \text{sec}$$

An assembly of such particles would reach thermal equilibrium state (M_r = 0) almost instantaneously.
No hysteresis

Magnetization Relaxation

- Two Regimes:

$\tau < t_m$ — t_m — $\tau > t_m$ — *time*

Superparamagnetic | *Measuring time (time needed to do a measurement)* | Blocked

- Standard Magnetic Measurements: $t_m \approx 100$ s
- Mössbauer: $t_m \approx 10^{-8}$ s

- Define a critical volume at constant T (e.g., RT$\equiv T_0$) by requiring $\tau = t_m$:

$$\ln\tau = \ln\underbrace{\tau_0}_{\approx 10^{-10}} + \frac{K_a V_{crit}}{k_B T_0} = \begin{cases} \ln 10^{2} \\ \cdots \\ \ln 10^{-8} \end{cases}$$

For $t_m \approx 100$ s:

$$\boxed{V_{crit} \approx \frac{25 k_B T}{K_a}}$$

$$D_{crit} = \left[\frac{6}{\pi} V_{crit}\right]^{1/3}$$

Magnetic blocking temperature

- The magnetic blocking temp, T_b, is the temp below which moment is blocked
- Blocking temperature depends on particle size and timescale of observation
- Larger particles have higher blocking temperatures
- The longer the observation time, the more likely it is that the moment will be observed to flip

Fluctuation timescales, τ

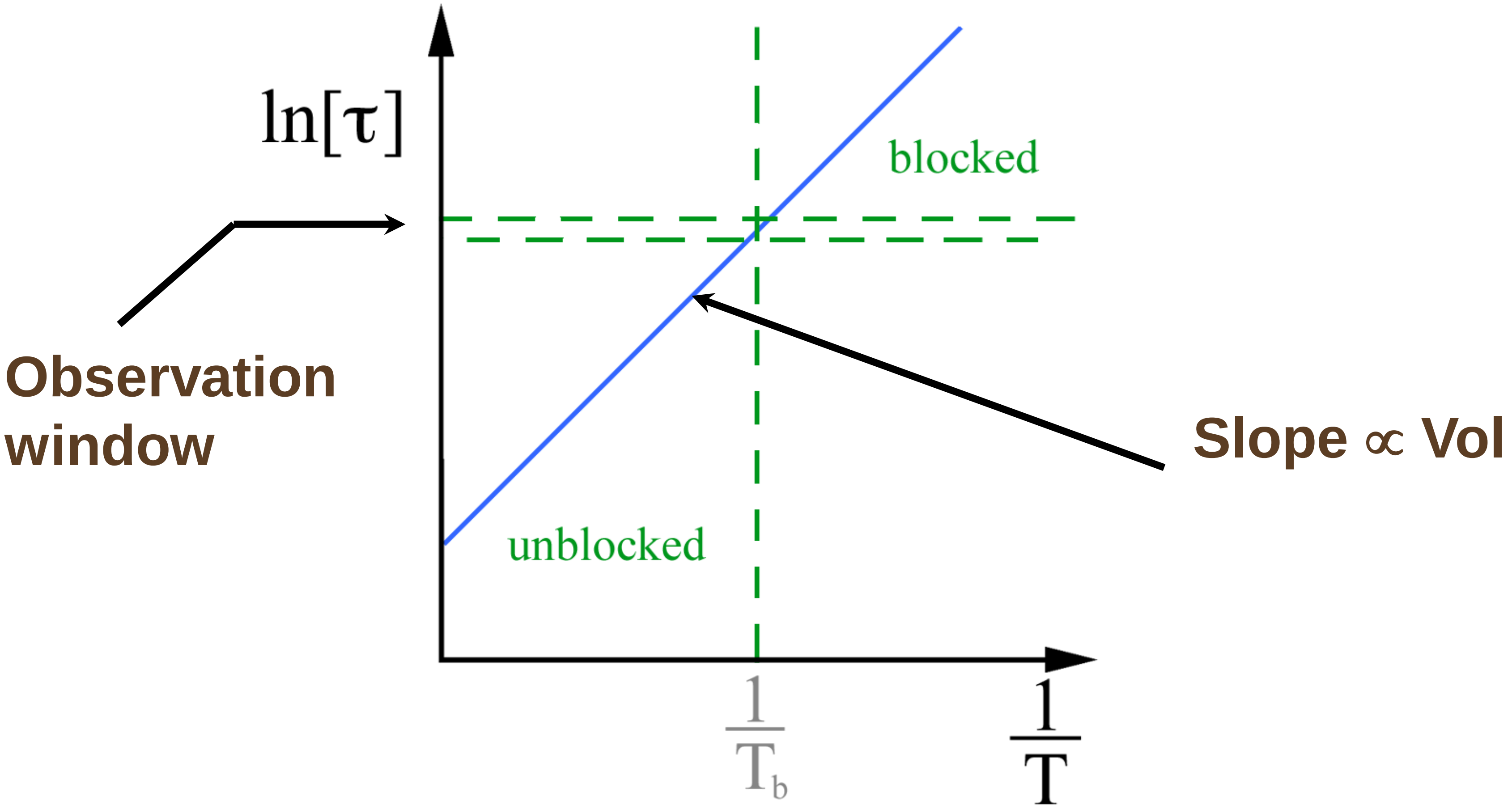

Effect of applied field on single domain particles

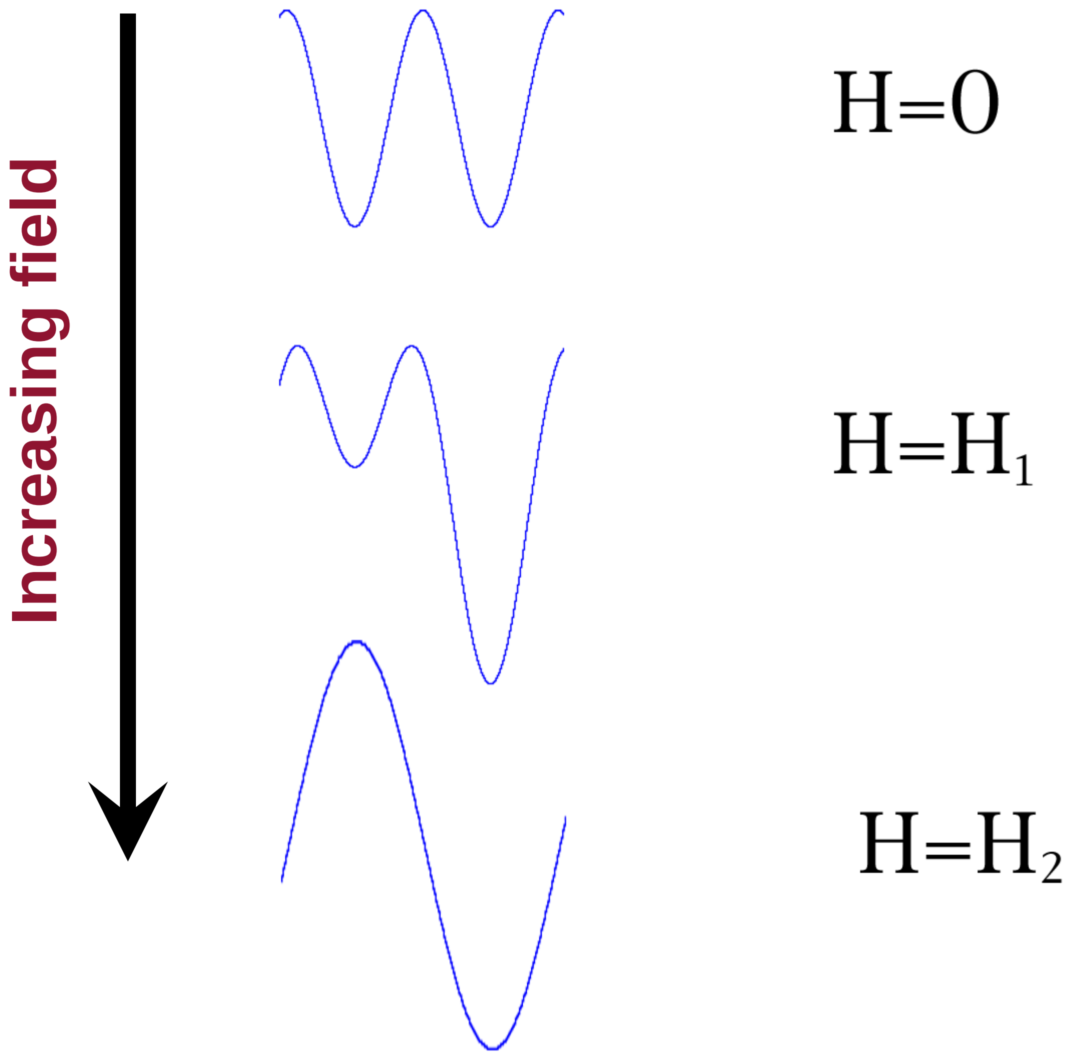

- **Applying field along easy axis favours moment aligned with field**
- **Above T_b this results in moment spending more time in lower well**
- **Particle exhibits time averaged magnetization in direction of field**

Superparamagnetism

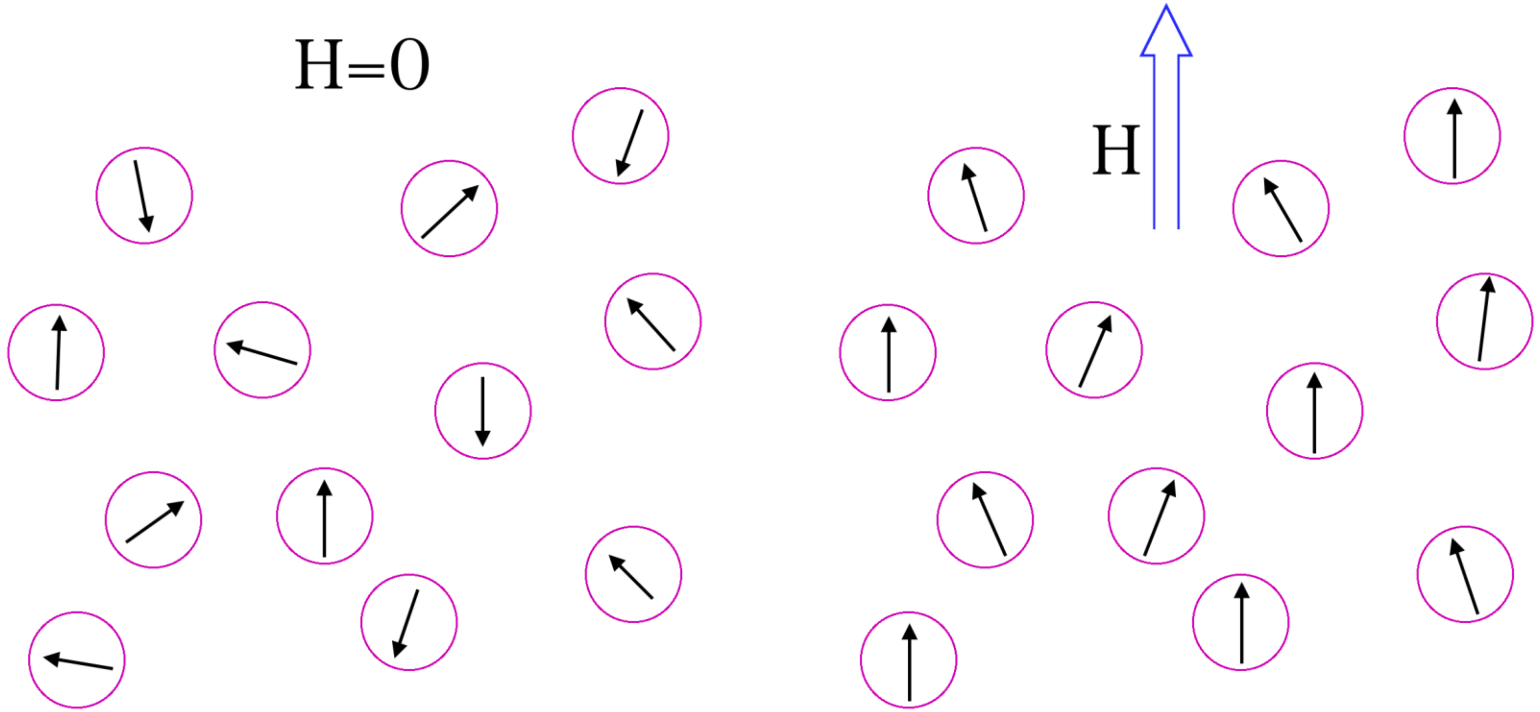

- Unblocked particles that respond to a field are known as superparamagnetic

Superparamagnetism

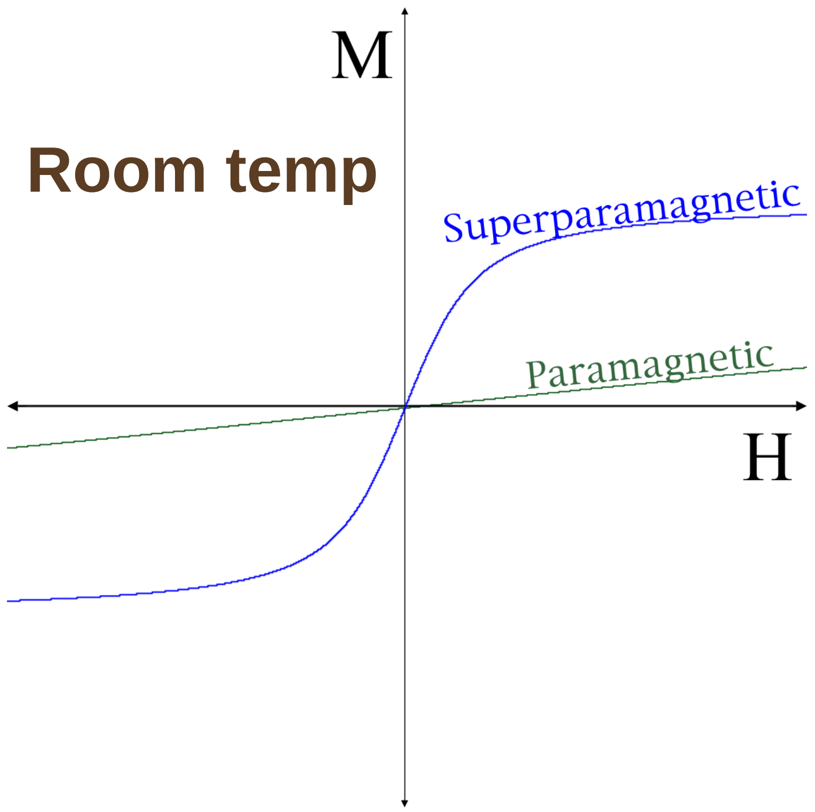

- Response of superparamagnets to applied field described by Langevin model
- Qualitatively similar to paramagnets
- At room temperature superparamagnetic materials have a much greater magnetic susceptibility per atom than paramagnetic materials

Superparamagnetism

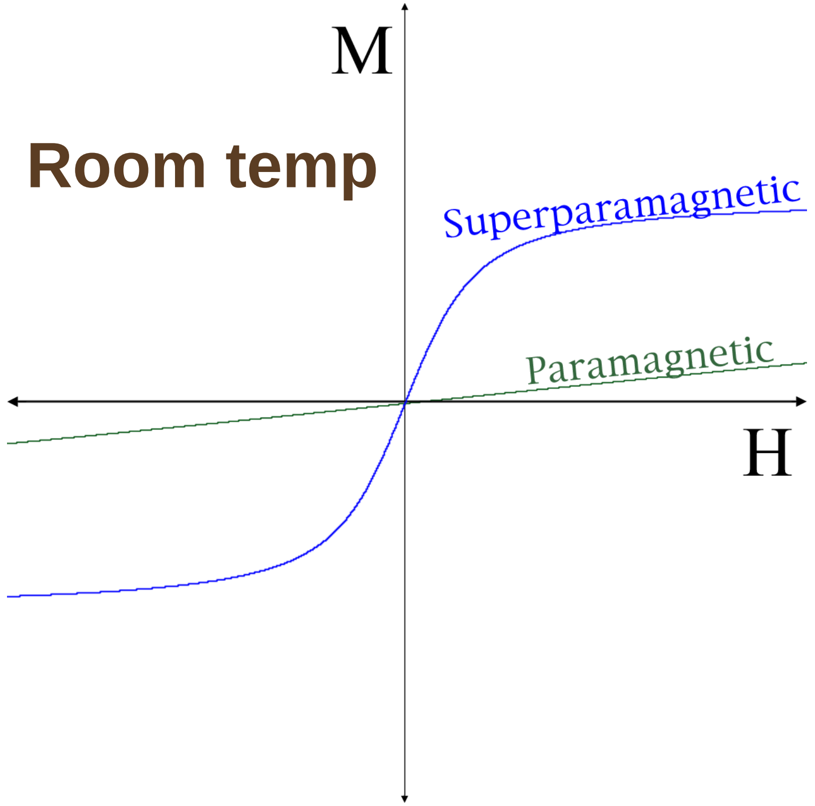

Superparamagnets are often ideal for applications where…

- **a high magnetic susceptibility is required**
- **zero magnetic remanence is required**

Ferromagnetic Resonance

FMR is a spectroscopic technique to probe the magnetization of ferromagnetic materials.

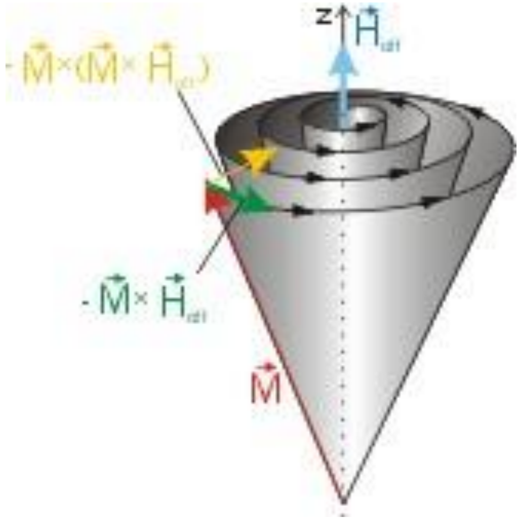

Landau-Lifshitz-Gilbert equation:

$$\frac{\partial \vec{M}}{\partial t} = -\gamma(\vec{M}\times\vec{H}_{eff}) + \frac{G}{\gamma M_S^2}\left[\vec{M}\times\frac{\partial \vec{M}}{\partial t}\right]$$

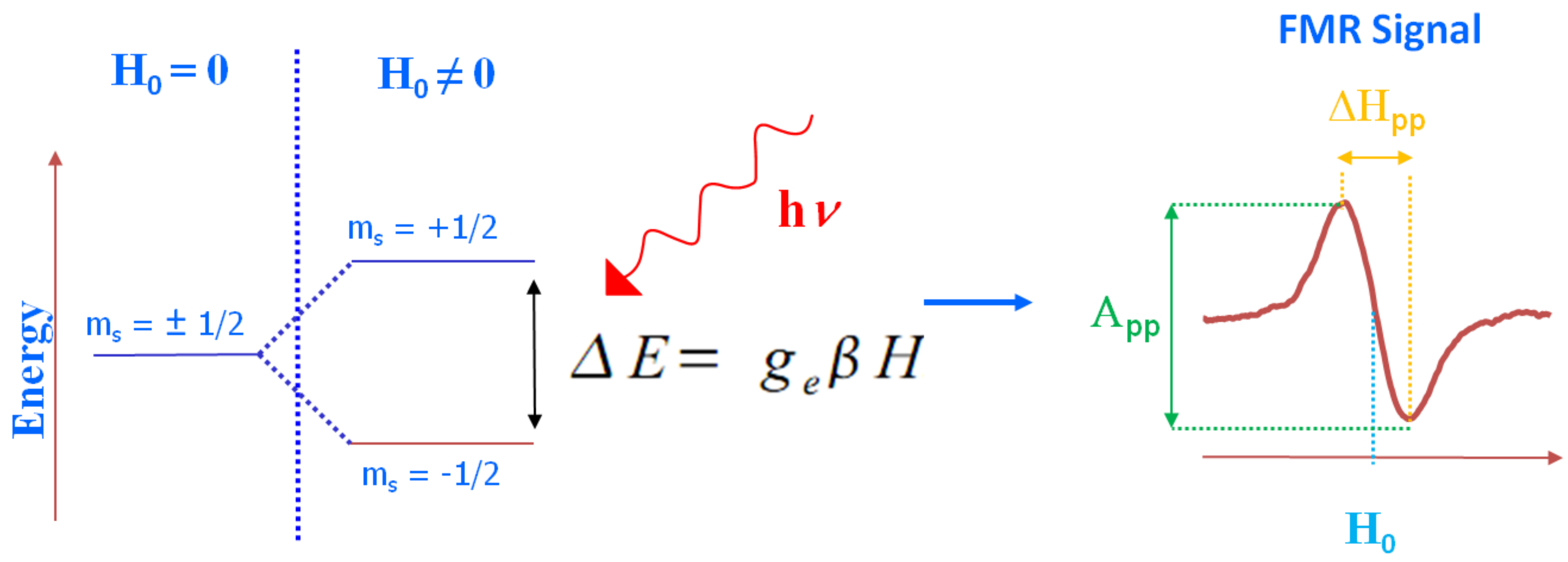

$H_0 = 0$
$H_0 \neq 0$
Energy
$m_s = \pm 1/2$
$m_s = +1/2$
$m_s = -1/2$
h ν
$\Delta E = g_e \beta H$
FMR Signal
ΔH_{pp}
A_{pp}
H_0

FMR: what we calculate?

The following parameters are directly determined from the FMR spectrum:	What are their physical meaning?
• amplitude of the first derivative absorption line A	No immediate meaning (indirectly number of spins)
• resonance field (apparent or true) B_r	Internal magnetic field
• peak-to-peak linewidth (apparent or true) ΔB_{pp}	Dynamics of the spin system
• integrated intensity $I_{int}=A\cdot(\Delta B_{pp})^2$	Magnetic susceptibility at microwave frequency and/or number of spins

Source: Janusz Typek, Institute of Physics, West Pomeranian University of Technology, Szczecin, Poland

JOURNAL OF MAGNETIC RESONANCE, Series A **122,** 100–103 (1996) ARTICLE NO. 0184

Investigation of the Magnetic Anisotropy in Manganese Ferrite Nanoparticles Using Magnetic Resonance

A. F. BAKUZIS,* P. C. MORAIS,* AND F. A. TOURINHO†

The dynamics of the magnetic moment of the particle is described by the Landau–Lifschitz equation, and for uniaxial particles the resonance condition is given by (*16*)

$$\omega_r = \gamma[H_r + 2(K/I_s)(L_2/L_1)P_2(\cos\theta)], \qquad [2]$$

where K is the effective anisotropy, $L_2 = 1 - 3(L_1/\xi)$, and $L_1 = \coth\xi - 1/\xi$ ($\xi = \mu H_r/kT$). The magnetic moment per particle (μ) is related to the saturation magnetization (I_s) by $\mu = I_s V$, where V is the particle volume. It must be pointed out that Eq. [2] is valid over a wide temperature range, including high temperatures, where the fluctuation field is typically of the order of the anisotropy field.

FMR resonance field

$$H_r = (\omega_r/\gamma) - (K/I_s)(3\cos^2\theta - 1).$$

Experimental Results

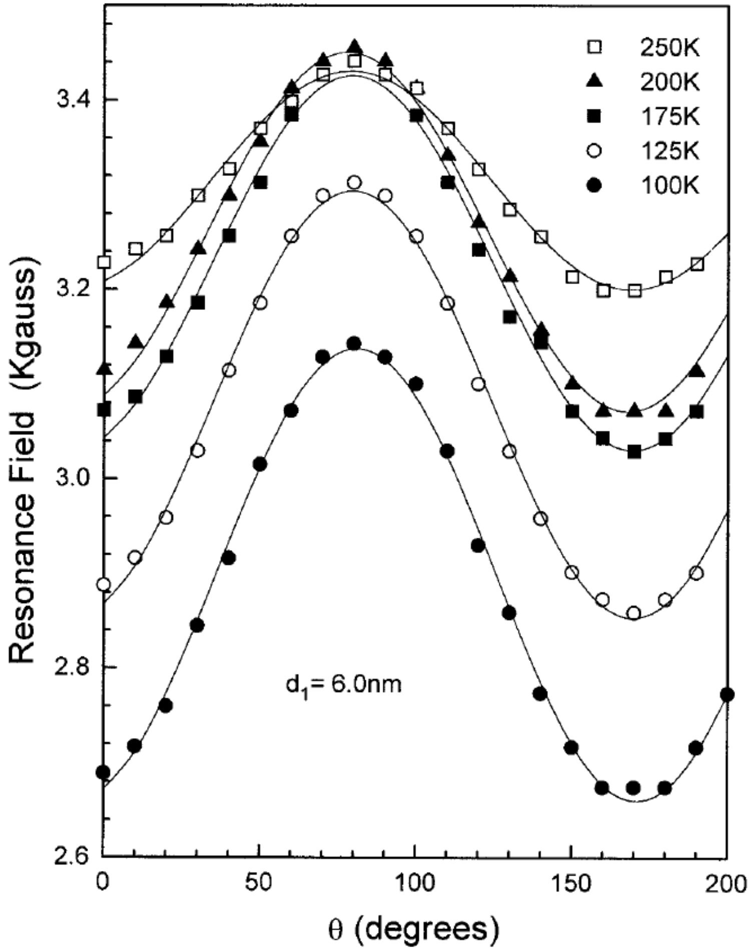

Angular dependence of the resonance field for a magnetic fluid sample of MnFe2O4 with particles having an average diameter of 6.0 nm. The solid lines represent the best fit of the experimental data according to Eq. [4].

Magnetization Curve

ifmpan.poznan.pl/~urbaniak/Wyklady2014/urbaniakUAM2014L2_magnetic%20measurements.pdf

M. Urbaniak Magnetic materials in nanoelectronics... IFM PAN Poznań 2014

Introduction

Measurement of magnetic field strength

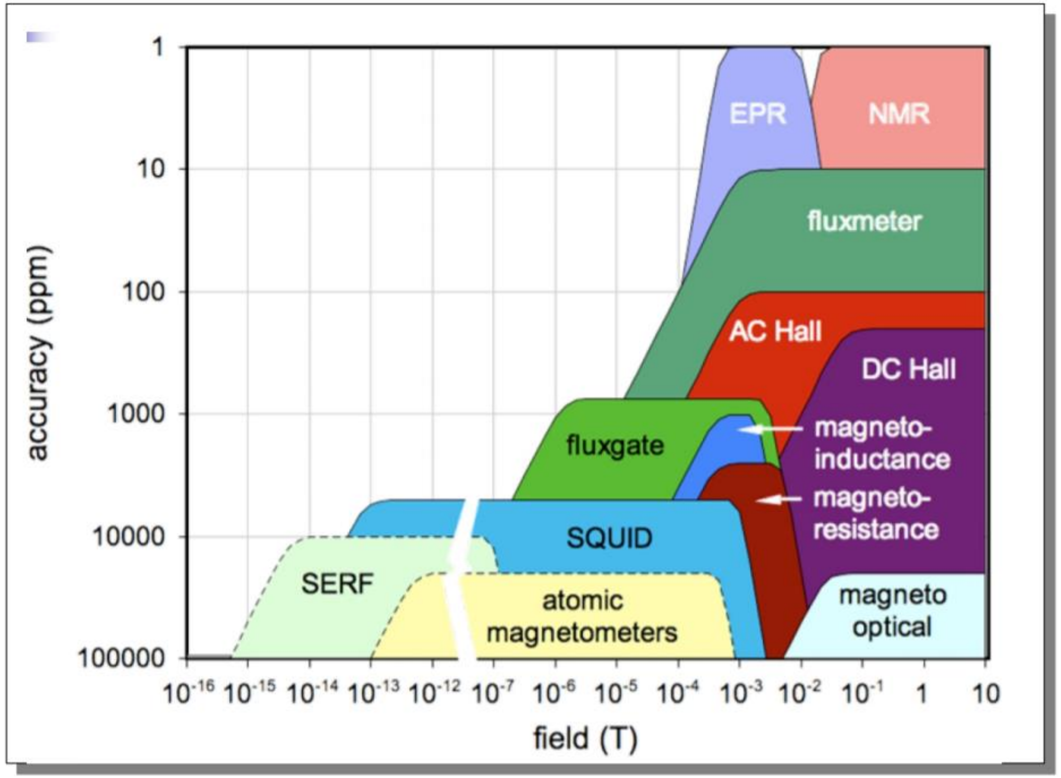

methods most relevant in spintronic measurements:
AC and DC Hall probes

The sensitivity range of the probe should cover whole range of fields in which magnetic configuration significantly changes

graphics from *Field Measurement Methods* lecture delivered during The Cern Accelerator School; Novotel Brugge Centrum, Bruges, Belgium, 16 - 25 June, 2009; author: Luca Bottura

Introduction

- Magnetic sensor can be divided according to different criteria:

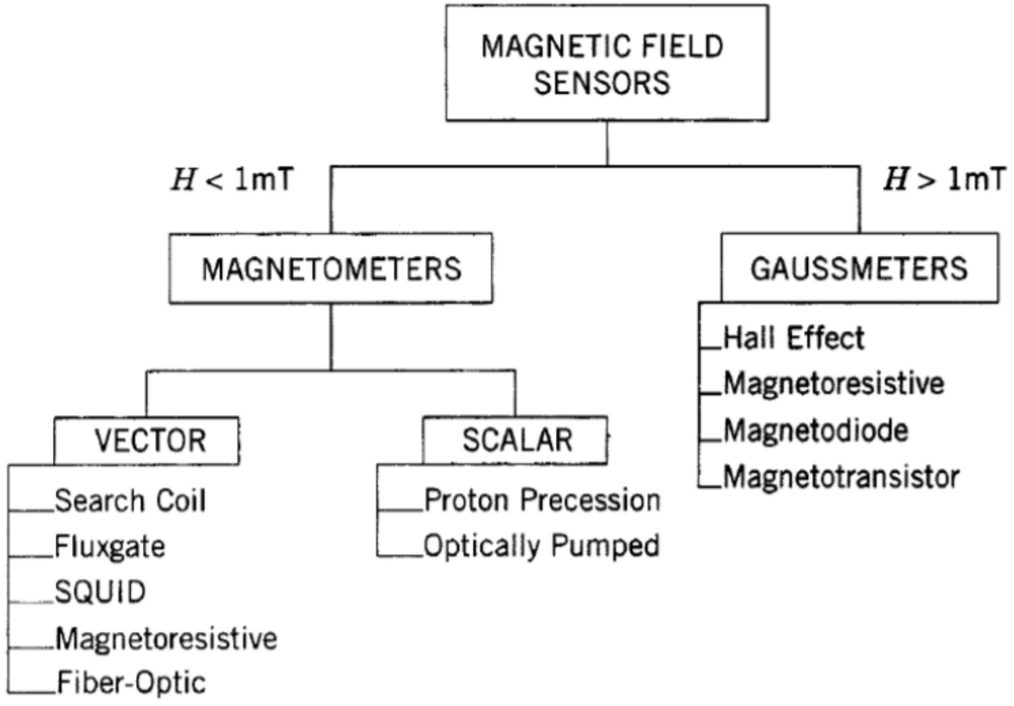

FIGURE 48.1 Magnetic field sensors are divided into two categories based on their field strengths and measurement range: magnetometers measure low fields and gaussmeters measure high fields.

- Distinction magnetometer-gaussmeter is rather arbitrary and not commonly used.

graphics from [7]: S.A. Macintyre, Magnetic Field Measurement

Introduction – Hall magnetometer

- Lorentz force acting on electrons in a circuit deflects them perpendicularly to drift direction:

$$\vec{F}_{Lorentz} = q\vec{E} + q\vec{v} \times \vec{B}$$

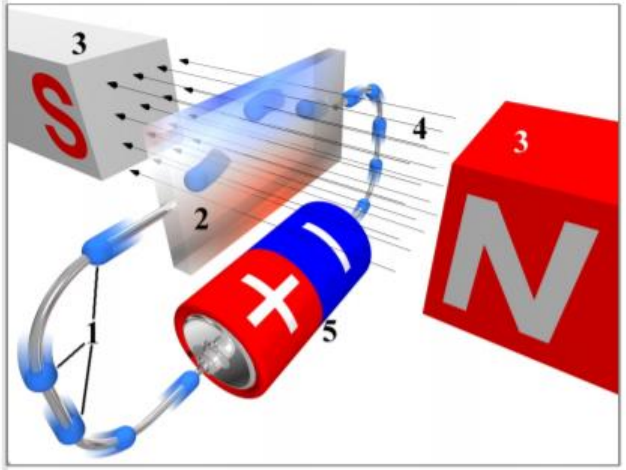

image from Wikimedia Commons; authors: Peo (modification by Church of emacs)

- The build-up of charges on outer limits of the circuit induces Hall voltage which depends on the field strength and is used to sense it.
- The Hall voltage is given by (t-film thickness, R_H-Hall coefficient*):

$$U_y = R_H \frac{I}{t} B_z$$

- The main figure of interest is field sensitivity of the sensor** (for a given driving current I_c):

$$\boxed{\gamma_b = \frac{U_y}{B_z} = \frac{R_H I_c}{t}}$$

- Semiconductors are used to obtain high sensitivity combined with temperature stability (InAs)
- The Hall sensors have a limited use at high fields and low temperatures (conductivity quantization)

The new HFC probe is able to measure intense fields in tiny gaps.

image from http://metrolab.com/

Hall sensors are relatively easy to miniaturize

*for InAs R_H is about 0.0001 m^3/As **some tenths of mV per kA/m for I_c of several mA (www.lakeshore.com/products/Hall-Magnetic-Sensors/pages/Specifications.aspx)

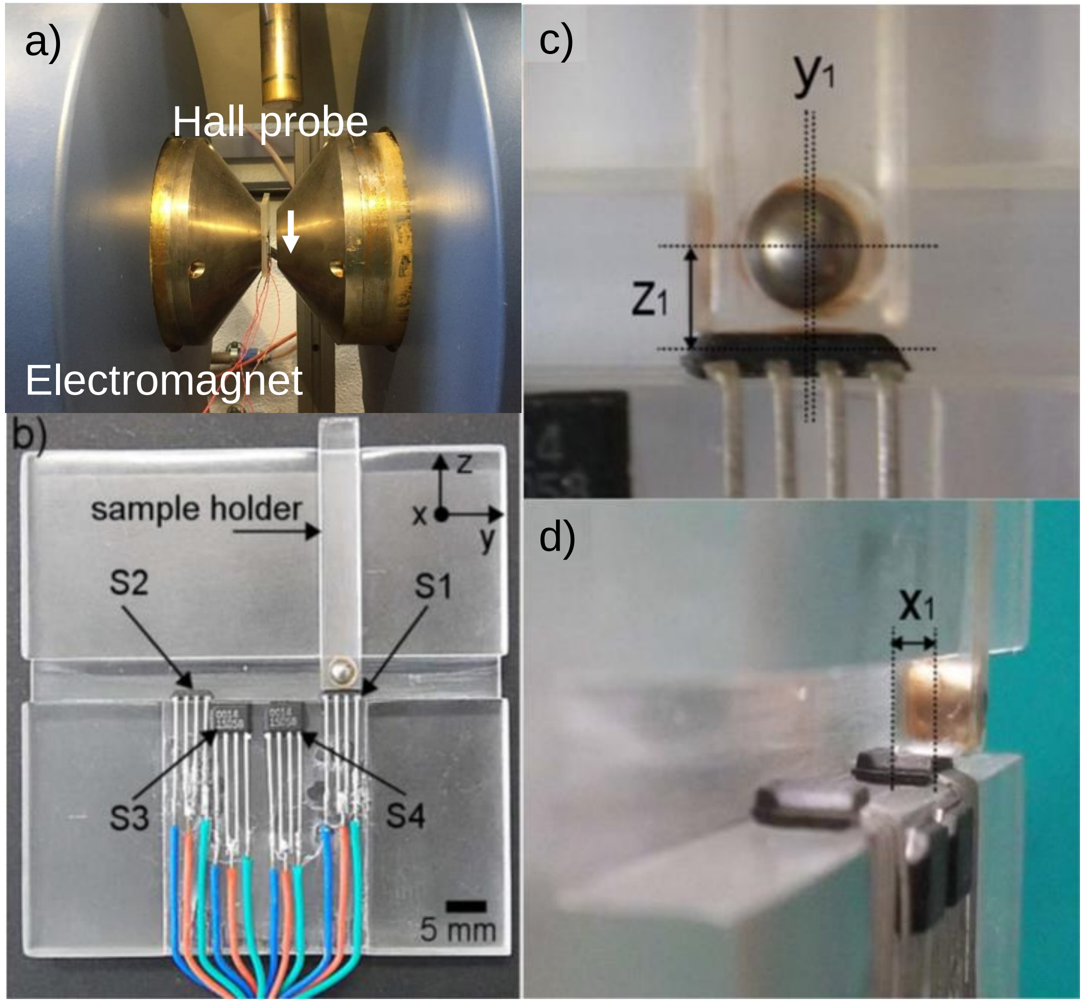

Jefferson F. D. F. Araujo, et al. *J. Magn. Magn. Mater*. 426, 159-162 (2017).

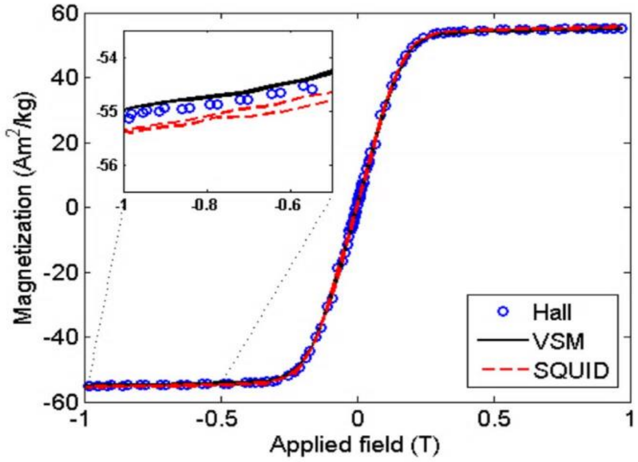

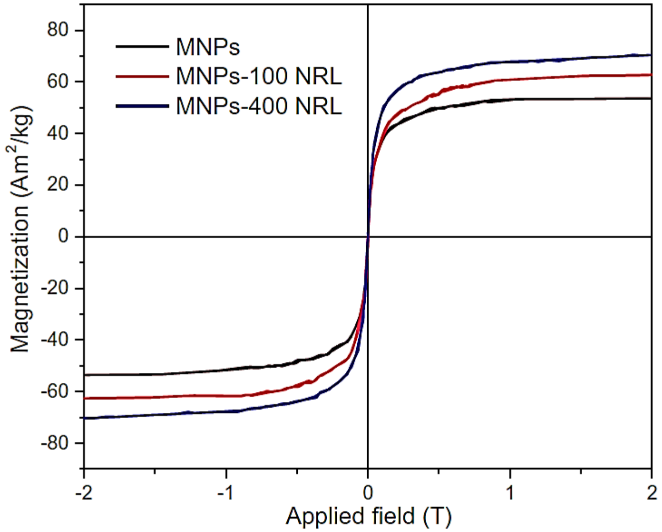

Soudabeh Arsalani, et al. *J. Magn. Magn. Mater*. 475, 458-464 (2019).

- Sensibilidade $3.5\text{x}10^{-7}$ Am^2
- Massa da Amostra 15 mg
- $B_{máx}$ 3.0 T

- Modelo Teórico

$$B_z(x,y,z)=\frac{\mu_0 I}{4\pi}\int_0^{2\pi}\frac{xasen\varphi}{r'^3}d\varphi$$

$$B_z(x,y,z)=\frac{\mu_0 m}{4\pi}[\int_{-L/2}^{L/2}\int_0^{2\pi}\frac{xasen\varphi}{r'^3}d\varphi dx]/\pi a^2$$

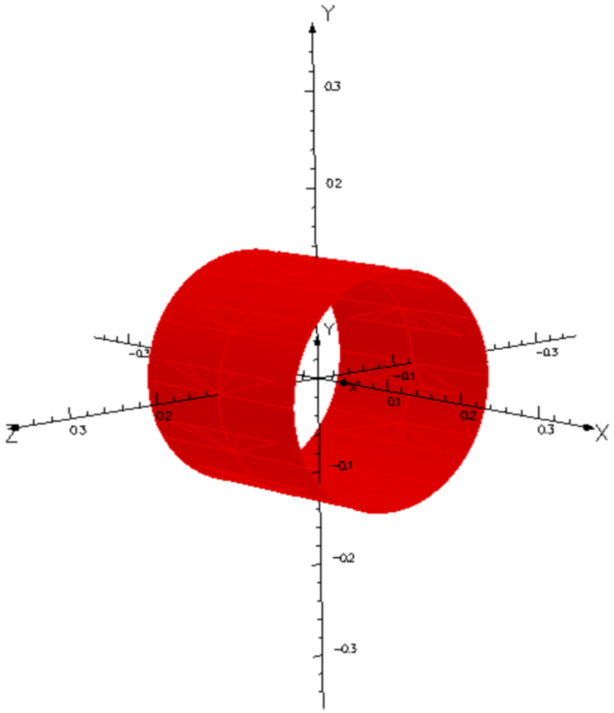

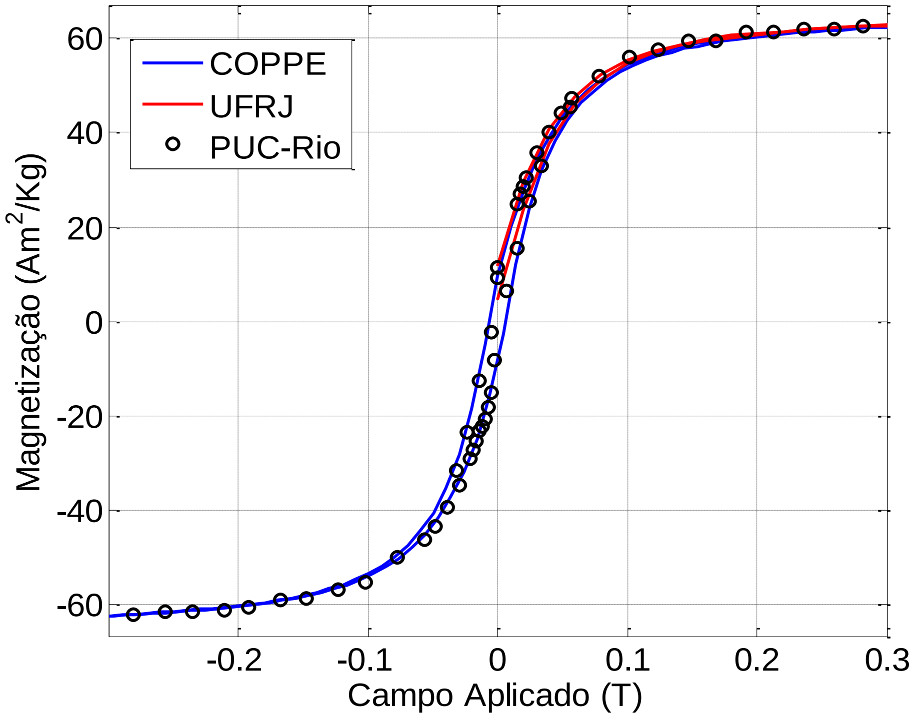

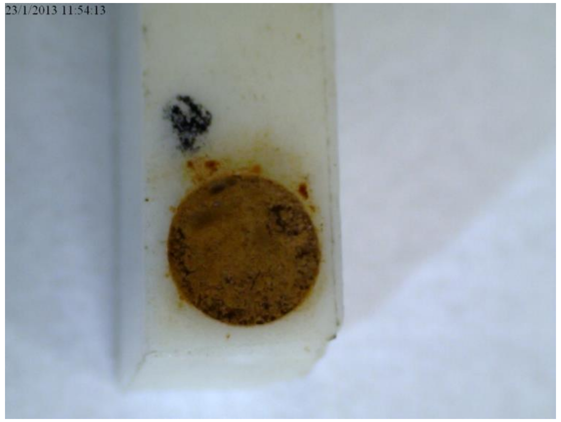

Jefferson F. D. F. Araujo, et al. *J. Magn. Magn. Mater*. 426, 159-162 (2017).

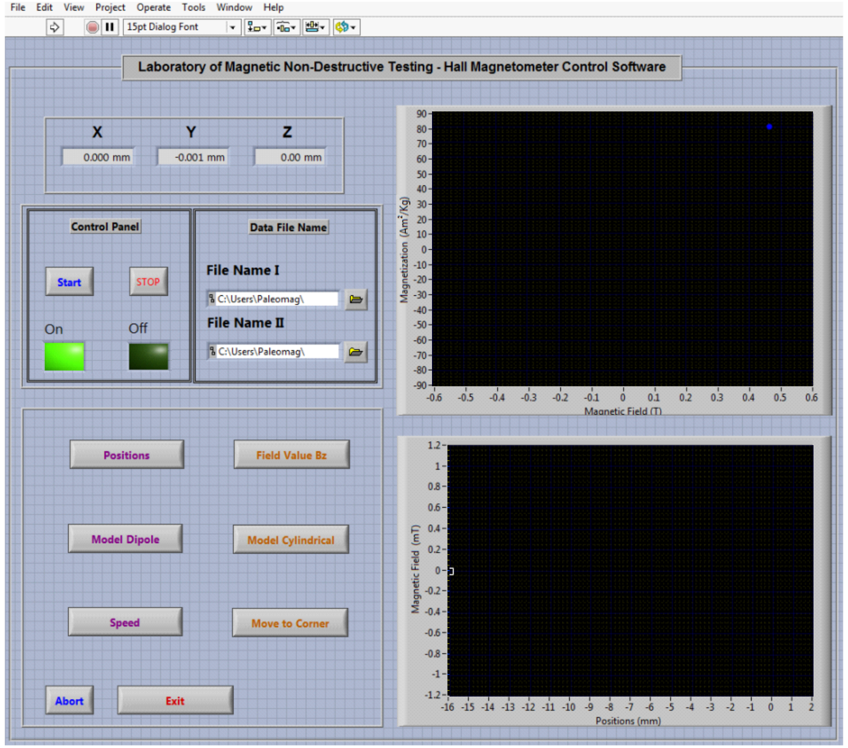
File Edit View Project Operate Tools Window Help
15pt Dialog Font
Laboratory of Magnetic Non-Destructive Testing - Hall Magnetometer Control Software
X
Y
Z
0.000 mm
-0.001 mm
0.00 mm
Control Panel
Start
STOP
On
Off
Data File Name
File Name I
C:\Users\Paleomag\
File Name II
C:\Users\Paleomag\
Positions
Field Value Bz
Model Dipole
Model Cylindrical
Speed
Move to Corner
Abort
Exit
Magnetization (Am²/Kg)
Magnetic Field (T)
Magnetic Field (mT)
Positions (mm)

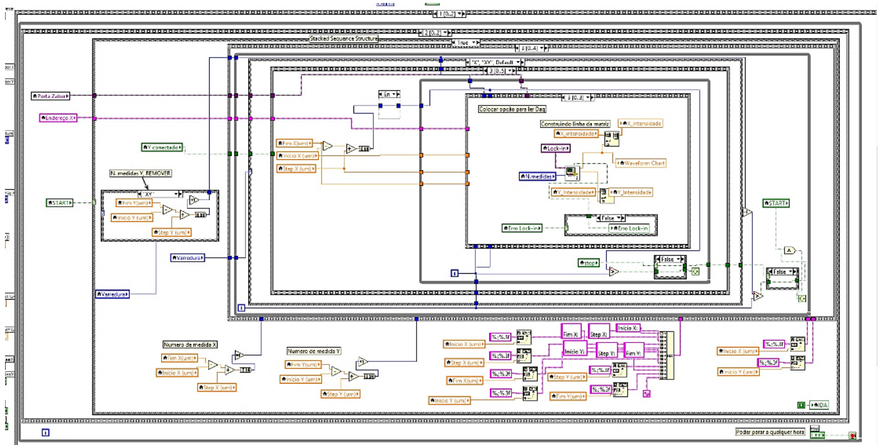

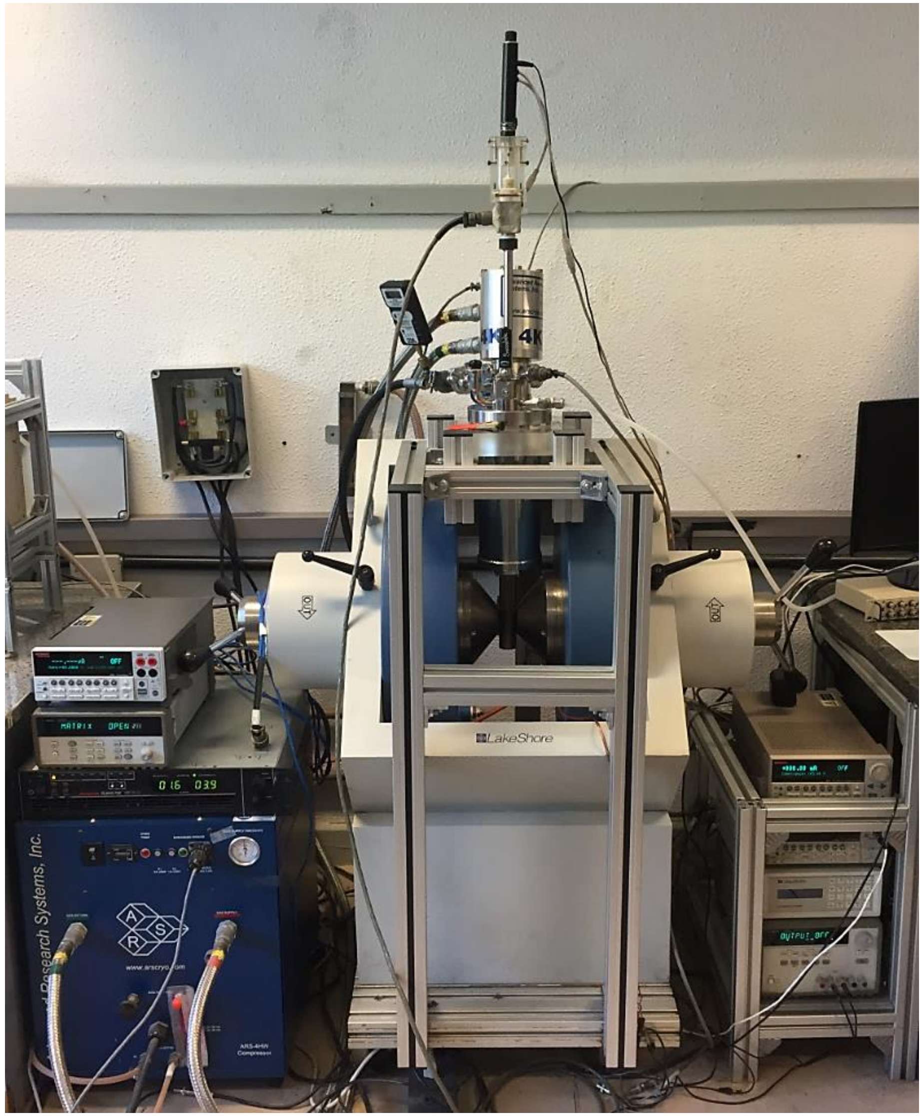

Jefferson F. D. F. Araujo, A. C. Bruno, and S. R. W. Louro, *Review of Scientific Instruments* 86, 105103 (2015).

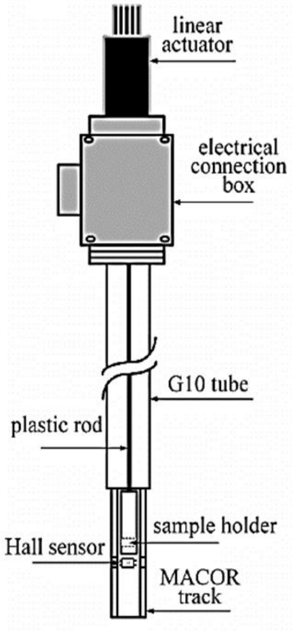

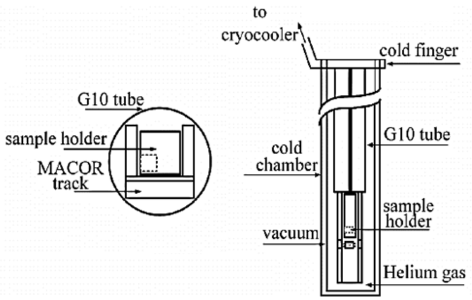

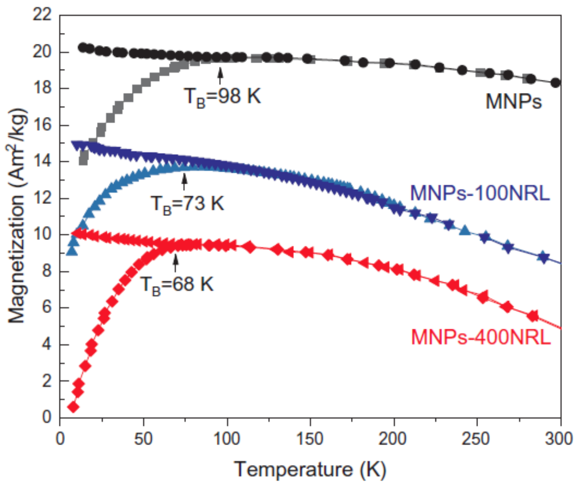

Soudabeh Arsalani, et al. *J. Magn. Magn. Mater*. 475, 458-464 (2019).

- Sensibilidade: $8.5x10^{-8}$ Am^2
- Massa da Amostra: 15 mg
- $B_{máx}$: 1.0 T
- T_{mim}: 6.0 K

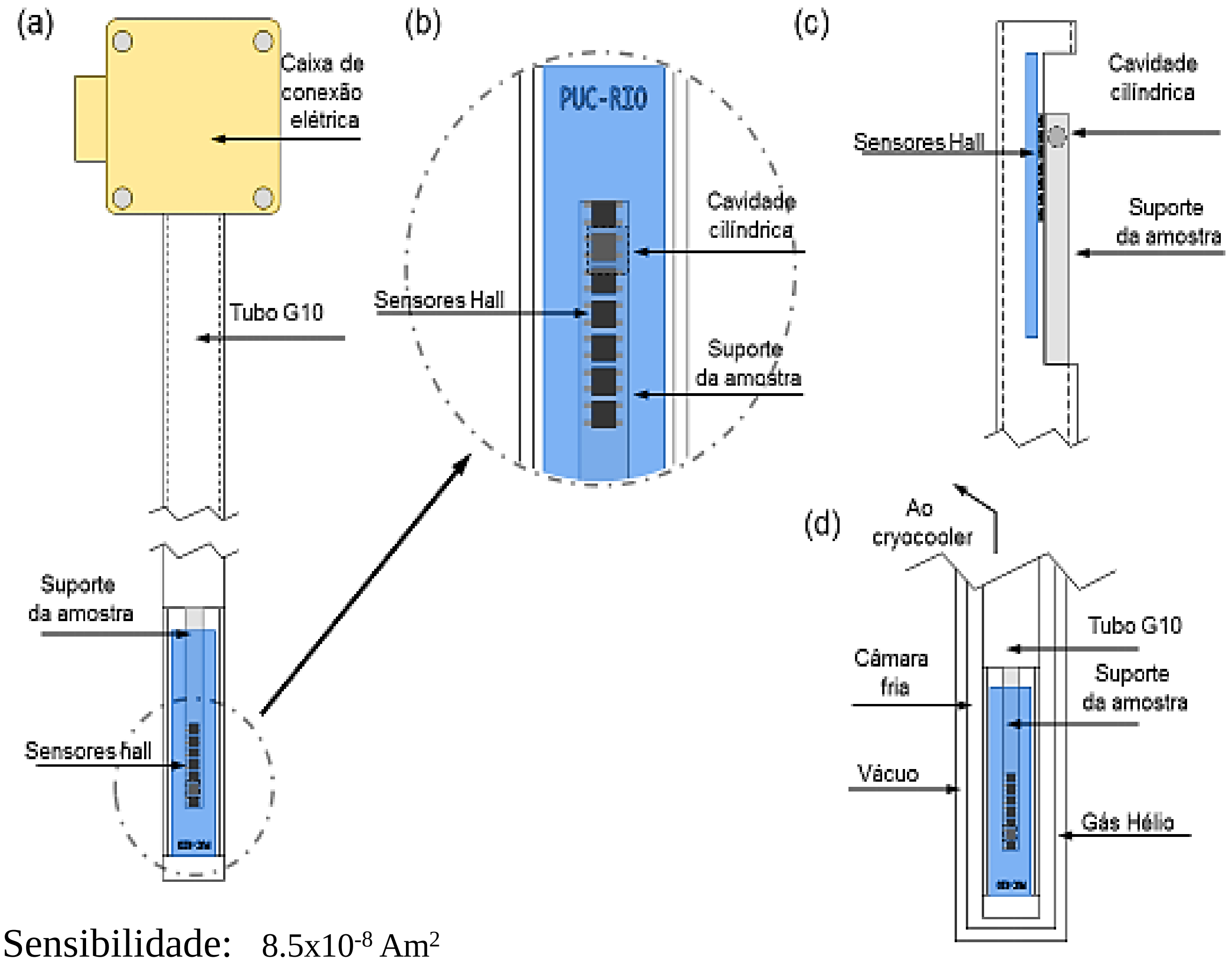

- Sensibilidade: 8.5×10^{-8} Am^2
- Massa da Amostra: 10 - 200 mg

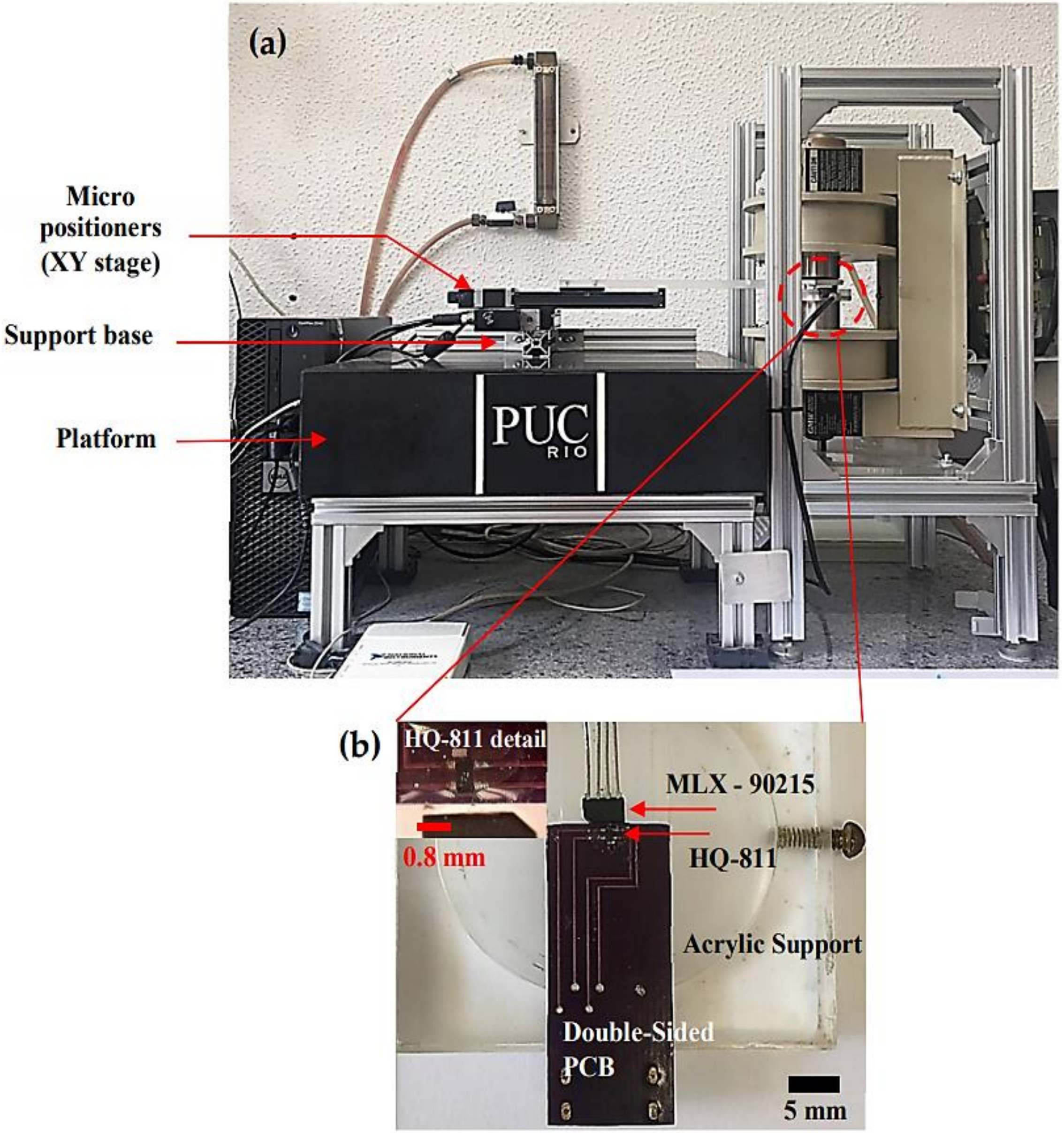

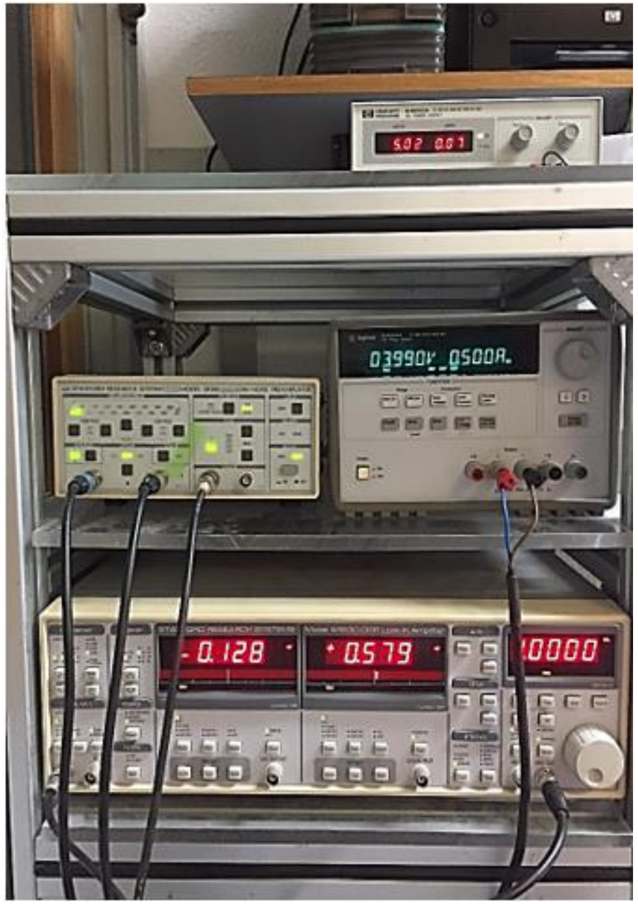

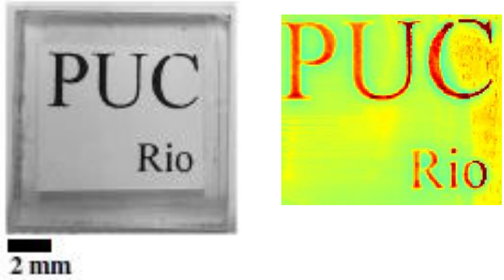

Desenvolvido de forma pioneira

Jefferson F. D. F. Araujo, et al. *J. Magn. Magn. Mater*. 499, 166300-9 (2020).

Gan.: 2 mV/mT @ 3 mA

BW: 100 kHz

Ruído: 300 nT/√Hz

Sens.: 2,5 x 10^{-11} Am^2

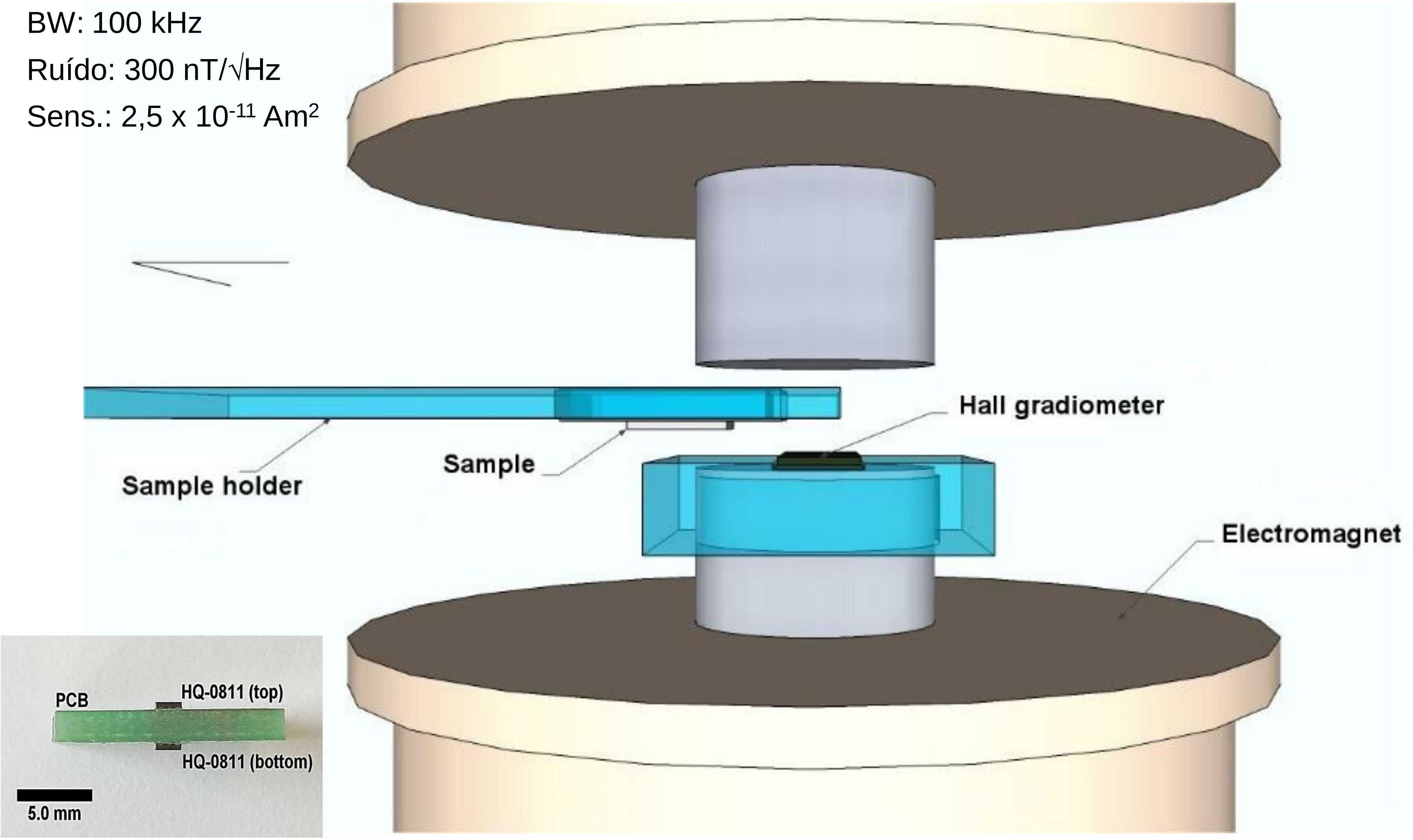

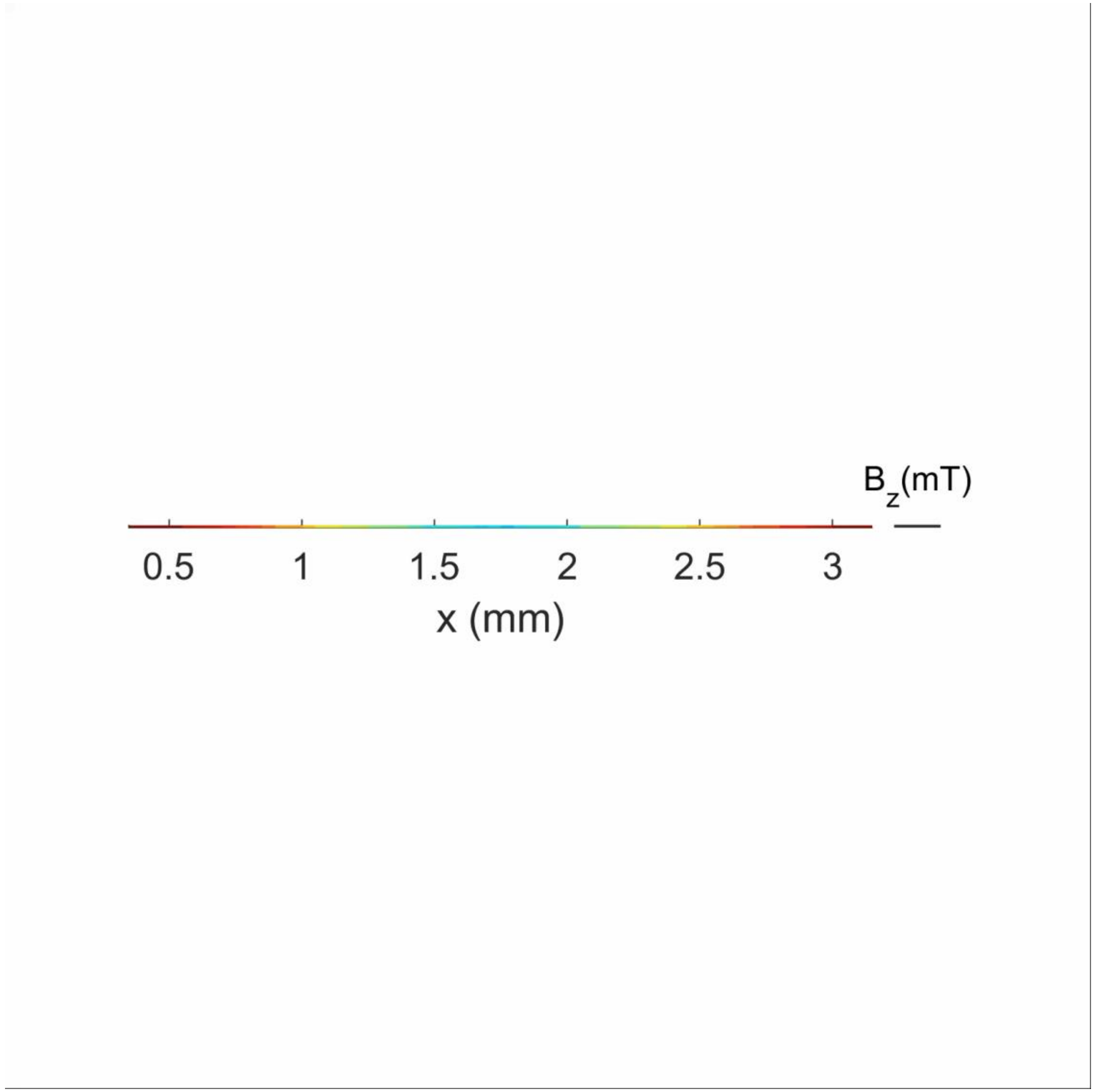

B_z(mT)
0.5
1
1.5
2
2.5
3
x (mm)

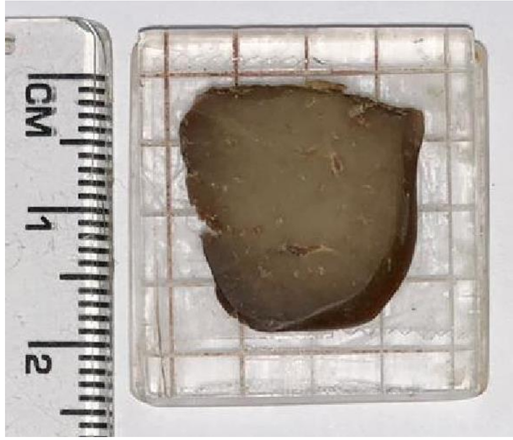

Colaboração: USP - UNESP
Prof. Oswaldo Baffa
Prof. José Ricardo de Arruda

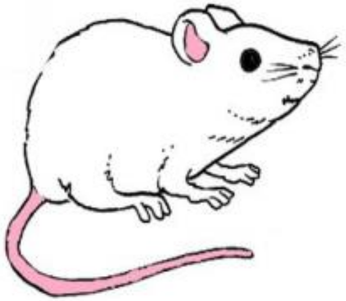

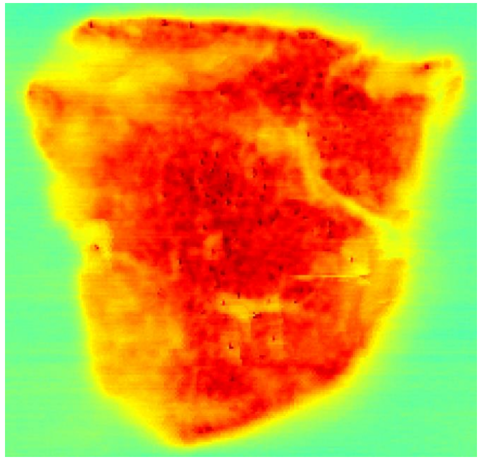

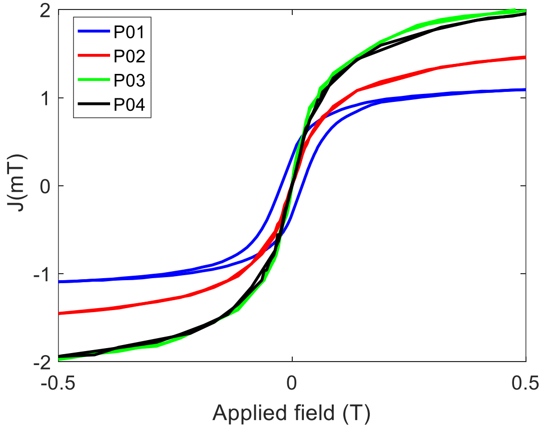

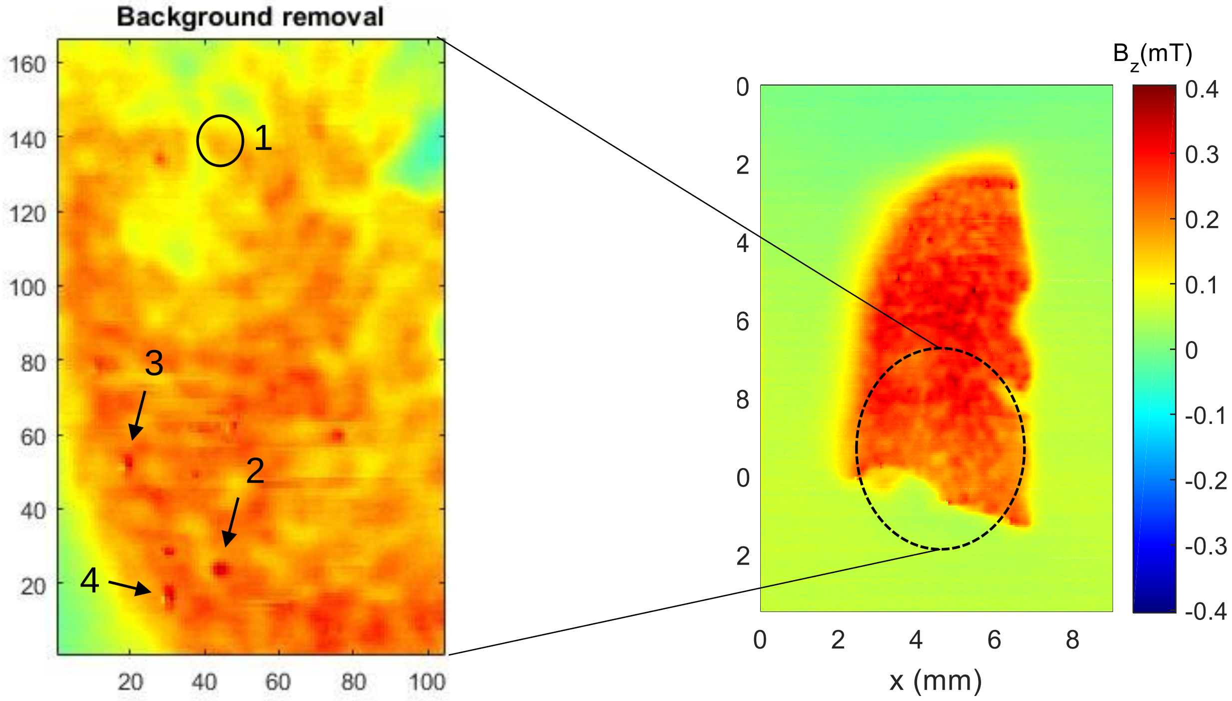

Magnetic Separation

Magnetic separation setup (magnetophoresis device)

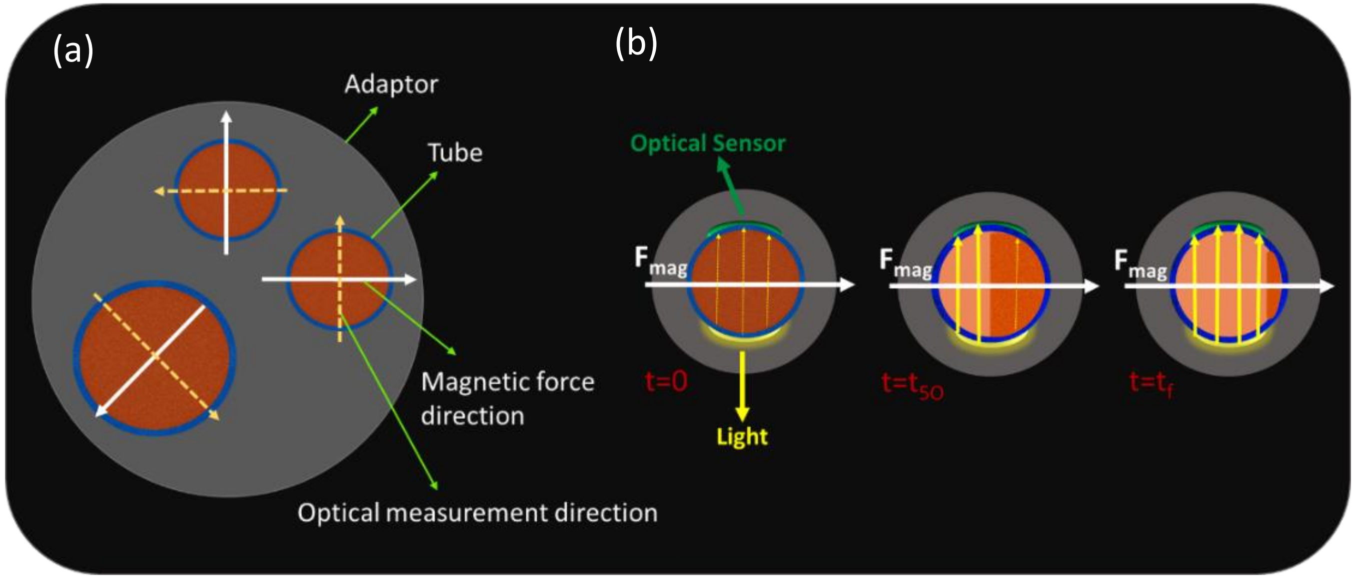

F_d= $6\pi r\eta v$

F_m=m$\mu_0 \frac{\partial H}{\partial r}$

Schematic setup of magnetophoresis device (top view) contains three cylindrical cavities, two of them for 2 mL volume tubes and one for 15 mL tube. (b) The MS process for one tube is illustrated.

Magnetophoresis curve and DLS

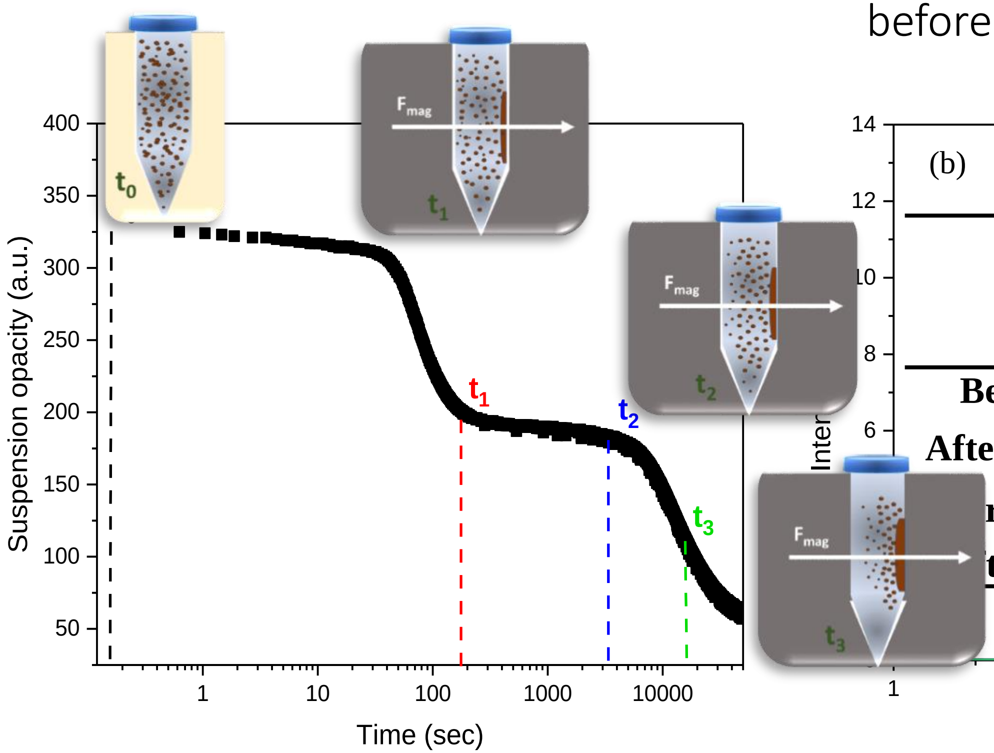

Characteristics of the EM10 sample before MS and during 3 h of MS by DLS.

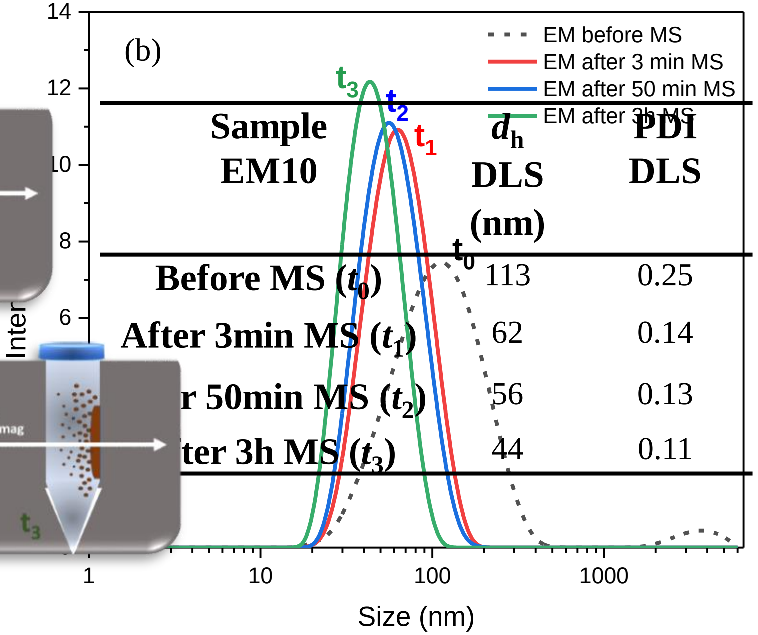

Sample EM10	d_h DLS (nm)	PDI DLS
Before MS (t_0)	113	0.25
After 3min MS (t_1)	62	0.14
r 50min MS (t_2)	56	0.13
ter 3h MS (t_3)	44	0.11

(a) The magnetophoresis curve of EM10 over a 14 h time period, and (b) DLS of EM10 sample at t_0 before separation, t_1 after 3 min, t_2 after 50 min, and t_3 after 3h of inserting sample in separation system.

Magnetic Particle Spectrometer

Single driving field-based MPS

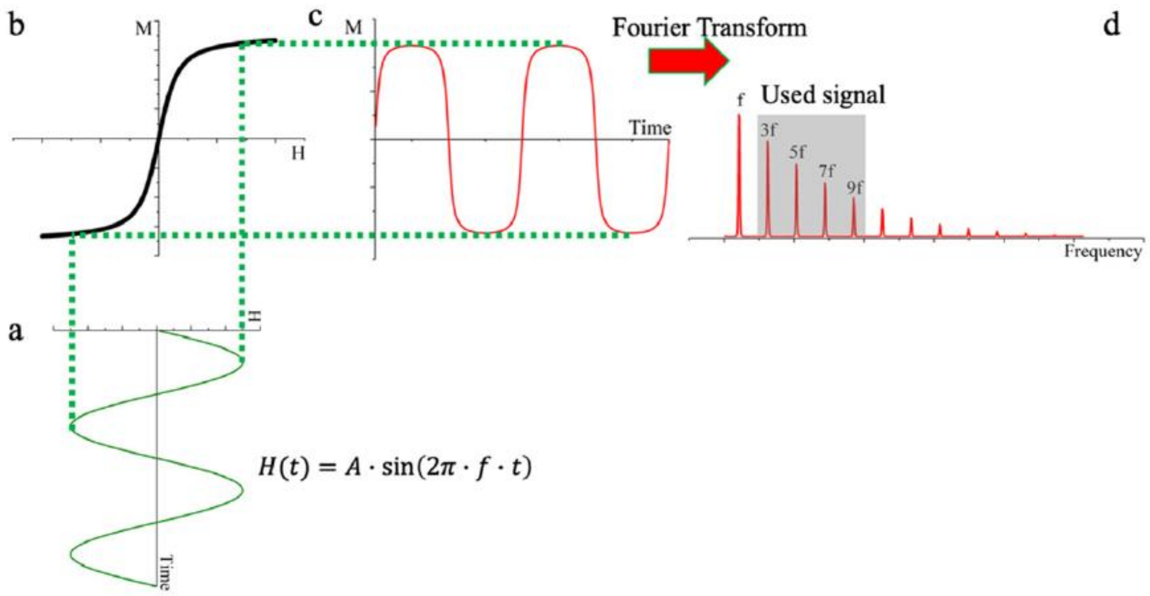

(a) Time varying sinusoidal magnetic field; (b) MH response curve of SPIONs; (c) time domain magnetization response of SPIONs; (d) power spectrum of collected signal contains higher harmonic components 3*f* (third harmonic), 5*f* (fifth harmonic), etc

Picture from: J. Phys. D: Appl. Phys. 52 (2019) 173001 (17pp)

Magnetization Coil Electrical and Geometrical Specifications

R_1= 35 mm

R_2= 41.5 mm

R_3= 52 mm

l=160mm

N= 1.360 turns

L=20.6 mH

R=8.7Ω

C= 12.3nF

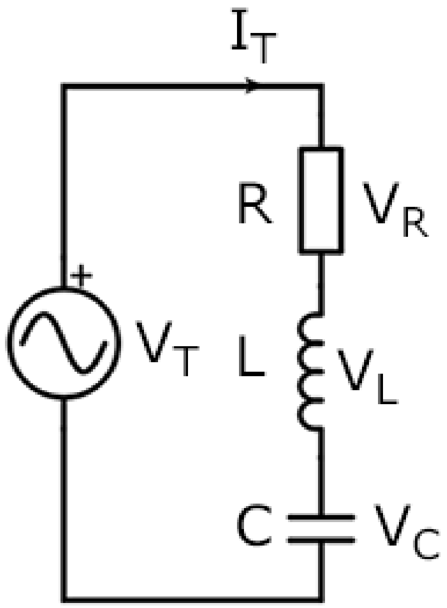

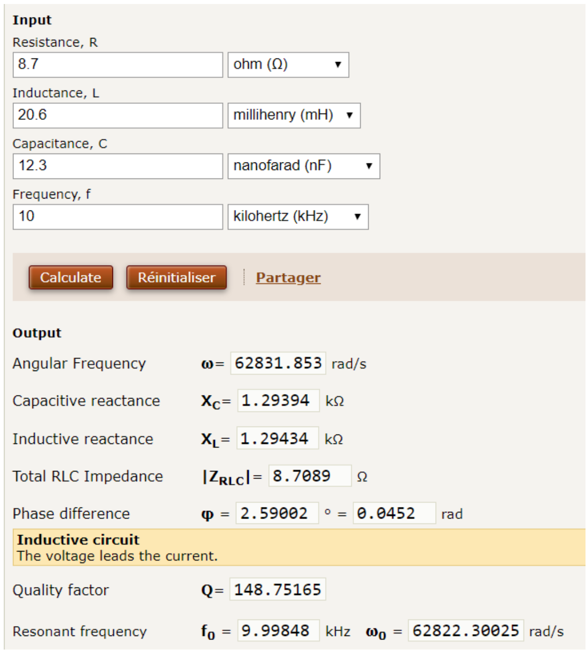

https://www.translatorscafe.com/unit-converter/fr/calculator/series-rlc-impedance/

Magnetic Characteristics

$$\oint_C \mathbf{B} \cdot d\mathbf{l} = \mu_0 I$$

$$\mu_0 = 4\pi \times 10^{-7} \frac{\mathrm{N}}{\mathrm{A}^2}$$

N= 1360 turns

L= 160 mm

B= 10.7 mT/A

Experimental Checks

Search coil positioned at the center of the magnetization coil

N= 10 turns

R= 5 mm

$V_{mag\text{-}coil}$ = 74Vpp

$V_{search\text{-}coil}$ = 81 mVpp

B_{exp}= 0.60 mT/A

Excitation, detection & monitoring coils

Detection coils, 1st order gradiometer

Monitoring coil (center)

Excitation coil-solenoid with two layers of winding.

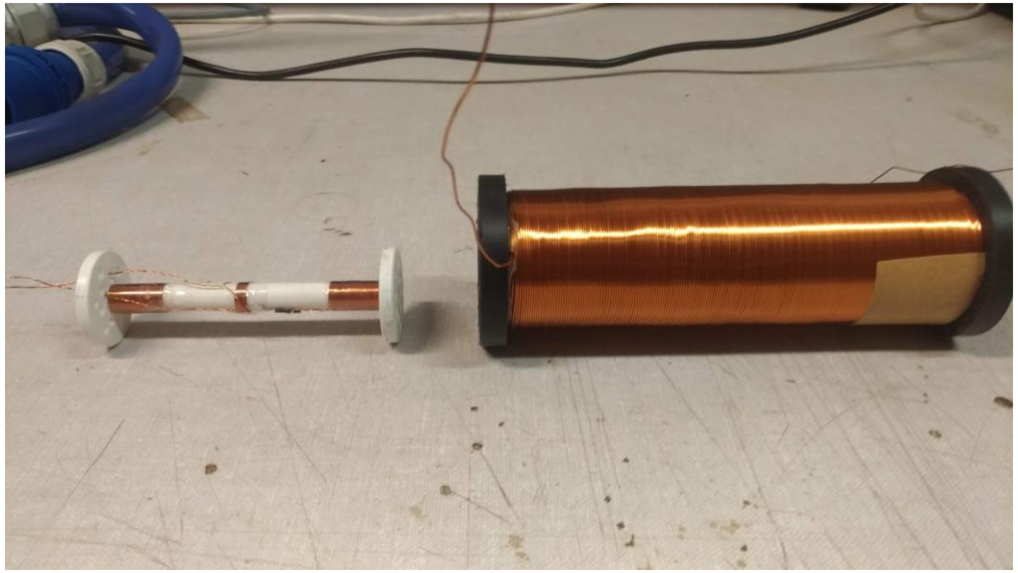

Resonance of Driving Coil

- The RLC circuit is usually driven at the resonance frequency to optimize power transfer from the power amplifier

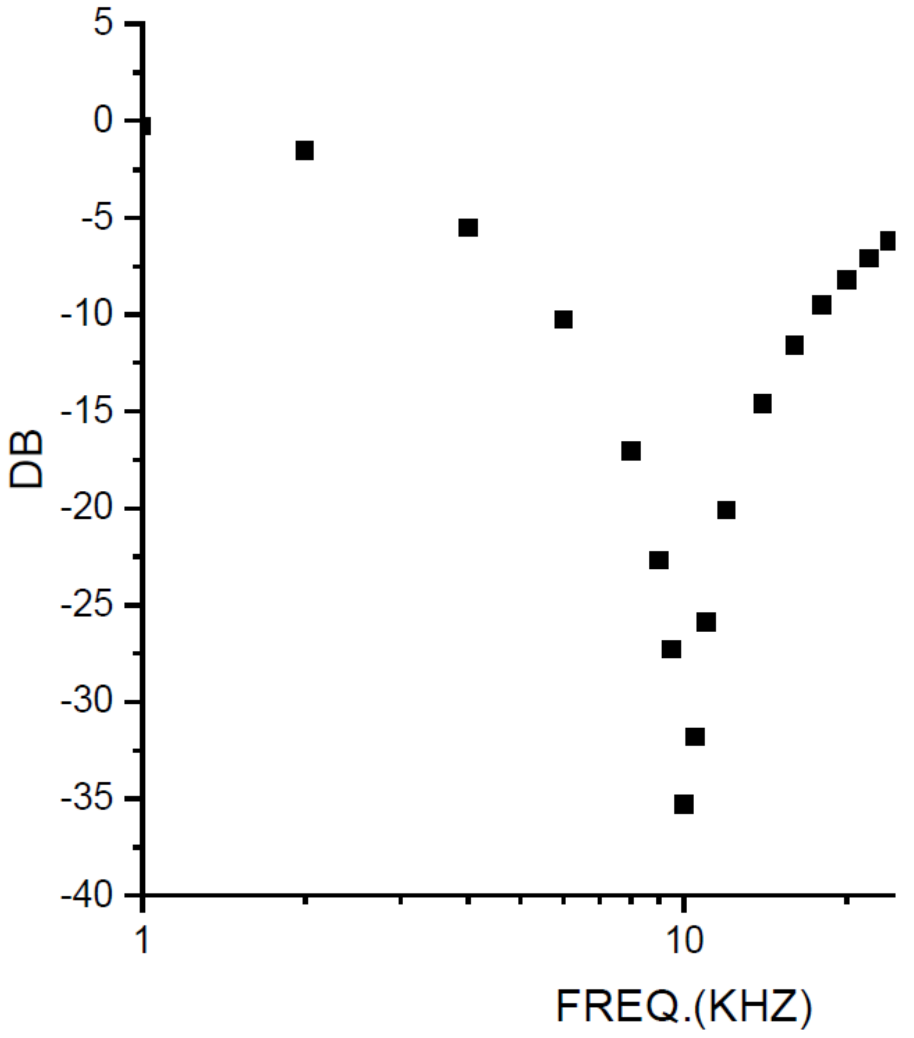

Power Amplifier

A power amplifier with low level of distortion must be employed in the excitation circuit.

Dual driving field-based MPS

(e) dual sinusoidal magnetic fields; (f) MH response curve of SPIONs; (g) time domain magnetization response of SPIONs;
(h) power spectrum of collected signal contains higher harmonic components
fH ± 2*fL* (third harmonics),
fH ± 4*fL* (fifth harmonics).

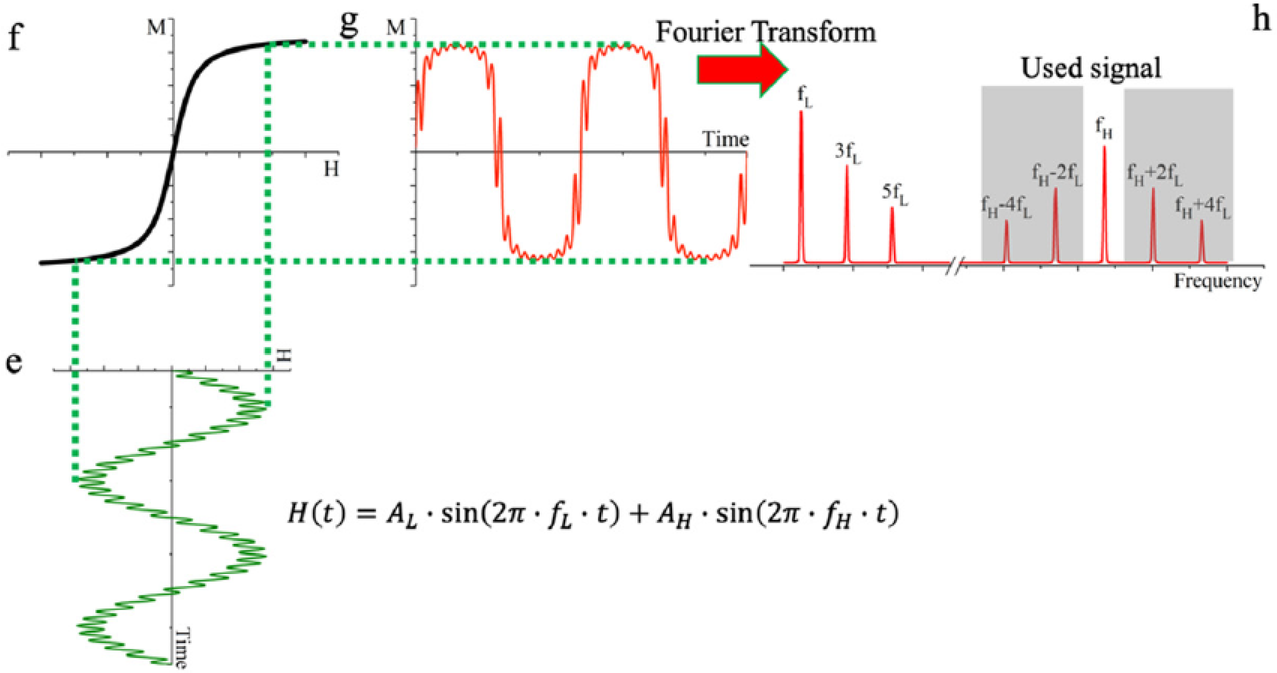

$$H(t) = A_L \cdot \sin(2\pi \cdot f_L \cdot t) + A_H \cdot \sin(2\pi \cdot f_H \cdot t)$$

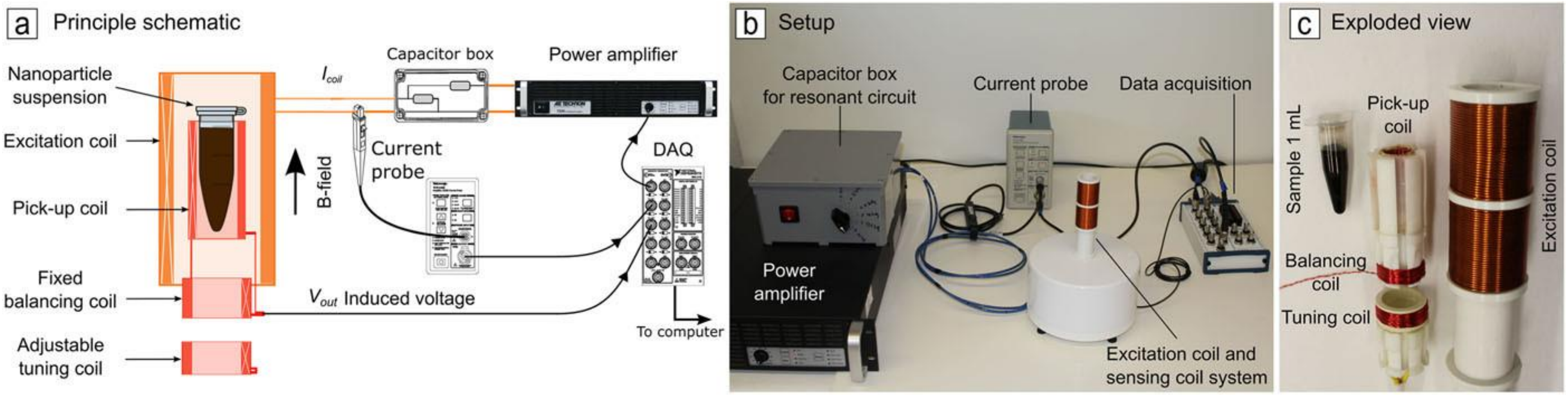

FIG. 1. The nanoparticle suspension is driven by a time-varying magnetic field provided by the excitation field. The sample magnetization change induces a voltage in a pick-up coil system which is recorded by a DAQ.

Published in: Nicolas Garraud; Rohan Dhavalikar; Lorena Maldonado-Camargo; David P. Arnold; Carlos Rinaldi; *AIP Advances* 7, 056730 (2017) DOI: 10.1063/1.4978003